UC Berkeley
UC Berkeley Electronic Theses and Dissertations

Title

Pseudomonas aeruginosa Adhesion To Soft Contact Lenses: Effects Of Cell Surface And Substrate Chemistry

Permalink
https://escholarship.org/uc/item/7pv3s0wp

Author
Tran, Victoria Blue

Publication Date
2011

Peer reviewed|Thesis/dissertation

eScholarship.org Powered by the California Digital Library
University of California

Pseudomonas aeruginosa Adhesion To Soft Contact Lenses: Effects Of Cell Surface And Substrate Chemistry

By

Victoria Blue Tran

A dissertation submitted in partial satisfaction of the

requirements of the degree of

Doctor of Philosophy

In

Chemical Engineering

In the

Graduate Division

of the

University of California, Berkeley

Committee in charge:

Professor Clayton J. Radke, Co-Chair
Professor Suzanne M.J. Fleiszig, Co-Chair
Professor Harvey Blanch
Professor Carolyn Bertozzi

Fall 2011

Pseudomonas aeruginosa Adhesion To Soft Contact Lenses: Effects Of Cell Surface And Substrate Chemistry

© 2011

by Victoria Blue Tran

Abstract

Pseudomonas aeruginosa Adhesion To Soft Contact Lenses: Effects Of Cell Surface And Substrate Chemistry

By

Victoria Blue Tran

Doctor of Philosophy in Chemical Engineering

University of California, Berkeley

Professor Clayton J Radke, Co-Chair
Professor Suzanne M.J. Fleiszig, Co-Chair

Bacterial adhesion to soft-contact lenses is a major risk factor for microbial keratitis. Microbial keratitis, a potentially blinding condition, is the most serious complication associated with soft-contact-lens wear. Thus, curtailing adhesion of bacteria to soft contact lenses is a method of preventing microbial keratitis. One of the most implicated bacteria in soft-contact-lens related microbial keratitis is *Pseudomonas aeruginosa*. However, binding of bacteria to solid substrates is complex and incompletely understood. This thesis investigates and elucidates the mechanisms of *P. aeruginosa* binding to soft-contact lenses in order to advance antifouling science.

This study consists of three main parts. First, the bacterium's motility appendages, which have been implicated in bacterial adhesion, were studied. Changes in bacteria surface association due to modifications of the appendages were investigated. Following this, the influence of anionic membrane surfaces on bacteria association was studied. Finally, utilizing what was learned, surface modifications via surfactants were explored for antifouling efficacy.

Most current studies involving binding to contact lenses report end-point analyses with little understanding of the mechanisms of adhesion. Under phase-contrast microscopy, a parallel plate flow chamber, which provides a well-defined flow field, was utilized. *P. aeruginosa* binding was visualized and investigated, and its binding mechanisms were dissected. *P. aeruginosa* swimming motility increased attachment rates by increasing the bacterium's effective diffusion but did not change the bacterium's ability to bind. Additionally, pili are not necessary for attachment. Hyperpiliation, infact, hinders attachment. By direct observation individual bacteria, it is shown that *P. aeruginosa* has multiple binding sites. Removal of one binding site givs way to binding via other binding sites.

Many contact lenses are anionic. Membranes with addition of anionic poly(methacrylic) and poly(acrylic acid) were investigated. Wild-type *P. aeruginosa* strain PAK exhibits an accumulation burst-attachment phenomenon on anionic hydrogel membranes when the suspending medium contains divalent cations and the membrane initially does not. Early-time accumulation rates of are larger than on counterpart nonionic

hydrogels. The initial high accumulation rate is followed by spontaneous bacterial detachment to a low number of strongly bound bacteria. The bursting phenomenon arises from reversible divalent-cation bridging between the anionic bacterium and anionic charged sites on the hydrogel surface. Few strongly bound PAK bacteria remain on the gel surface is most likely due to increased water wettability compared to the nonionic hydrogels.

Soft-contact-lens surface wettability can be increased by addition of surfactants. The ability of polymeric surfactants to modify contact lenses and prevent adhesion was studied. A polyethylene oxide/polypropylene oxide surfactants (Pluronic F127) and ethylene oxide/butylene oxide (EOBO) polymeric surfactants were capable of increasing the wettability of soft-contact lenses. Surfactants absorbed into the lens matrix. Over time, the surfactants leach from the lens matrix and adsorb at the external lens surface. The surfactants increase the lens wettability by decreasing the air/water surface tension while also increasing the adhesion tension of the lens surface. A highly wettable surface slightly reduces bacterial adhesion of PAK bacteria in agreement with previous studies. However, prevention of PAO1 bacteria was not possible, as surface wettability did not play a role.

This study emphasizes the delicate balance of forces at play during bacterial adhesion to substrates. In addition, the many factors such as substrate, bacterium, and adhesive factors that play a role stress the difficulty of preventing adhesion.

Acknowledgments

I would like to thank all the people who made this project possible and helped me complete it. First, I would like to acknowledge my family. They have struggled with so much in their lives with only the hope that I can succeed. Knowing that they have been there for me has guided me through this project over the years.

Next, I would like to thank my advisors: Professor Clayton Radke and Professor Suzanne Fleiszig. Thank you for taking me into your labs and advising and teaching me through the years. I have enjoyed our conversations and scientific discussions. Without your enthusiasm and scientific inquisitiveness, this project would not have beeen possible. Aside from the duties of advisors, they went above and beyond. They made my graduate experience fun and enjoyable.

In addition, I would like to thank my lab members (past and present) in the Radke Lab and the Fleiszig lab. Thank you especially to Tatyana Svitova and Kendra Copley in the Radke Lab to David Evans in the Fleiszig lab for guidance. All my lab members have been there for me both academically and emotionally. Whether it was help with experiments, knowledge or pure scientific input, they were always there. I never felt alone in my project because of them.

I would in particular like to thank my undergraduate student researcher, Nicole Sung. She helped me with my project for 4 years and was always enthusiastic to learn and help. Her spirit was never ending and I found it very inspirational.

This project was also made possible by the incredible support staff available to me at UC Berkeley. Thank you so much to Eric Granlund in the machine shop for making my experimental setups possible. Thank you to Phil Simon for helping me in the student shop. Also, thank you to the administrative staff: Aileen Harris, Rocio Sanchez and Patricia Schaible.

Thank you to my thesis committee: Professor Harvey Blanch and Professor Carolyn Bertozzi for taking the time to read this thesis and for your input.

Finally I would like to acknowledge my funding sources: The National Science Foundation Graduate Fellowship, The UC Berkeley Chancellor's Fellowship and Alcon Labs.

Table of Contents

Abstract **1**

Acknowledgments ..... **i**

Table of Contents ..... **ii**

Chapter 1: Introduction and Background **1**
1.1 Preface to Chapter 1
1.2 Microbial keratitis 2
1.3 *Pseudomonas aeruginosa* 3
1.4 Soft-Contact Lenses 5
1.5 Bacterial Adhesion to Soft-Contact Lenses 5

Chapter 2: Dynamics of Flagellar and Pilus-mediated *Pseudomonas aeruginosa* Surface Association with Contact Lenses **7**
2.1 Abstract 7
2.2 Introduction 8
2.3 Methods and Materials 8
2.3.1 Bacterial strains and culture conditions 8
2.3.2 Parallel-Plate Flow Chamber 9
2.3.3 Microscopy 12
2.3.4 Statistics 12
2.4 Results 13
2.4.1 Swimming Motility and Association Kinetics 13
2.4.2 Pili and Association Kinetics 16
2.4.3 Association Phenotypes 18
2.4.4 Distribution of Association Phenotypes 22
2.5 Discussion 25

Chapter 3: Dynamics of *Pseudomonas aeruginosa* association with anionic hydrogel surfaces in the presence of aqueous divalent-cation salts. **28**
3.1 Abstract 28
3.2 Introduction 29
3.3 Experiment 29
3.3.1 Materials 29
3.3.2 Bacteria preparation 30
3.3.3 Hydrogel synthesis 30
3.3.4 Membrane wettability 31
3.3.5 Hydrogel swelling/shrinking 32
3.3.6 Bacteria association assays 35
3.4 Results and Discussion 35
3.4.1 Bacterial uptake 35
3.4.2 Burst etiology 46
3.5 Conclusions 50

Chapter 4: Effects of Polymeric Surfactants On Silicone Hydrogel Soft Contact Lens Wettability and Bacterial Adhesion of *Pseudomonas aeruginosa* **51**
4.1 Abstract 51
4.2 Introduction 52
4.3 Materials and Methods 52

4.3.1 Materials ... 52
4.3.2 Contact-Lens Preparation ... 52
4.3.3 Surfactants ... 53
4.3.4 Contact-Angle and Surface-Tension Measurements ... 53
4.3.5 Bacteria Preparation ... 54
4.3.6 Bacterial-Adhesion Assays ... 54
4.3.7 Bacteria-Hydrocarbon-Adhesion Assay ... 55
4.4 Results ... 55
4.4.1 Wettability ... 55
4.4.2 Bacterial Adhesion ... 59
4.5 Discussion ... 61
4.5.1 Wettability ... 61
4.5.2 Bacterial Adhesion ... 65
4.6 Conclusions ... 66

References ... 67

Appendix A: Bacterial Adhesion Studies With a Flow-Chamber designed for Viable-Cell Counting ... A-1
A.1 Abstract ... A-1
A.2 Background ... A-2
A.3.1 Contact Lenses ... A-2
A.3.2 Contact angles ... A-2
A.3.3 First Flow Chamber ... A-3
A.3.4 Bacterial Adhesion Assays ... A-4
A.3.5 Addition of Surfactants ... A-4
A.4 Results and Discussion ... A-4
A.4.1 Contact Angles ... A-4
A.4.2 Bacterial Adhesion ... A-5
A.4.3 Role of Polymeric Surfactants in Bacterial Adhesion ... A-8
A.4.4 Adhesion kinetic model ... A-9
A.5 Conclusions ... A-10

Appendix B: Determination of Effective Diffusion Coefficient of motile *Pseudomonas aeruginosa* via Restricted Diffusion ... B-1
B.1 Abstract ... B-1
B.2 Introduction ... B-2
B.3 Methods ... B-2
B.3.1 Bacteria preparation ... B-2
B.3.2 Restricted Diffusion ... B-2
B.4 Results and Discussion ... B-3

Appendix C: Micro - Flow Chamber Information ... C-1
C.1 Introduction ... C-1
C.2 Flow chamber preparation ... C-1
C.3 Flow chamber, pump and microscope set-up ... C-1
C.4 Flow chamber hydrodynamics ... C-2

Appendix D: Sterile Media Washout After Bacterial Adhesion Experiment ... D-1

Appendix E: Passage of Air Water Interface Across Bound Bacteria ... E-1

List of Figures

Figure 1.1 *Pseudomonas aeruginosa* keratitis 2
Figure 1.2 *Pseudomonas aeruginosa* strain PAO1 and its flagellum 4
Figure 1.3 *Pseudomonas aeruginosa* strain PAO1 and its pili. 4
Figure 2.1 Parallel-plate flow chamber for bacterial adhesion assays. 10
Figure 2.2 Atomic force microscopy pictures of an O_2Optix lens surface 11
Figure 2.3 PAK bacteria and flagellum mutants association with O_2Optix lens surface 14
Figure 2.4 Rates of wild-type PAK bacteria associating with contact-lens surface as a function of bulk bacteria solution concentration. 16
Figure 2.5 PAK bacteria and pilin mutants association with O_2Optix lens surface 17
Figure 2.6 Schematic of five surface-association phenotypes. 19
Figure 2.7 Time-lapse phase-contrast images of bacteria rotating and moving laterally 20
Figure 2.8 Fluorescence microscopy of rotating PAK bacteria 21
Figure 2.9 Distribution of surface-association phenotypes for wild-type PAK and its swimming-motility mutants. 23
Figure 2.10 Distributions of surface-association phenotypes for wild-type PAK and its pili mutants. 24
Figure 3.1 Advancing contact angles for surfaces: p-HEMA pretreated with PBS (pH=7.4), p-MAA pretreated with PBS (pH=7.4) with 100-mM $MgCl_2$, clean glass, and silanated glass each immersed in aqueous PBS (pH=7.4) 32
Figure 3.2 Volume swelling/shrinking kinetics of 4-μL p-MAA beads: a.) initially soaked in distilled/deionized water (pH=6.2) and immersed in PBS (pH 7.4) b.) initially soaked in PBS (pH=7.4) and immersed in PBS (pH 7.4) with 10 mM NaCl 34
Figure 3.3 Surface uptake kinetics of PAK suspended at $5x10^6$ cfu/mL in Mian's medium accumulating on a p-HEMA surface pretreated in PBS (pH=7.4). 36
Figure 3.4 Surface uptake kinetics of PAK at $5x10^6$ cfu/mL suspended in Mian's medium accumulating on a 70% p-HEMA /30% p-MAA surface pretreated in PBS 37
Figure 3.5 Total surface uptake kinetics of PAK at $5x10^6$ cfu/mL suspended in Mian's medium accumulating on anionic-polycarboxylate homopolymers 38
Figure 3.6 Total surface uptake kinetics for PAK at $5x10^6$ cfu/mL suspended in Mian's medium accumulating on p-MAA membranes with differing pretreatments: aqueous 100-mM NaCl in PBS solution (pH=7.4) (filled circles) or distilled/deionized water (pH=6.2) (open triangles). 39
Figure 3.7 Volume shrinking kinetics of 4-μL p-MAA beads initially soaked in PBS (pH=7.4) followed by immersion in PBS (pH 7.4) with 10-mM $MgCl_2$. 40
Figure 3.8 Total surface uptake kinetics of PAK at $5x10^6$ cfu/mL accumulating on p-MAA membranes pretreated in Mian's medium, in 10-mM $MgCl_2$ aqueous PBS solution (pH=7.4), and in 100-mM $MgCl_2$ aqueous PBS solution (pH=7.4) 41
Figure 3.9 Burst initiation with divalent cations. 42
Figure 3.10 Volume swelling kinetics of 4-μL p-MAA beads upon exposure to EDTA. 44
Figure 3.11 Magnesium burst recovery with EDTA. 45
Figure 3.12 Calcium burst recovery with EDTA. 46
Figure 3.13 Schematic of proposed bridging/collapse mechanism for PAK bursting. 48

Figure 3.14 PAK total uptake rates at $5x10^6$ cfu/mL on p-HEMA pretreated with PBS (pH=7.4), p-MAA pretreated with PBS (pH=7.4) with 100 mM $MgCl_2$, glass, and silanated glass. 49
Figure A.1 Advancing(a) and receding angles (b) A-3
Figure A.2 Schematic of viable-cell count flow cell for bacterial adhesion assays A-3
Figure A.3 COMSOL results from velocity field in viable-cell counting flow-cell A-4
Figure A.4 Advancing contact angles for Pure Vision, Acuvue 2 and Acuvue Advance after soaking in PBS, Tetronic or AL-52700 solutions. A-5
Figure A.5 Bacterial uptake versus time for viable-cell-count flow cell. A-6
Figure A.6 Bacterial uptake vs. bulk bacteria concentration for Pure Vision lenses A-7
Figure A.7 Effect of surfactant addition in contact lenses on bacterial adhesion A-8
Figure A.8 Kinetic model to describe bacterial adhesion to soft contact lenses. A-9
Figure B.1 Schematic of the restricted-diffusion method. Upward diffusion of the bacteria is detected by UV/vis absorbance B-3
Figure B.2 Restricted diffusion results for 0.5 M copper sulfate . B-4
Figure B.3 Variation in absorbance vs. time for various values of (a) diffusion coefficient where v is 3E-6cm/s and settling velocity (b) where D is 3E-6cm^2/s B-6
Figure B.4 Restricted diffusion results. B-7
Figure B.5 Restricted diffusion fit for 5 hours. B-8
Figure C.1 COMSOL simulated velocity profile of optical-flow chamer. C-2
Figure C.2 COMSOL simulated Reynold's number in optical-flow chamber C-3
Figure C.3 COMSOL simulated shear rate of optical-flow chamber. C-3
Figure C.4 COMSOL simulated velocity at bottom surface of flow chamber. C-4
Figure D.1 PAK bacteria associating with O_2Optix lens before and after washout D-1
Figure E.1 GFP labeled PAO1 at O_2Optix lens after passage of air water interface. E-2

Chapter 1: Introduction and Background

1.1 Preface to Chapter

Microbial keratitis is a serious, vision-threatening disease most commonly associated with soft-contact lens wear. Normally, the eye is highly resistant to infection but soft-contact lens wearers who are otherwise healthy, are victims of these infections. There are more than 30 million soft-contact-lens wearers in the United States with the population growing.[1] The most common gram negative bacterium found with contact-lens-related microbial keratitis is *Pseudomonas aeruginosa*[2]. Studies have shown that *P. aeruginosa*-laden soft-contact lenses and lens cases are a major risk factor for microbial keratitis.[3] Additionally, *P. aeruginosa*-laden contact lenses have been shown to induce microbial keratitis in a murine model.[4] Thus, prevention of *P. aeruginosa* adhesion to soft-contact lenses is a worthwhile endeavor. This chapter provides background to microbial keratitis, *P. aeruginosa*, contact lenses, and previous studies regarding bacterial adhesion.

1.2 Microbial keratitis

Microbial keratitis is a serious ocular disease caused by infiltration and replication of microbes in the cornea.[3] The cornea is a crucial part of the vision as it is responsible for 2/3 of the refractive power of the eye.[5] The components of the cornea are particulary well structured and organized to allow light to pass. As a result of microbial keratitis, bacteria penetrate the cornea disrupting its optical regularity.[3] Further, the host immune responses cause immune cells such as white blood cells to attack the bacteria.[6] Recruitment of immune cells into the cornea disrupt the cornea transparency even further thus causing even more damage and vision loss. This damage manifests as opacity as seen in Figure 1-1.[6]

There are a number of predisposing factors to microbial keratitis such as ocular trauma, ocular surface disease, and ocular surgery[2]. However, contact-lens wearers are at times, the most frequent victims.[2,3,6] In most incidences, contact-lens-related-microbial keratitis is rare[6]. However, its onset is unknown as it infects healthy contact-lens wearers with no other pre-existing conditions. In addition, microbial-keratitis characteristics vary with population and location[2].

Microbial keratitis is difficult and costly to treat.[3] If not treated promptly, it can cause severe and permanent eye damage and vision loss. In most cases, it is treated with antibiotics and/or steroids. However, microbial resistances to antibiotics are progressing which makes the disease even more hazardous and difficult to treat.[7]

There are numerous microbes that are involved in microbial keratitis.[2] The bacteria are often found in cultures taken directly from the eye, contact lenses and contact-lens cases. Common microbes include: *Staphlococcus aureous*, coagulase negative *Stapholococcus*, *Serratia marcecens*, *Pseudomonas aeruginosa,* and the fungus acanthomeaba. The most prevalent gram-negative bacterium is *Pseudomonas aeruginosa.*[3]

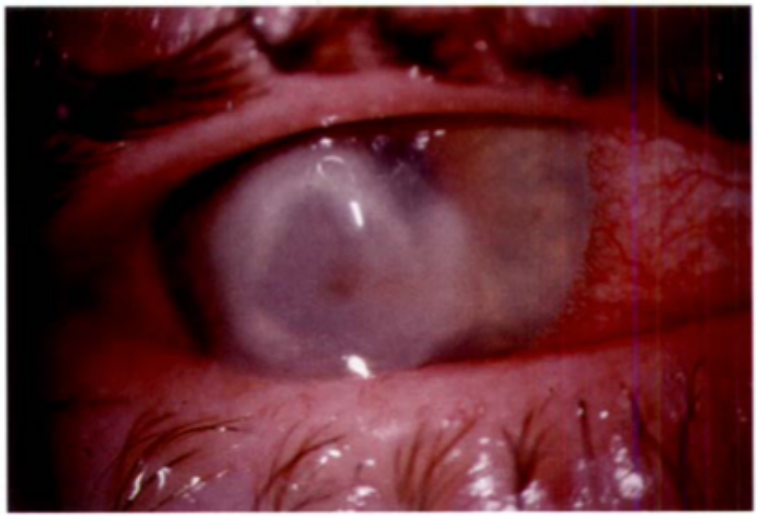


Figure 1.1 *Pseudomonas aeruginosa* keratitis

1.3 *Pseudomonas aeruginosa*

Pseudomonas aeruginosa is a ubiquitous bacterium found in the water, soil, plants, insects, and sewage. This bacterium can be found in such diverse locations because of its low nutritional requirements. Additionally, it can grow both aerobically and anaerobically.[8]

P. aeruginosa is a notorious opportunistic pathogen that is likely to attack and infect immune-compromised individuals. It is responsible for a number of nosocomial infections such as those found with burn wounds, surgical wounds, otitis externa (swimmer's ear), bacteremia, microbial keratitis, puncture wounds, and in others with suppressed immune systems. Infections by *P. aeruginosa* are difficult to treat, as the outcomes can be very damaging. *P. aeruginosa* is the number one gram-negative bacteria associated with bacterermia with a 40-60% mortality rate. Importantly, there are many antibiotic resistances that are associated with the bacteria, making treatment even more difficult.[8] Additionally, the bacterium has many virulence factors such as secreted, protein effectors and lipopolysaccharides on the cell surface that allow it to antagonize a host and cause inflammatory responses.[6]

Pseudomonas aeruginosa is a gram negative rod of approximately 1-2 microns in length[8]. Many strains of the bacterium are capable of swimming motility through a single flagellum. The flagellum as shown in Figure 1.2 and is essentially a tail extending out from one of the bacterium's poles.[9] This flagellum is approximately 2 microns in length and is formed by polymerization of protein subunits called flagellin.[10] Through rotation of the flagellum by a motor within the bacterium, the bacterium can swim at speeds of 30-50 μm/s. *P. aeruginosa* swimming gives the bacterium great advantages for seeking nutrients, eluding toxins, and finding optimal locations for colonization. In many cases, the bacterium swims in straight lines interrupted by random tumbles.[10] The movement is analogous to a random walk and can be described by an effective diffusion coefficient.[11] When the bacterium senses a concentration gradient and wishes to swim away or towards it, the bacterium is capable of more direct movement. This directed movement is called chemotaxis.[12] Additionally, the bacteria can signal to one another by excreting chemicals that can be sensed by another bacterium. This is described as quorum sensing.[13]

P. aeruginosa is also capable of surface-associated mobility attributed to its pili. The pili are hair-like appendages also on the surface of the bacterium as shown in Figure 1.3.[9] By extension, the bacterium can contact the end of the pili to a surface. When the pilus is retracted, it pulls the bacterium to the point of adhesion to a surface. This jerky, translational motion at a substrate surface is called twitching motility.[10]

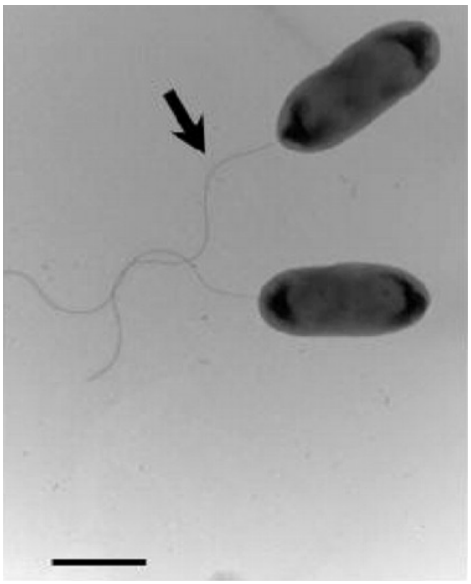


Figure 1.2 *Pseudomonas aeruginosa* strain PAO1 and its flagellum. The arrow points to the bacterium's flagellum. The scale bar represents 1 μm.[9]

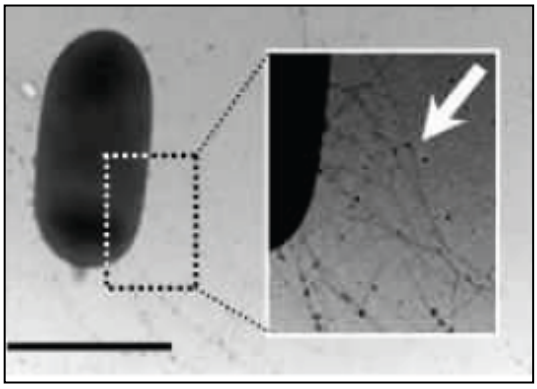


Figure 1.3 *Pseudomonas aeruginosa* strain PAO1 and its pili. The white arrow points to its external pili. The scale bar represents 1 μm.[9]

1.4 Soft-Contact Lenses

Soft contact lenses are hydrogels, crosslinked polymers with an affinity for water. Soft-contact lenses are on the order of 100 μm thick.[14] They are placed in the tear film, surrounding the cornea and ride closely and directly in front of the cornea.[15] There are two major types of soft-contact lenses: traditional hydrogels and silicone hydrogels. Traditional hydrogels are comfortable, hydrophilic, and can be high in water content (e.q. up to 70 wt% water). These types of lenses although comfortable, have low oxygen permeability. Hence, they are not marketed for overnight wear.[16] Since the cornea is avascular, the lack of oxygen supply through the lens results in complications such as hypoxia. Hypoxia is the depravation of oxygen to the eye and has been considered a risk factor for microbial keratitis.[17] Oxygen is relatively soluble in silicone. Thus to counter low oxygen permeability, many if not most modern soft-contact lenses, incorporate silicone into the cross-linked, polymer backbone. Silicone hydrogels have markedly better oxygen permeability and are approved for extended wear (i.e., continuous wear for up to weeks). [16]

Despite the advent of silicone hydrogels, contact-lens-related complications still exist. These include: superior epithelial arcuate lesions (SEALs), contact lens-induced peripheral ulcers (CLPU), corneal infiltrates, contact-lens-induced papillary conjunctivitis (CLPC), corneal erosions, and microbial keratitis. Of all these complications, microbial keratitis is the most serious.[17]

1.5 Bacterial Adhesion to Soft-Contact Lenses

Bacteria-laden contact lenses can supply bacteria to the nearby cornea, thereby promoting greater chances of infection.[18] Thus, understanding and preventing adhesion is a goal.

The traditional manner of understanding particle adhesion to a substrate is to apply classical DLVO (Derjaguin, Landau, Verway and Overbeek) theory for a colloidal particle. Long-range attraction/repulsion caused by electrical double layer and van der Waals forces create an adsorption interaction potential energy causing bacteria to adhere. At short distances bacterial rearrangement allows for irreversible attachment. However, DLVO theory assumes that bacteria and the substrates are smooth and of uniform chemistry thereby neglecting surface roughness, charge or chemical non uniformity, hydrophobic, and solvation forces.[19] It is unlikely that bacteria can be treated simply as colloidal particles; bacteria are by no means surface chemically uniform. Also as mentioned, bacteria such as *Pseudomonas aeruginosa* are capable of quorum sensing or signaling to other bacteria [13] in addition to chemotaxis or movement due to chemical gradients.[12] In addition, bacterial adhesion is complicated because bacteria can aggregate, attach reversibly and irreversibly, replicate, die and lyse. Further, bacteria are able to adhere by both specific and non-specific interactions. At short distances from substrates, there are complex coatings on the bacterial surfaces that aid in adherence to surfaces.[20] *P. aeruginosa* is capable of specifically interacting with a substrate through adhesins. Adhesins located internally and externally such as on their pili allow for chemical specificity to substrates.[21]

Substrate surface hydrophobicity is thought to be important to bacterial adhesion. Lipopolysaccarides on the surface of *P. aeruginosa* have been shown to be a major component in its virulence in addition to aiding bacterial adhesion. It may be possible that a hydrophobic O-side chain in some lipopolysaccarides help *P. aeruginosa* adhere to

hydrophobic surfaces.[22] Salerno et al established that lens material and surface hydrophobicity play a role in bacterial adhesion where hydrophobic bacteria are more likely to adhere to hydrophobic surfaces.[23] Garcia-Saenz et al indicate that bacteria are more likely to adhere to hydrophobic lenses of low water content.[24] However, other researchers report conflicting results.[25]

Numerous techniques to measure bacterial adhesion have been employed including substrates suspended in bacterial solutions, radial flow chambers, and parallel plate flow chambers. [9,23-25] Studies using suspended substrates in bacterial solutions seem flawed because they do not have good control over mass transport limitations, especially if the suspension is shaken to prevent bacteria from settling. Flow systems are beneficial because mass transport can be predicted. The shear rate, concentrations etc. can be controlled thereby allowing quantitative analysis of adhesion kinetics.

There are a number of adhesive factors associated with *P. aeruginosa* that may modulate its ability to bind. A set of important factors includes its motility appendages: pili and flagella. Studies have shown that these appendages aid in the bacterium's ability to bind.[9,25-34] Methods for assistance include transporting the bacterium to optimal locations for binding in addition to binding by the appendage. Despite the advancement in understanding the roles of the motility appendages, there is still controversial data the roles of these appendages and how they later contribute to biofilm formation.[33-39] [9,32,40-44]

Chapter 2: Dynamics of Flagellar and Pilus-mediated *Pseudomonas aeruginosa* Surface Association with Contact Lenses

2.1 Abstract

Flagella and pili are appendages that modulate attachment of *Pseudomonas aeruginosa* to solid surfaces. However, previous studies have mostly reported absolute attachment. Neither the dynamic roles of these appendages in surface association nor those of attachment phenotypes have been quantified. Video-microscopy was used to address this issue. Unworn, sterile, soft contact lenses were placed in a laminar-flow optical chamber. Initial lens-association kinetics for *P. aeruginosa* strain PAK were assessed in addition to lens-surface association phenotypes. Comparisons were made to mutants in flagellin (*fliC*), pilin (*pilA*), or those in flagella (*motAB*) or pilus (*pilU*) function. PAK and its mutants associated with the contact-lens surface at a constant rate according to first-order kinetics. Non-swimming mutants associated ~30-40 times slower than wild-type. PAK and its *pilA* mutant associated at similar rates, but each ~4 times faster than the *pilU* mutant. Lens attachment by wild-type PAK induced multiple phenotypes: static, lateral and rotational surface movement, each showing only minor detachment. Flagellin (*fliC*) and flagellar-motility (*motAB*) mutants did not exhibit surface rotation. Conversely, mutants in pilin (*pilA*) and pilus retraction (*pilU*) lacked lateral-surface movement, but displayed enhanced surface rotation. Slower surface association of swimming-incapable *P. aeruginosa* mutants was ascribed to slower convective-diffusion-arrival rates, not an inability to adhere. Flagella function (swimming) enhanced lens association, attachment, and rotation; hyperpiliation hindered lens association. *P. aeruginosa* bound through three different adhesion sites: flagellum, pili, and body. Reduction of bacterial attachment to contact lenses thus requires blockage of multiple adhesion phenotypes.

2.2 Introduction

Pseudomonas aeruginosa is a ubiquitous bacterium notorious for causing serious infections in the airways, urinary tract, and cornea.[45-47] Healthy corneas are inherently resistant to *P. aeruginosa* infection, [48,49] but appear more susceptible with soft-contact-lens wear, especially overnight or extended-wear modalities. [3,50] Since most *P. aeruginosa* corneal and other infections are difficult to treat, there is an urgent need to understand infection pathogenesis and develop novel methods of treatment and prevention.[51,52] One possible mitigating measure against infection is the reduction/prevention of bacterial adhesion to tissues and medical devices including the contact lens.[52,53]

P. aeruginosa adhesion to substrates, including soft-contact lenses, has been studied extensively, [25,27-31,54] and roles for pili and flagella have been documented.[9,32-34] For example, pili are hair-like appendages on the surface of *P. aeruginosa*; they are responsible for surface lateral motility (i.e., twitching).[55,56] Some studies argue that pili are responsible for surface attachment while others refute that role.[33-36,38,39] Some strains of *P. aeruginosa* also exhibit a polar flagellum that allows the bacteria to swim.[57] Flagella are argued by some to provide only a means for transport to a surface.[40] Conversely, other investigators suggest that flagellin, the structural unit of the flagellum, is an adhesive factor that permits surface binding.[38,41,44,57]

Many measurements of bacterial uptake expose a fixed aqueous concentration of bacteria to a surface in a poorly defined flow field for a fixed time and count the number of viable bacteria after washing away "loosely" held material.[24,58-60] In such studies, the rate of bacterial arrival to the surface, the fraction of those arriving that stick, and the uptake kinetics cannot be quantified. Moreover, bacteria in some surface-adhesion studies have been treated as inanimate colloids instead of as living organisms.[25,26,61,62] It is well known that bacteria attached to solid surfaces exhibit motion.[21,35,57,63-66] Due to the limitations of many current assays, little mechanistic information is available on the roles of bacterial appendages in surface association.

To understand the mechanism(s) of initial bacterial uptake to soft contact lenses and the underlying roles of appendage adhesins, video microscopy was utilized in a transparent micro-flow cell. The optical flow chamber was specially designed to provide well-defined laminar parabolic flow across the lens allowing calculation of the transport rate to the surface. The hypothesis was that *P. aeruginosa* binds to a soft contact lens in multiple ways that manifest as different attachment phenotypes. To distinguish the relative roles of pili and flagella in surface association, the uptake kinetics were quantified and phenotypes of *P. aeruginosa* pilin and flagellin structural and functional mutants by time-lapse and real-time phase-contrast microscopy.

2.3 Methods and Materials

2.3.1 Bacterial strains and culture conditions

P. aeruginosa strain PAK and its motility mutants, PAK*ΔfliC* and PAK*ΔmotAB* were kindly provided by Dr. Stephen Lory (Harvard Medical School). PAK*ΔfliC* lacks flagellin, hence the entire flagellum, and thus is unable to swim.[67] PAK *ΔmotAB* has a flagellum, but not a functional motor, and also cannot swim.[67] *P. aeruginosa* strain PAK and its twitching

motility mutants PAK*ΔpilA* and PAK*ΔpilU* were also studied. The pili parent/mutant set was previously constructed and characterized by Dr. John S. Mattick (University of Queensland, Australia), [68,69] and was kindly provided by Dr. Joanne Engel (University of California, San Francisco) with Dr. Mattick's permission. PAK*ΔpilA* is a non-piliated, isogenic mutant, and thus is also twitching-motility defective.[68] PAK*ΔpilU* has pili, but is unable to retract them, and thus is also twitching-motility negative. Indeed, PAK*ΔpilU* is hyperpiliated from the expression of paralyzed fully extended pili.[69]

Bacteria were recovered from frozen stocks by growth on trypticase soy agar at 37°C overnight. Single colonies were inoculated into 12 mL of a modified Mian's minimal medium: sodium phosphate monobasic monohydrate (7.5 mM), potassium phosphate anhydrous (16.8 mM), magnesium sulfate heptahydrate (10 mM), sodium nitrate (23.5 mM), and sodium acetate (10 mM) (reagent grade, Fisher) in ultra-pure water and filter sterilized.[4,70] Except for sodium acetate, all reagents were reagent grade from Sigma (St. Louis, MO, USA). All were used without further purification. Modified Mian's minimal medium was employed since it is transparent, chemically well defined, and supports bacterial growth at a slower rate than nutrient-rich media. Importantly, the low-nutrient content of Mian's medium more closely mimics the low-nutrient content of contact-lens-care solutions. Bacteria were grown in a rotary shaker at 37 ºC and 250 rpm until the culture reached an optical density of OD_{650} = 0.15 corresponding to a late-exponential growth phase. The resulting culture was then diluted to the desired concentration of ~5×10^6 cfu/mL by diluting 6 mL of the culture into 210 mL of fresh modified Mian's minimal medium and used immediately for attachment assays. Bacterial concentrations were confirmed by viable cell counts.

In some experiments, *P. aeruginosa* was fluorescently labeled with Alexa Flour 546 carboxylic acid succinimidyl ester (Molecular Probes) as previously described, [71] but with slight modification. Briefly, a single colony of bacteria was inoculated into 5 mL of trypticase soy broth (TSB) and grown overnight (37 ºC, shaking 250 rpm). 100 μL of that culture was then used to inoculate 10 mL of fresh TSB. The culture was then grown for 4.5 h (37 ºC, shaking 250 rpm), washed by centrifuging at 2000 rcf (2000 x *g*) for 10 min, and recovered and re-suspended in sterile PBS (10 mL, pH 7.4, Sigma, lab grade). The wash step was repeated twice. Alexa Flour 546 carboxylic acid succinimidyl ester was added, and the culture was incubated for 1 h in the dark with gentle shaking. Unreacted dye was removed by washing as described above. The labeled bacteria were then suspended in 1 mL of Mian's minimal medium.

2.3.2 Parallel-Plate Flow Chamber

As illustrated in Figure 2.1, bacteria interactions with a soft-contact-lens surface were studied in a transparent, parallel-plate laminar-flow chamber designed to rest on a phase-contrast microscope. The flow chamber provided fully-developed laminar flow across the soft contact lens. Bacteria were thereby introduced to the lens surface at a constant and known surface-shear rate. The chamber frame was constructed of G10 fiber-glass epoxy resin. A standard 3 x 1-inch glass microscope slide (Fisher Scientific) served as the chamber top while the bottom was a 60 x 24 mm cover glass slip (Fisher Scientific). The soft contact lens was mounted to the cover glass 35 mm downstream of the chamber entrance and was held in place with a 60 x 24 mm, 0.25 mm thick G10 fiber-glass epoxy resin sheet with a 5-mm diameter aperture allowing for lens exposure to the flow stream.

New cover glass and microscope slides were used for each experiment. Flow entered and exited the flow cell via 0.125-cm diameter ports. A 2-mm baffle near the flow-chamber entrance evenly distributed the flow into a parabolic profile. One-dimensional parabolic flow at the location of the soft contact lens was confirmed with Multiphysics simulations (COMSOL) as shown in Appendix C.

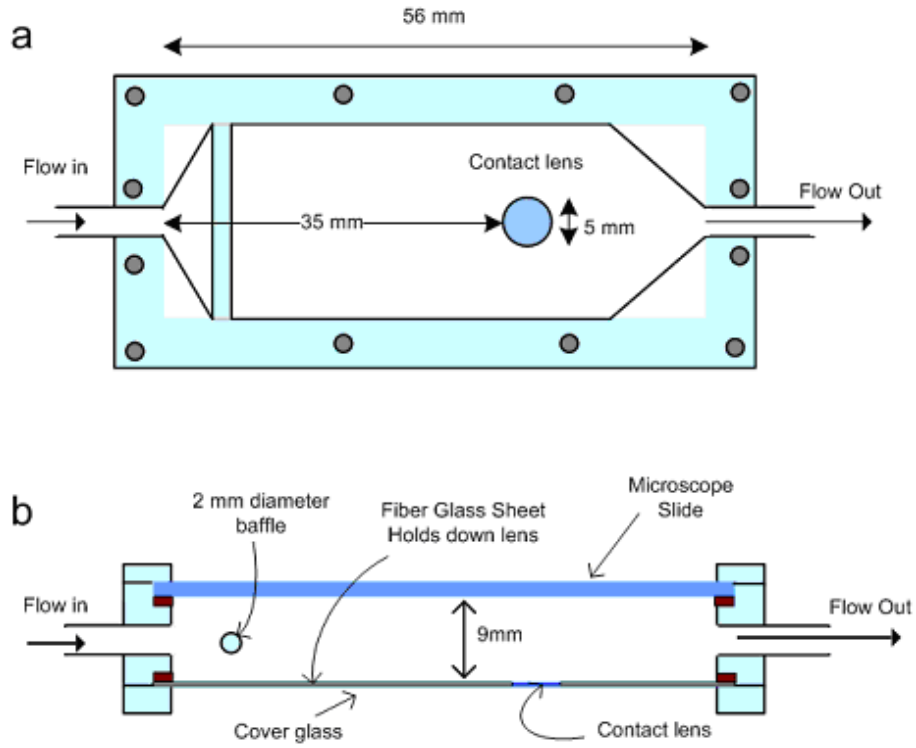


Figure 2.1 Plan a) and side b) views of the parallel-plate flow chamber for bacterial adhesion assays. A baffle at the entrance of the flow chamber more uniformly distributes the bacteria.

For each surface assay, a new O_2Optix™ (Balafilcon A, CIBA Vision, Duluth, GA) silicone-hydrogel lens was soaked in sterile phosphate buffered saline (PBS), pH 7.4 (Sigma) for two days to remove blister-pack impurities. O_2Optix™ lenses were chosen for their relatively uniform plasma surface coating [72,73] as verified by atomic force microscopy in Figure 2.2. Figure 2.2a shows the topography of an O_2Optix lens varies only in a range of 0-35 nm. Figure 2.2b shows the phase of the O_2Optix lens is relatively uniform as well with only a range of 0-20 °. Lens quarters were soaked in PBS for 2 days and then dried overnight prior to being mounted to a 1-cm^2 silicon wafer.

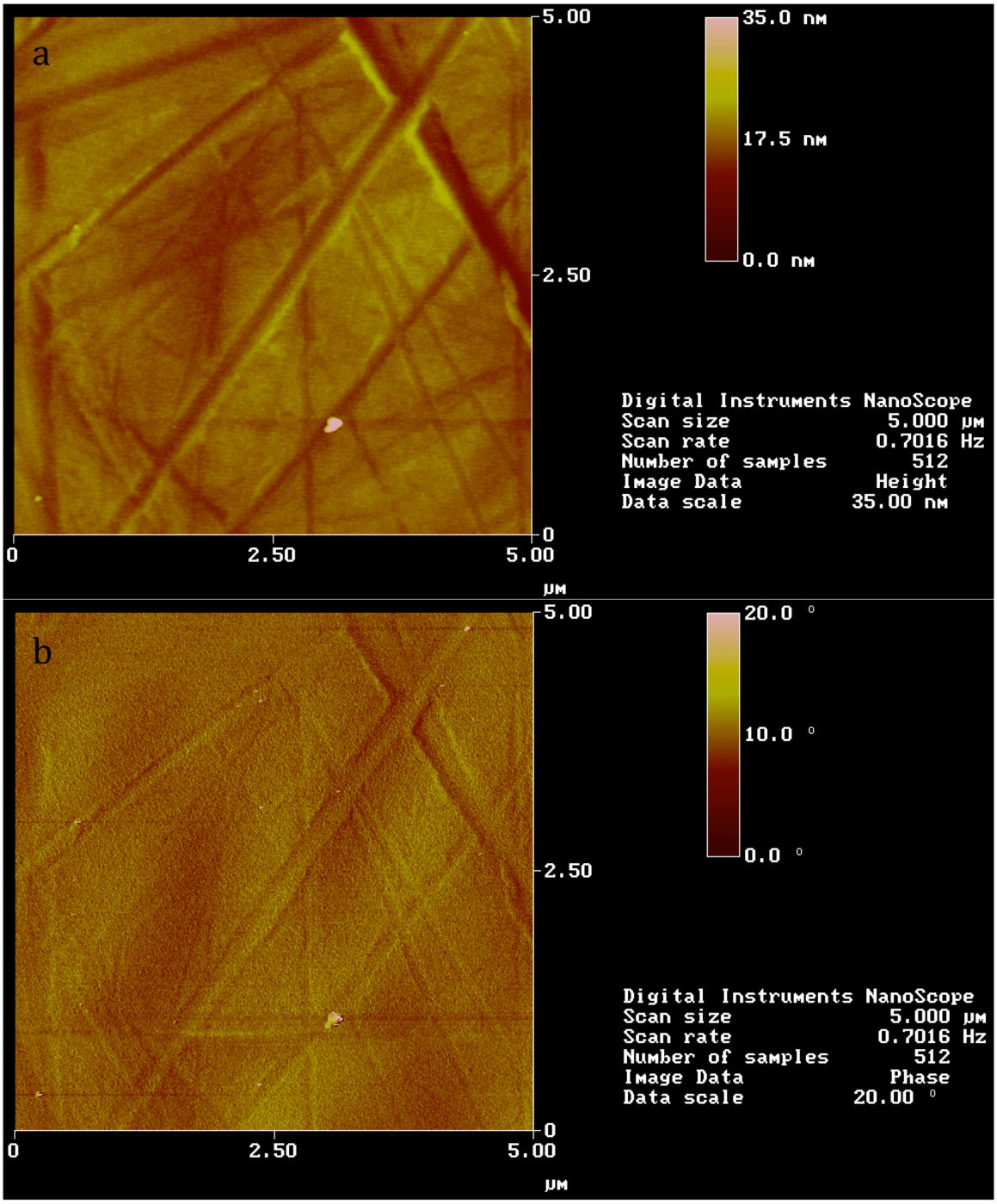


Figure 2.2 Atomic force microscopy pictures of an O_2Optix lens surface a.) the topography b.) the phase

A 10-mm diameter circular section was cut from the lens using a corer and was mounted in the flow chamber such that the bacterial suspension flowed past the lens's posterior side. The posterior side of the lens was chosen for examination since under contact-lens wear, it is the side in closest contact with the cornea. Before surface assay with phase-contrast microscopy, the flow cell was primed with modified Mian's minimal

medium while the pump (Pharmacia LKB-Pump P-500*)* and all lines entering the flow cell were primed with the freshly prepared bacterial suspension. During bacterial deposition, a flow rate of 210 mL/hr was set corresponding to a surface shear rate of 0.2 s^{-1}. This low shear rate was chosen to provide a well-defined and reproducible mass-transfer rate to the lens surface. In addition, entrained, non-adherent bacteria drifted past the contact lens. As described below, these bacteria were counted as part of those associated with the surface. Each attachment assay lasted 1-2 h. There was no detectable bacterial growth during that time frame.

For bacteria labeled with Alexa Flour 546 carboxylic acid, 20 μL of fluorescently labeled bacteria suspension were added to an Attofluor cell chamber (Molecular Probes) containing a mounted 25-mm diameter glass cover slip and 980 μL of fresh Mian's medium and viewed under fluorescence microscopy.

2.3.3 Microscopy

In each experiment, *P. aeruginosa* adhesion was visualized by time-lapse or real-time video-phase-contrast microscopy (Olympus IX70). To assess the rate of bacterial surface association, a 40X objective was focused through the contact lens onto its posterior side (Total magnification: 400X). Images were captured with a black-and-white camera (Hammatsu ORCA ER CCD), and subsequently magnified and displayed digitally on a computer screen. Images were captured every 20 s with Volociy 4.0 imaging software. The number of bacteria associated with the surface of the lens in each captured image was quantified with Image J software (NIH). Bacteria were considered associated if they were within focus with the contact surface. Thus, all bacteria located within about 4 μm from the surface, the depth of focus of the microscope, were counted. Sequential video frames were analyzed for the number of bacteria associated with the surface over a 1-2 h period. The rate of bacterial association with the contact-lens surface was scaled a 1-mm^2 viewing area. As determined by viable cell counting, each bacterial suspension had a somewhat different concentration. Hence, the rate of surface association was also scaled linearly to the nominal bulk bacterial concentration of 5 x 10^6 cfu/mL.

For experiments studying attachment phenotypes, phase-contrast microscopy with 600X magnification was used. An analog camera captured bacterial behavior at the contact-lens surface in real time. Eye TV™ (elgato) converted the analog signal to digital for compression in QuickTime video. 1 h after bacteria were detected at the contact-lens surface, a 1-min interval of video was reviewed and examined for distinct phenotypes. For fluorescence microscopy experiments, the bacteria were viewed through a rhodamine filter at 600X or 1000X total magnification. Images were captured with a black-and-white Hammatsu ORCA ER CCD camera using Volociy 4.0 imaging software at a minimum of 9 frames/s. They were subsequently magnified and displayed digitally on a computer screen.

2.3.4 Statistics

All rate and phenotype distribution data are reported as mean +/- the standard deviation. Experiments were repeated at least three times. Student's t-Test was used to determine the statistical significance of differences between two groups with $p < 0.05$ considered significant.

2.4 Results

2.4.1 Swimming Motility and Association Kinetics

Figure 2.3a shows the number of bacteria per unit surface area associated with the contact lens as a function of time for PAK and its structural and functional flagella mutants: PAK*ΔfliC* and PAK*ΔmotAB*. PAK*ΔfliC* has no flagellum. To investigate the role of operative versus non-operative flagella in surface association, PAK*ΔmotAB* was also studied. This mutant has a flagellum, but lacks a functional motor apparatus and, thus, cannot swim.[67] Uptake data for PAK*ΔfliC* and PAK*ΔmotAB* are indistinguishable in Figure 2.3a. Dark-vertical arrows denote the first arrival of bacteria to the contact-lens surface. Wild-type PAK exhibited a short lag of ~2-5 min before bacteria were observed at the surface. Swimming-deficient mutants, PAK*ΔfliC* and PAK*ΔmotAB*, however, exhibit a much longer lag of ~30 min. After arrival, all strains accumulated linearly in time at the surface. The slope of the kinetic uptake curve gave the rate of association with the surface that, in all cases, was constant over the time range studied. As summarized in Figure 2.3b, different strains clearly exhibited much different rates of association. Surface uptake rate for PAK*ΔmotAB* (filled triangles) was nearly the same as that for PAK*ΔfliC* (filled cirles). Wild-type PAK, however, associated with the SCL surface ~30-40 times faster than its non-swimming capable mutants. Separate uptake experiments with another *P. aeruginosa* strain (PAO1) similarly demonstrated a linear increase in time and 30-40 times faster association of motile bacteria than non-swimming capable mutants (data not shown). It is concluded that the drastically lower association rates observed in Figure 2.3 for the flagella mutants reflect an inability to swim rather than increased attachment via the flagellum in the wild-type strain.

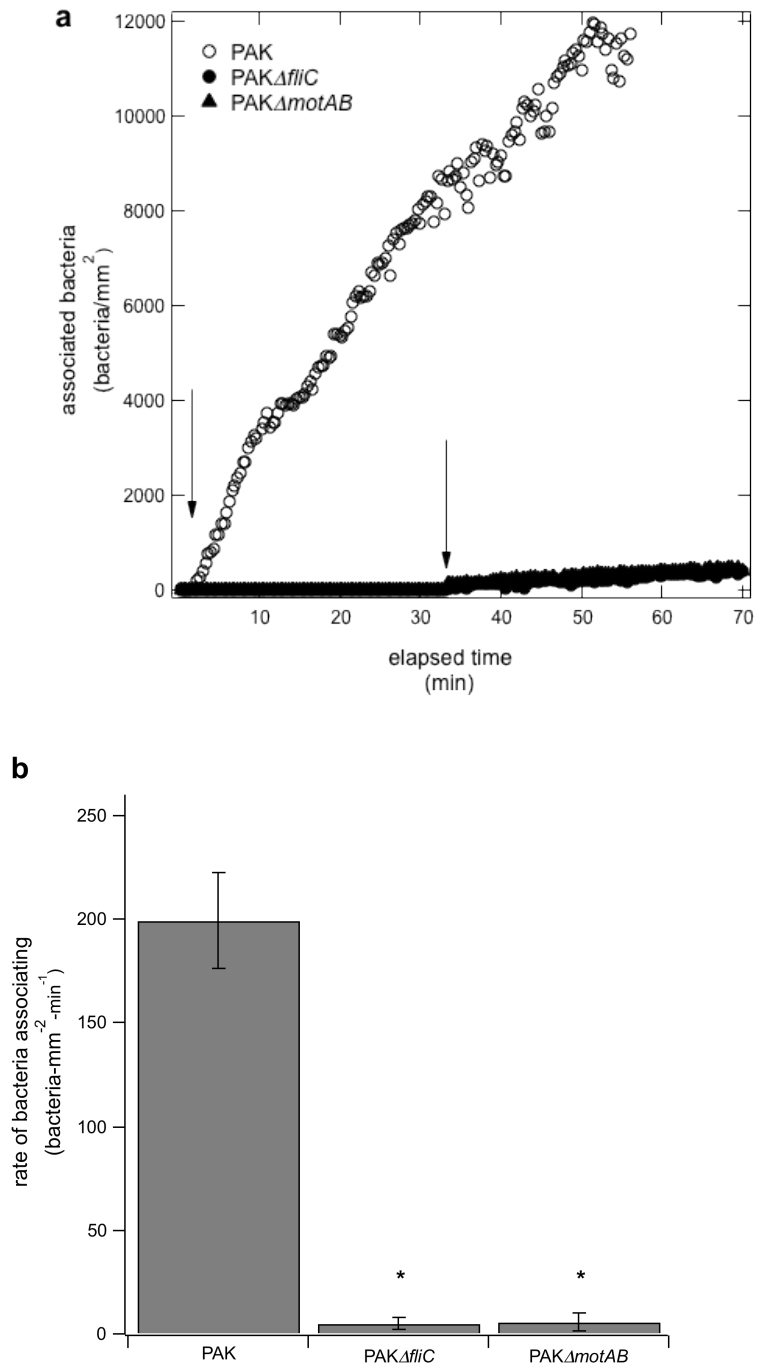


Figure 2.3 a) Number per unit of PAK (open circles), PAK*ΔfliC* (filled circles), and PAKΔ*motAB* (filled triangles) bacteria associated with the contact-lens surface as a function time. Data for PAK*ΔmotAB* (filled triangles) are hidden by those for PAK*ΔfliC* (filled circles). Arrows indicate the arrival time of the bacteria to the lens. b) Rates of surface association from slopes of the linear regression in (a). The superscript * indicates that the p-value is less than 0.05 compared to wild-type.

As shown in Figure 2.4 for over a 100-fold range of concentration (2 x 10^5 to 2 x 10^7 cfu/mL), PAK obeys a linear increase of association rate with increasing concentration. If Γ denotes the number of bacteria associated with the surface per unit area. Then the uptake-rate observations mean that:

$$\frac{d\Gamma}{dt} = kC \tag{2-1}$$

where t is time, C is the bulk concentration of bacteria, and k is a first-order rate constant. Since k and C are constant, integration of Eqn 2-1 explains the straight-line increase in transient uptake seen in Figure 2.3a for wt PAK and its motility mutants. Also explained is the observed linear increase in rate with bacterial concentration. Equation 1 holds only for dilute bacterial suspensions at early times where surface coverage is minimal. For a bacterial mean size of ~1 μm, only 2-4 % of the contact-lens surface was covered by wild-type PAK after 1 h. These results suggest that the bacteria arrived and associated with the surface uninfluenced by the presence of other bacteria. Further, if a significant number of bacteria initially adhered to the surface and then detached, association rates in Figure 2-3a must decline in time; equation 1 is no longer valid. Since this is not the case, it can be concluded that detachment is minimal. Consequently, bacterial detachment rates are slow at the low surface coverages studied. Further, washout of wild-type PAK by Mian's medium (containing no bacteria) after 1 h of loading demonstrates little decline in surface coverage (Appendix D). This conclusion holds for the imposed 0.2 s^{-1} shear rate. It has not been ascertained whether adhered bacteria detach under the higher shear rates of 1000 s^{-1} typical of on-eye contact-lens motion, or if they detach due to phenotype changes after longer times.

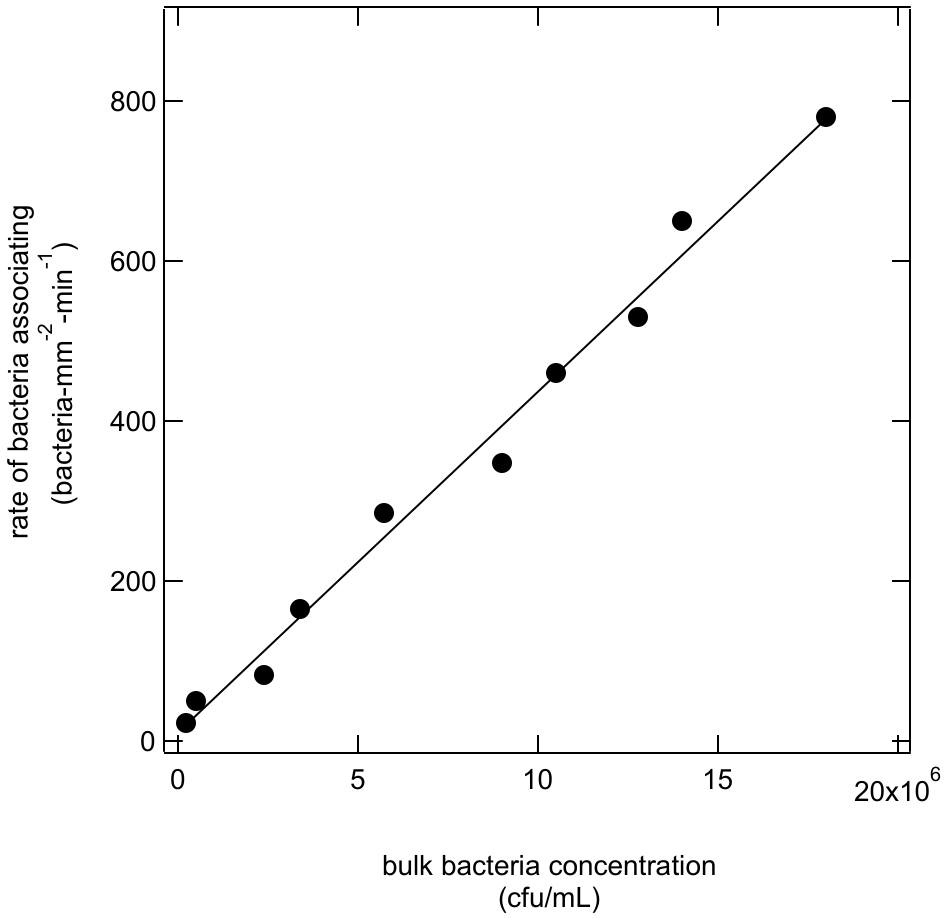


Figure 2.4 Rates of wild-type PAK bacteria associating with contact-lens surface as a function of bulk bacteria solution concentration.

2.4.2 Pili and Association Kinetics

Pili are often implicated as a mediator for bacterial attachment.[33,37-39] Consequently, if pili are removed, a smaller rate of surface association is anticipated. A pilin mutant, PAK*ΔpilA*, was studied to determine the possible influence in attachment rate when pili are lacking. Association kinetics to the soft contact lens for PAK*ΔpilA* and wild-type PAK are compared in Figure 2.5. No significant difference in the rate of bacterial association with the contact-lens surface was seen.

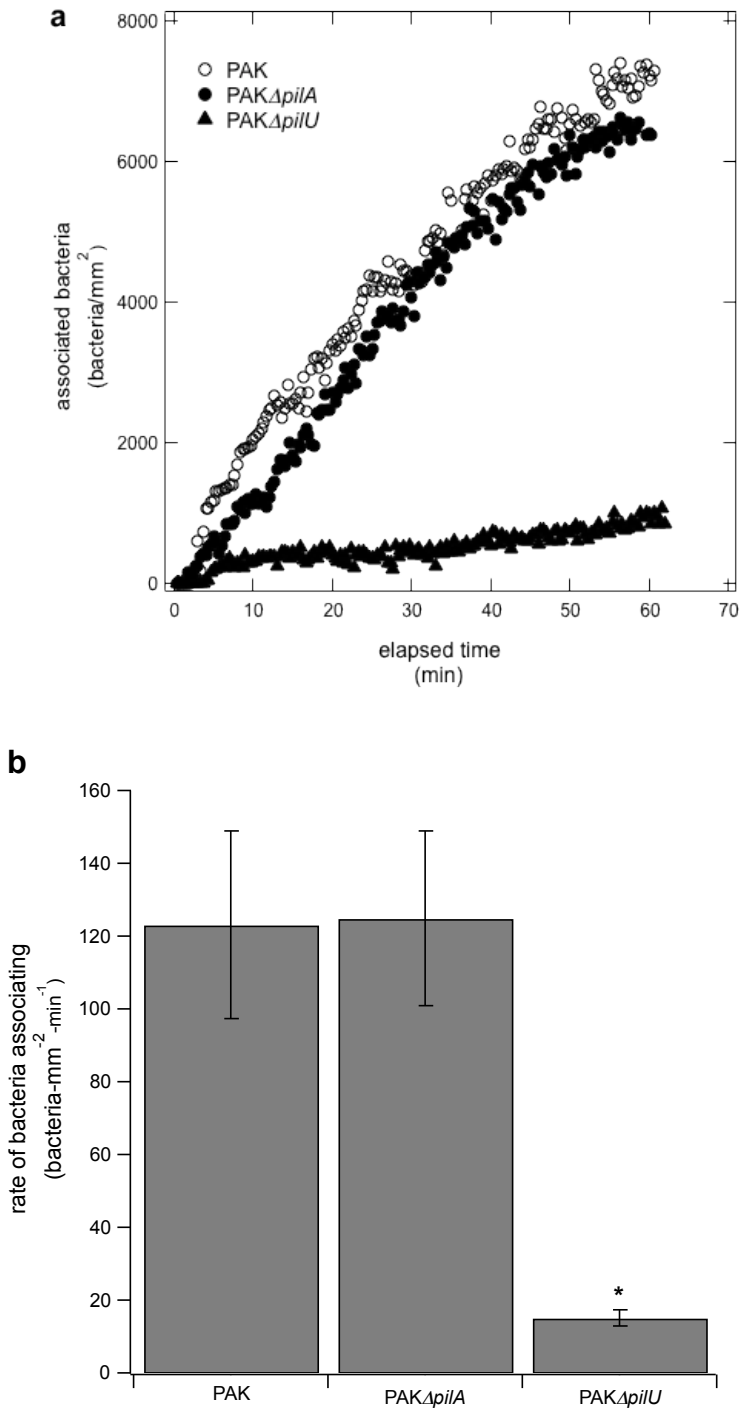


Figure 2.5 a.) Number per unit area of PAK (open circles) bacteria and its pili mutants, PAK*ΔpilA* (filled circles) and PAK*ΔpilU* (filled triangles), associated with the contact-lens surface as a function of time. b) Corresponding rates of surface association from slopes of the linear regression in (a). The superscript * indicates that the p-value is less than 0.05 compared to wild-type.

PAK*ΔpilU* was also studied. It has pili but lacks the ability to retract them and, thus, cannot participate in surface-associated twitching motility. The rate of association of PAK*ΔpilU* in Figure 2.5 was only 25% that of the wild-type PAK or the pilin-deficient PAK*ΔpilA*. The three bacteria in Figure 2.5 are capable of swimming; they all reached the contact-lens surface within minutes from the start of the experiment. Thus, lower association rates for PAK*ΔpilU* were not due to slower surface-arrival rates, but rather to an adsorption barrier to binding.

2.4.3 Association Phenotypes

Video-phase-contrast microscopy was used to observe the behavior of individual wild-type PAK associating with the contact-lens surface. Figure 2.6 pictures the 5 different attachment phenotypes expressed by the PAK population. One group appeared to be "tethered" to the lens surface (Figure 2.6a); these bacteria rotated randomly about a fixed point, as documented in Figure 2.7a. The rotation phenotype is similar to that documented by Toutain et al. [66] Another fraction of bacteria remained fixed at the contact-lens surface and did not exhibit observable movement (Figure 2.6b). Some bacteria appeared attached to the lens surface, but moved slowly along, even against the flow of fluid (Figure 2.6c), as confirmed in Figure 2.7b. Some bacteria approached the surface, but did not stop and attach over the 1-min observation period (Figure 2.6d). These non-attached bacteria either drifted with the flow stream for swimming-deficient mutants, or swam randomly near the surface, including against the flow, for swimming bacteria. Non-attached bacteria were still considered surface associated because they were close enough to the lens surface to be interacting with it. Finally, small numbers from each of these classes detached and left the surface (Figure 2.6e). Some of the phenotype classifications in Figure 2.6 bears resemblance to that of Singh et al.[74] and who designated fixed, stationary bacteria as squatters, lateral movement as ramblers, and detaching as flyers.

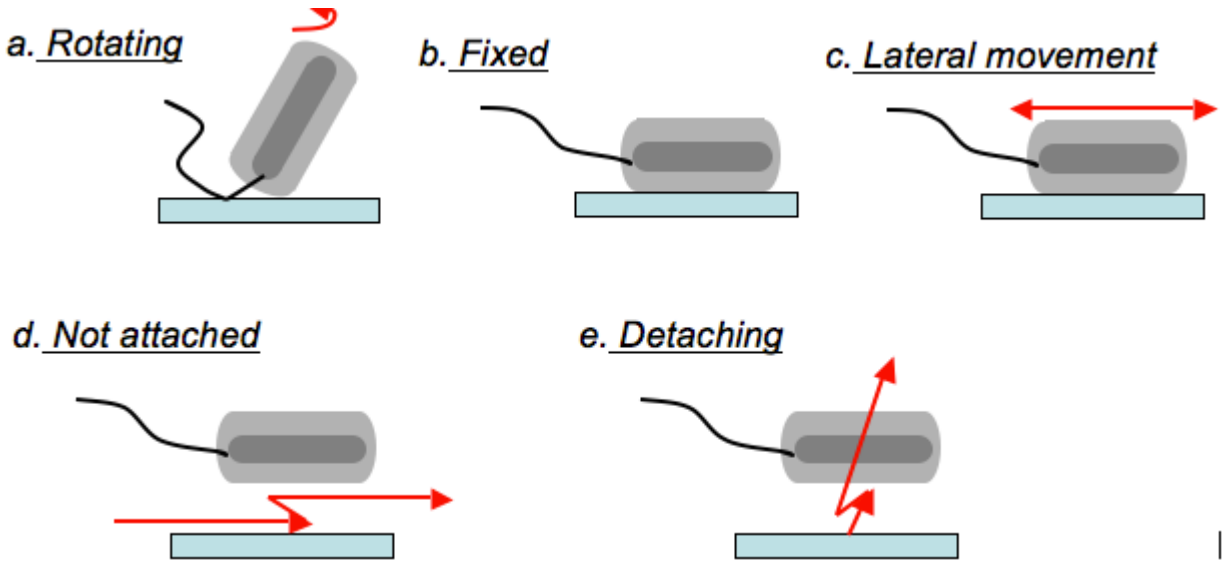


Figure 2.6 Schematic of five surface-association phenotypes. Dark gray corresponds to bacterial body. Light gray represent bacterial pilin. Phenotypes a-c adhered to the surface. Phenotype d did not. As discussed in the text, phenotypes a and d each exhibited two subclasses.

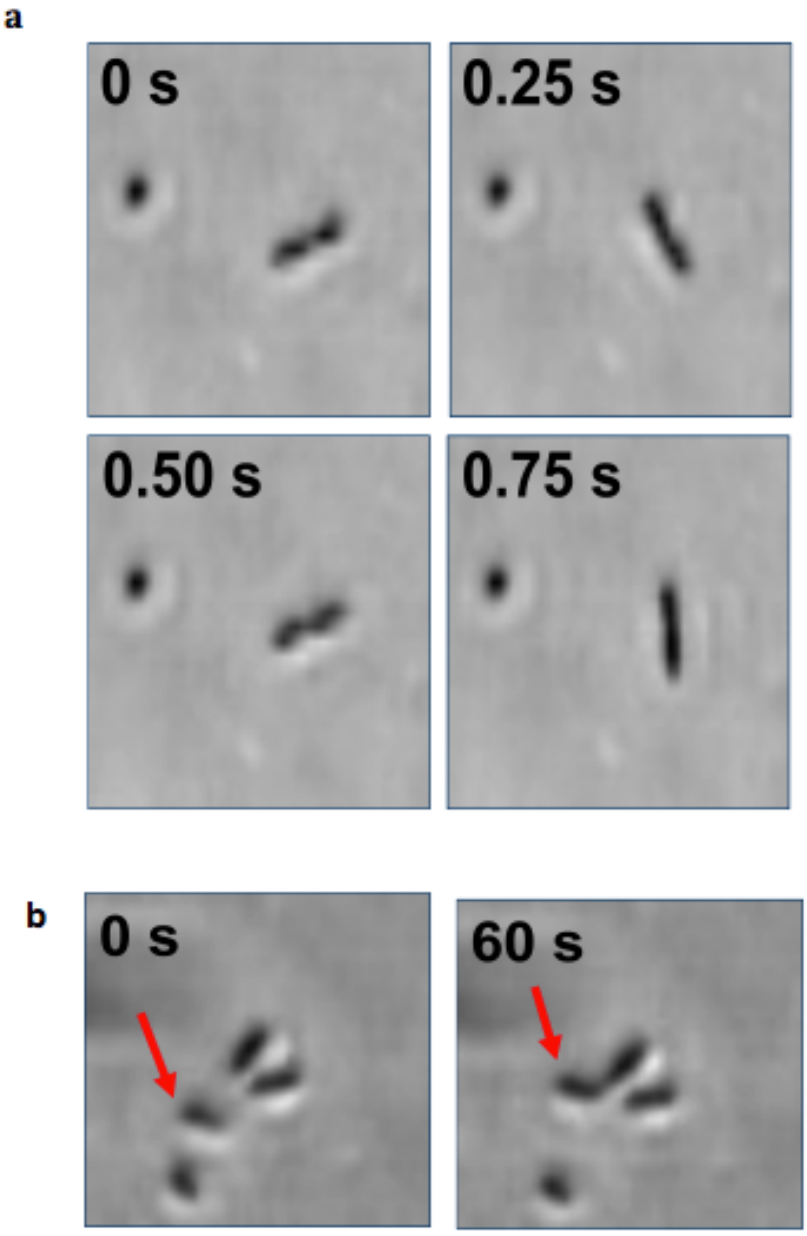


Figure 2.7 Time-lapse phase-contrast images of bacteria: a) rotating, b) moving laterally (twitching). Rotating bacteria appear tethered to the contact lens by a single point and spin around that point at least once in 60 s. Laterally moving bacteria move at least one bacterial body width while remaining at the contact-lens surface. Flow direction was from left to right

P. aeruginosa flagella can be directly viewed when the bacteria are labeled with Alexa Flour 546 carboxylic acid. Wild-type PAK bacteria were seen attaching to a glass cover-slip surface, and at times rotating while attached to the surface, similar to that seen by phase-contrast microscopy of the bacteria attached to the soft contact lens. Figures 2.8 a-d and e-h reveal that the rotational phenotype displayed at least two distinct subpopulations. Figure 2.8 a-d shows that the wild-type bacteria adhered to the glass

surface *via* their flagella, and rotated their body while their flagella remained fixed. Additionally, bacteria attached to the glass cover-slip and rotated both body and flagellum in concert, as shown in Figure 2.8 e-h. Here, the attachment point was on the body since the flagellum rotated in tandem.

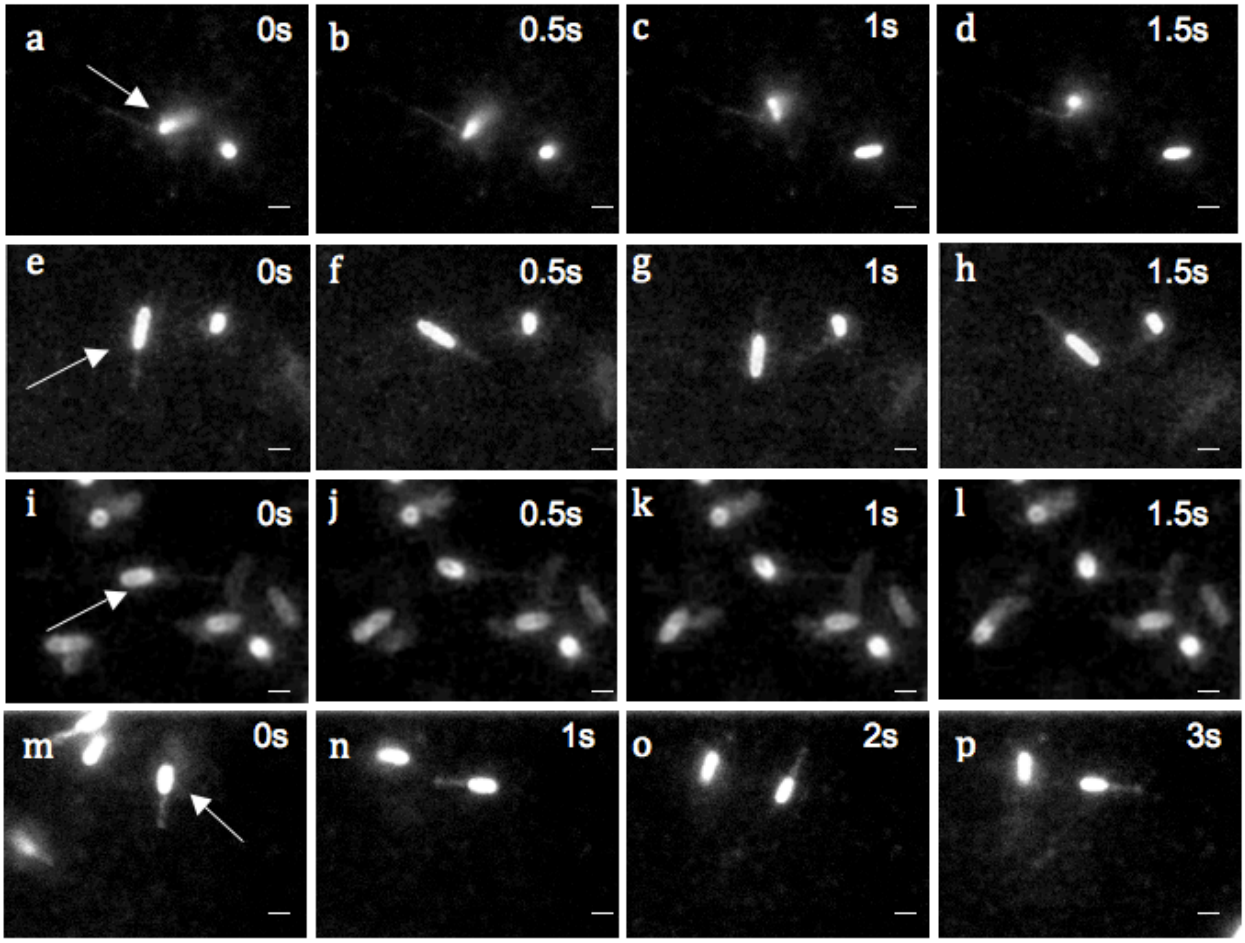


Figure 2.8 Fluorescence microscopy: a-d) rotation of wild-type PAK body while attached to cover-slip by its fixed flagellum; e-h) PAK attached to a cover-slip at a point with both body and flagellum rotating together; i-l) PAK*ΔpilA* attached to cover-slip by its flagellum; and m-p) PAK*ΔpilA* attached to cover slip at a point on its body with both body and flagellum rotating together. The scale bar represents 1 μm.

To determine whether bacteria rotate when not attached by pili, PAK*ΔpilA* was fluorescently labeled. Figure 2.8 i-l shows a pilin mutant attached to the cover-slip surface by its flagellum with the body rotating, similar to wild-type PAK in Figure 2.8 a-d. Similar to wild-type PAK in Figure 2.8 e-h, PAK*ΔpilA* mutant in Figure 2.8 m-p also bound to the glass surface and rotated its body and flagellum in tandem. Thus, PAK*ΔpilA* bound to the surface and exhibited a rotational phenotype while attached to a point on its body, even though the bacterium has no pili.

2.4.4 Distribution of Association Phenotypes

Video microscopy allowed not only observation of the 5 association phenotypes but also the fraction of bacteria expressing each phenotype. Figure 2.9 illustrates results for wild-type PAK and its swimming-motility mutants, PAK*ΔfliC* and PAK*ΔmotAB*. For wild-type PAK, over 95 % of the individual bacteria associated with the contact-lens surface were adhered. Most of these were fixed and remained stationary. A small fraction of the adhered bacteria rotated; a more substantial portion moved laterally (i.e., twitched). Less than 5 % of surface-associated bacteria detached over the 1-min observation period. A small but measureable fraction of wild-type bacteria did not attach at all and appeared to swim randomly along the contact-lens surface. The linear uptake kinetics in Figure 2.3a and the distribution of surface phenotypes in Figure 2.9 are in concert: wild-type PAK binds to the surface at this time-point with minimal desorption.

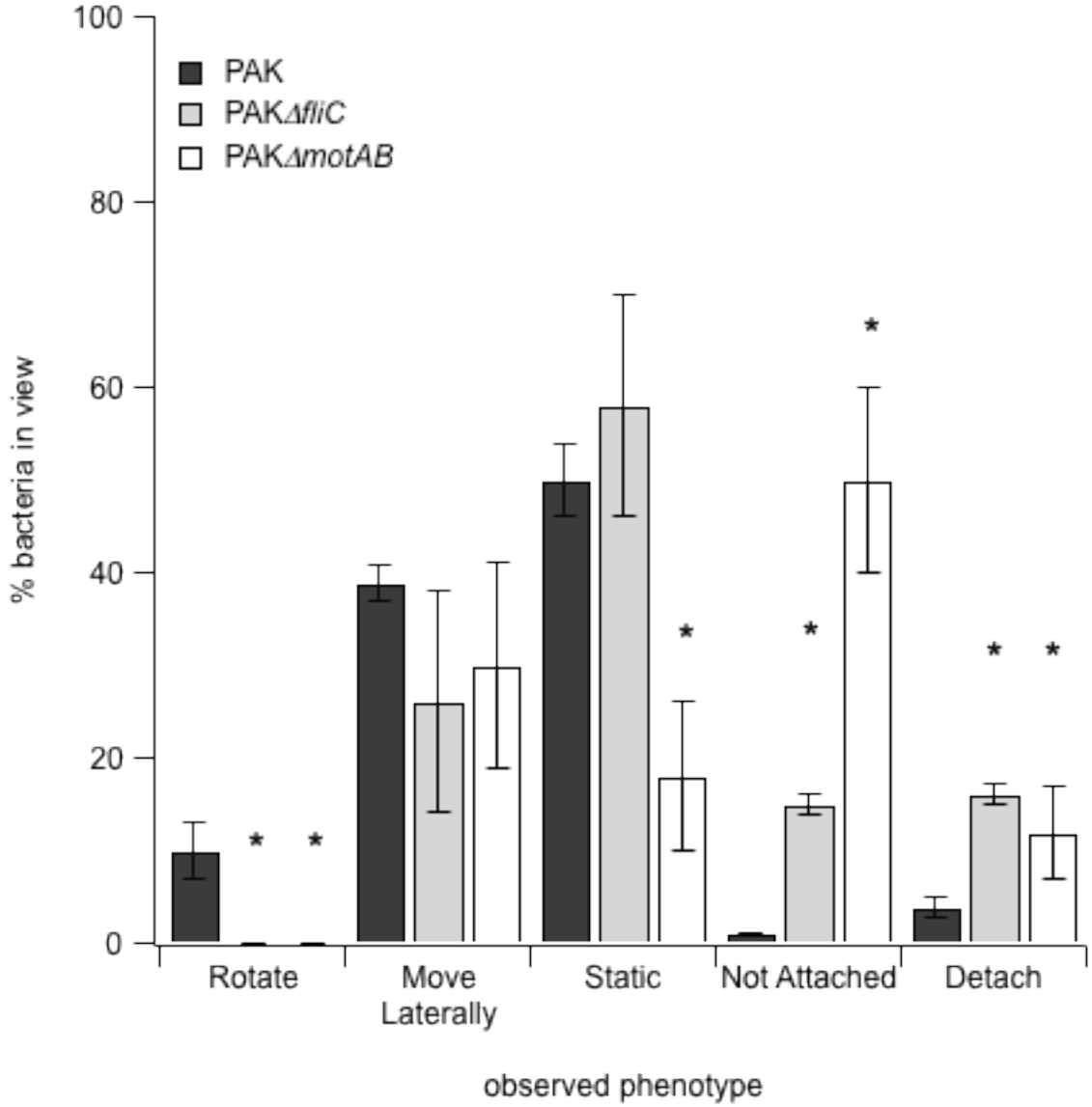


Figure 2.9 Distribution of surface-association phenotypes for wild-type PAK and its swimming-motility mutants. Typical error bars are shown. The superscript * indicates that the p-value is less than 0.05 compared to wild-type.

For the flagellum mutant, *ΔfliC*, no bacteria were observed to rotate on the lens surface. Similar findings were seen for the *ΔmotAB* mutant. Loss in swimming motility removed the rotational phenotype. Consequently, surface rotation demands an active flagellum. Notably, PAK*ΔmotAB* showed a significant fraction of entrained bacteria associating with, but not binding to, the contact-lens surface.

Figure 2.10 presents analogous results for phenotype distributions of wild-type PAK and its pili mutants, PAK*ΔpilA* and PAK*ΔpilU*. As expected, the lack of pili on PAK*ΔpilA* and

the lack of pili retraction on PAK*ΔpilU* completely eliminated lateral movement. Upon loss of twitching motility, the fraction of rotating bacteria increased ~3-fold compared to the wild-type bacteria with the remaining phenotype populations remaining about the same. In all cases, the fraction of pili mutants not attached or detaching was small.

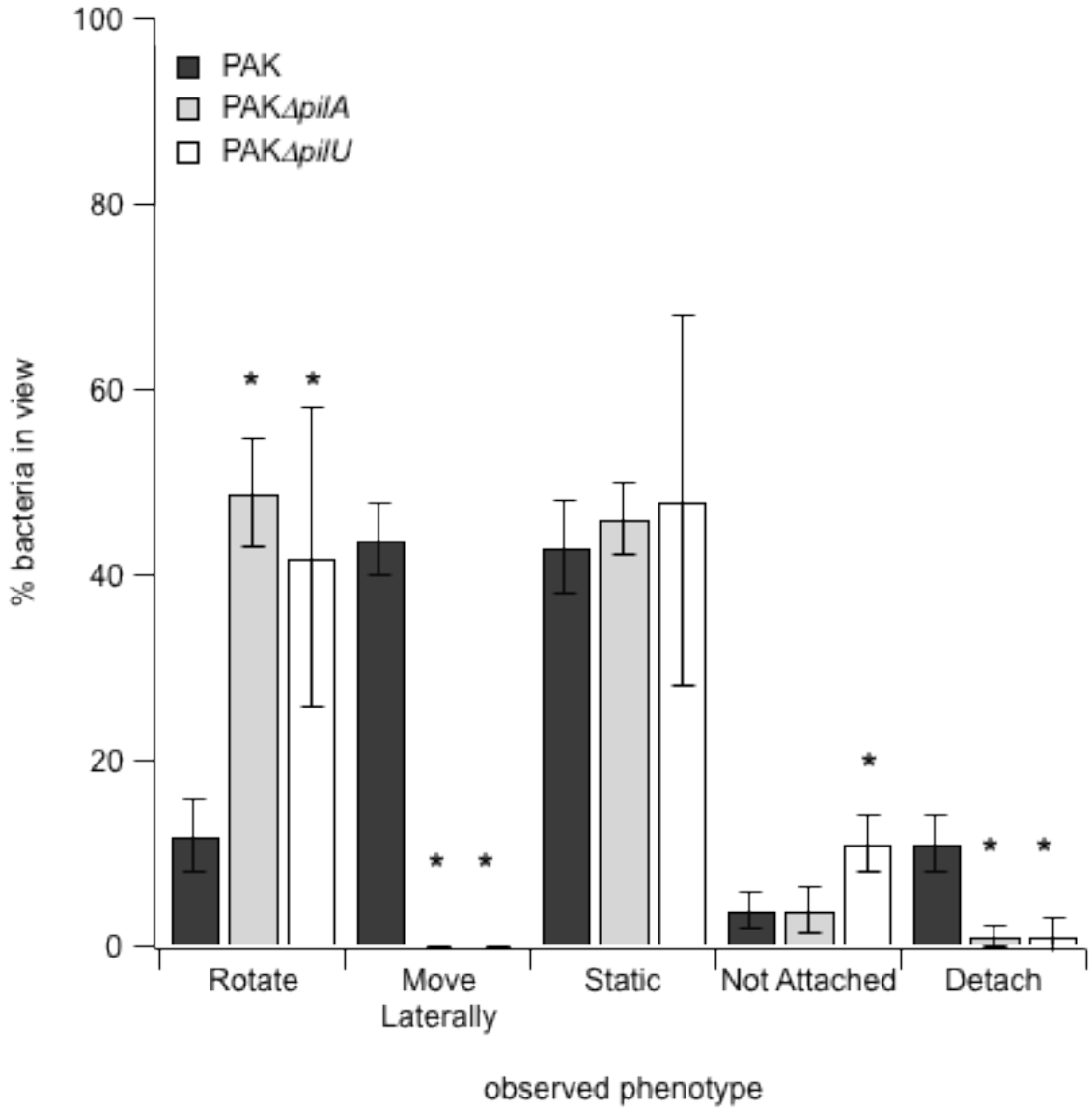


Figure 2.10 Distributions of surface-association phenotypes for wild-type PAK and its pili mutants. Typical error bars are shown. The superscript * indicates that the p-value is less than 0.05 compared to wild-type.

2.5 Discussion

The data show that wild-type *Pseudomonas aeruginosa* strain PAK, and each of its-structural and functional flagellum and pilus mutants, initially associate with a soft-contact lens surface by linear uptake kinetics, as seen in Figures 2.3a and 2.5a. Linear uptake kinetics indicates a constant rate of bacterial accumulation at the surface. Rates of surface association also increased linearly with bacterial concentration revealing that bacteria arrive and interact with the surface individually. Although constant arrival rates were found for all bacteria in this study, Figures 2.3b and 2.5b reveal that non-swimming mutants accumulated at a ~30 – 40 times slower rate. In the laminar flow chamber, bacteria in dilute suspension reached the focal depth of the contact-lens surface by convective diffusion from an axial, parabolic velocity field to a sparsely covered surface. These conditions suggest arrival to the surface according to Lèvêque theory.[75-77] In this situation, the ratio of association rates scales by the ratio of bacteria diffusion coefficients each raised to the 2/3 power (i.e., $D^{2/3}$). Several studies have shown that *P. aeruginosa* swimming motility is correctly modeled as a random walk with an effective diffusion coefficient on the order of $\sim 10^{-6}$ cm^2/s [11,78]. To estimate the effective diffusion coefficient of the non-swimming PAK mutants, Stokes-Einstein theory of Brownian motion is adopted: $D=k_bT/6\pi\mu r$, where k_b is Boltzmann's constant, T is absolute temperature, μ is the solution viscosity, and $r=a/ln(2a/b)$ with a the half the length of the bacterium (0.5 μm) and b the half the width of the bacterium (0.25 μm).[9,11] It is thus estimated that the diffusion coefficient of the non-swimming bacteria as 6×10^{-9} cm^2/s. When these values are adopted in Lèvêque theory, the ratio of arrival rates at the surface for the swimming strains to the non-swimming strains is about 30, in good agreement with the experimental data. This result indicates that PAK association with the SCL surface is governed by convective diffusion.

The significantly smaller diffusion coefficient of the non-active flagella mutants also explains why they do not first appear at the contact-lens surface until about ½ h after the motile strains first appear. This is an important finding since the rate of bacterial uptake to a surface, such as in Figures 2.3a and 2.5a, cannot be correlated with ability to adhere to the surface. Although PAK*ΔfliC* arrived at the surface much slower than did wild-type PAK, Figure 2.9 reveals that the fraction of bacteria bound to the surface after 1 h is similar for both PAK wt and PAK *ΔfliC*. The non-motile bacteria simply required more time to reach the same surface coverage as the motile wild-type.

Since bacterial approach rates to a surface are influenced by convective diffusion, different apparatus assess different uptake kinetics and mechanisms. Thus, bacteria uptake to a surface studied in a stagnant cell is slower than that studied in a flow cell. Using a microtitre- plate assay under an observation time frame of hours, O'Toole and Kolter found that flagella are required for biofilm formation.[32] However, Klausen et al. [40] using a flow cell under a time frame of days refute that finding. To distinguish phenotype binding mechanisms and strengths, surface adhesion studies must account quantitatively for the role of solution transport.

Figure 2.5a demonstrates that pili are not required for binding since PAK*ΔpilA* accumulated at the same rate as wild-type PAK. PAK*ΔpilU* also can swim, and, hence, should arrive to the surface at the same rate as did the *pilA* mutant. However, it is found here along with others [34,37,79,80] that surface association is small for hyperpiliated mutants

of *P. aeruginosa*. Comolli et al.[37] proposed that twitching motility is required for binding and that PAK*ΔpilU's* lack of pili retraction precludes twitching, and, thus, prevents binding. Since pili were not required here for initial adhesion to a SCL, it is hypothesized, in agreement with Fletcher et al. [34], that hyperpiliation sterically hinders binding. Hyperpiliated bacteria are able to swim away and not accumulate at the contact-lens surface.

If the non-attached mutant had no flagellum or if the flagellum was disabled, then non-attached motion was entrainment in the flow stream. For the disabled mutant, PAK*ΔmotAB*, the fraction of entrained bacteria was almost 50 % indicating that despite being at the surface, many of the bacteria were unable to bind. It is also possible that like the hyperpiliated PAK*ΔpilU*, a paralyzed flagellum prevents adhesion by steric hindrance.

Within the attached class, bacteria may rotate, either about the body or about the flagellum (rotate); translate laterally along the surface by twitching (move laterally); attach stationary (fixed); and desorb (detach). Only bacteria with active flagella rotated on the surface. Rotation was either about a point on the body or on the flagellum. Rotation upon pili attachment was not observed. Rotation about the body does, however, signify point attachment rather than multiple attachment locations along the bacterial body. Attachment to the contact lens *via* lipopolysaccharides may be implicated.[22,38] Toutain et al. [66], however, suggest that rotation of *P. aeruginosa* is attributed to binding sites at the bacterium poles, rather than along the body.

The distribution of each phenotype in the surface-associated population differed significantly depending on mutant type. Still several general observations can be made for PAK bacteria attaching to the surface of the SCL. Arrival rate to the surface was governed by convective diffusion. Attachment occurred through the flagellum, the pili, or the body. When any single attachment site was eliminated or disabled, the others could be substituted to provide sticking. In all cases studied here, there were at least two attachment sites available to the bacteria

In all phenotypes, the percentage of fixed bacteria was a majority, typically over 50 %. Real-time observations occurred after 1 h of initial detection of bacteria at the lens surface. Presumably, the longer bacteria remain attached to the surface, the stronger they attach. If so, most all attached bacteria evolve towards complete irreversible attachment. Interestingly, Singh et al. [74] found that for attached PAO1 bacteria under growth conditions, nearly 50% of the bacteria were squatters (stationary bacteria) in good comparison with the results. Surprisingly, despite using the same assay as that of Singh et al., Kirisits et al. [81] found few stationary wild-type PAO1 bacteria. Initial binding of PAK under non-growth conditions was focused on rather than early biofilms. For all phenotypes studied in the experiments, the fraction of detachment was small. However, it is possible that phenotypic changes in the attached population over longer times could permit dispersal from the lens.[13]

For mutants without pili, but with an active flagellum (i.e. PAKΔ*pilA*), the fraction of surface-attached bacteria undergoing rotation increased significantly. For this class of mutant, it appeared that the fraction exhibiting twitching motility was replaced by rotation. Since non-piliated mutants can rotate about their bodies, surface attachment in this case was via an adhesive site other than pili.

Since PAK exhibits body-attachment sites other than pili, this suggests initial binding by the body, followed by pili-propelled motion along the surface. Such a mechanism has significant implications for biofilm formation. All else being equal, lateral motion at the surface of individual bacteria permits surface collisions and aggregation in support of the current biofilm-formation model [82]. However, if biofilm formation occurs primarily during growth at the surface, twitching motion hinders biofilm growth as progeny bacteria migrate away from the parent [74].

Assays performed in a well-defined flow field are necessary to understand bacterial adhesion to surfaces. Non-swimming mutants of *PAK* associated with the contact-lens surface at a much slower rate than that of the swimming strains. Thus, the ability to swim enhanced the arrival rate to the surface. Arrival rates, however, do not correlate with adherence effectiveness, as illustrated by the results for *PAK* wt and PAK*ΔfliC*. It was also found that direct visual observation and enumeration of surface-associating subpopulations were crucial for understanding mechanisms of binding. *P. aeruginosa* bound to the contact lens through three different adhesion sites. Prevention of *P. aeruginosa* attachment requires blockage of all three adhesive locations. Thus, development of antifouling agents cannot focus on overcoming only one of the binding sites. Examination of surface phenotypes seems requisite to understanding the behavior of possible antifoulants. Although the findings only apply specifically to *P. aeruginosa* strain PAK and its interaction with the O_2Optix™ SCL (and glass) surfaces, it is likely that other strains of *P. aeruginosa*, and other bacterial species with multiple appendages, display similar surface phenotypes on other contact-lens surfaces.

Chapter 3: Dynamics of *Pseudomonas aeruginosa* association with anionic hydrogel surfaces in the presence of aqueous divalent-cation salts.

3.1 Abstract

Binding of bacteria to solid surfaces is complex with many aspects incompletely understood. *Pseudomonas aeruginosa* uptake kinetics onto hydrogel surfaces representative of soft contact lenses made of nonionic poly(2-hydroxyethylmethacrylate) (p-HEMA), anionic poly(methacrylic acid) (p-MAA) and poly(acrylic acid) (p-AA) were studied. Using a parallel-plate flow cell under phase-contrast microscopy, a kinetic "burst" at the anionic hydrogel surface is documented: dilute aqueous *P. aeruginosa* first rapidly accumulates and then rapidly depletes. Upon continuing flow, divalent cations in the suspending solution sorb into the hydrogel network causing the previously surface-accumulated bacteria to desorb. The number of bacteria eventually bound to the surface is low compared to the nonionic p-HEMA hydrogel. It is proposed that the kinetic burst is due to reversible divalent-cation bridging between the anionic bacteria and the negatively charged hydrogel surface. The number of surface bridging sites diminishes as divalent cations impregnate into and collapse the gel. *P. aeruginosa* association with the surface then falls. Low eventual binding of *P. aeruginosa* to the anionic hydrogel is ascribed to increased surface hydrophilicity compared to the counterpart nonionic p-HEMA hydrogel.

3.2 Introduction

Binding of the common bacterium, *Pseudomonas aeruginosa*, to solid substrates is important in bioremediation and biomedical devices [4,50,83-87]. Of special interest is the attachment of *P. aeruginosa* to soft-contact lenses because this bacterium can cause serious and difficult-to-treat infection.[85] In general, *P. aeruginosa* does not infect healthy individuals. The majority of time, infection occurs only for those with compromised immune systems.[47] Even though the human eye is particularly resistant to infection [88], *P. aeruginosa* can infect healthy contact-lens wearers.[3,50] Recent studies also demonstrate that *P. aeruginosa* bound to soft-contact lenses can initiate infection.[4] Thus, a promising method for alleviating infection is to prevent binding to soft-contact-lens surfaces.

P. aeruginosa attachment to substrates is complex because the bacterium possesses a number of different binding mechanisms arising from a variety of appendages.[89] For example, wild-type *P. aeruginosa* have a propelling flagellum that enhances attachment rates to surfaces. Additionally, pili, another appendage of *P. aeruginosa,* allow both specific and non-specific binding to surfaces [41,90-92] (Nonspecific binding includes hydrophobic and double-layer electrostatic interactions.[20] Proteins, lipopolysacharides, and exopolysacharides expressed on the surface of the bacterium further modulate both specific and nonspecific binding to surfaces.[93-95]

Soft-contact lenses are transparent hydrogels designed to ride closely and comfortably on the cornea.[96] Traditionally, they are composed of poly(2-hydroxyethyl methacrylate) (p-HEMA) sometimes copolymerized with polyeletrolytes, such as poly(methacrylic acid) (p-MAA) or poly(acrylic acid) (p-AA), to enhance water content and wearability.[97-99] Copolymerization with varying amounts of MAA/AA creates a cross-linked anionic hydrogel with differing properties including matrix charge, mesh size, elastic modulus, ion and solute uptake, and surface wettability.[98,100,101] Possible roles of p-MAA/p-AA in the binding of *P. aeruginosa* to p-HEMA hydrogels are unknown. Further, incorporation of MAA/AA into hydrogels provides a direct means to investigate the specific role of matrix charge in bacterial binding.

P. aeruginosa interaction with the surfaces of traditional p-HEMA-based soft-contact-lens materials and how these interactions change upon co-polymerization with polycarboxylic acids was investigated, MAA and AA, to produce anionic-charged hydrogels. Because the bacterial growth medium contains magnesium sulfate, the importance of calcium and magnesium cations in bacterial attachment was also investigated.

3.3 Experiment

3.3.1 Materials

2-hydroxyethylmethacrylate (HEMA, 97%), ethylene glycol dimethacrylate (EGDMA, 98%), methacrylic acid (MAA, 99%), acrylic acid (AA, 99%), 0.01M phosphate-buffered saline (PBS, (0.138-M NaCl) molecular biology grade), SigmaCote™, ethylene diamine tetra-acetic acid terasodium salt dihydrate (EDTA, 99%), potassium chloride , sodium phosphate monobasic monohydrate, potassium phosphate anhydrous, magnesium sulfate heptahydrate , and sodium nitrate (reagent grade) were purchased from Sigma-Aldrich (St. Louis, MO) and used as received. 2,4,6-Trimethyl-benzoyl-diphenyl-phosphineoxide (Daracure TPO) was kindly supplied by CIBA Specialty Chemicals (Tarrytown, NY).

Anhydrous ethanol, acetonitrile (99.9%), and sodium acetate (reagent grade) were purchased from Fisher Scientific. Distilled/deionized water was obtained via a Milli Q system (Millipore, Billerica, MA). Tryptic soy agar and MacConkey agar were purchased from Becton, Dickinson, and Company (Franklin Lakes, NJ).

3.3.2 Bacteria preparation

Bacteria preparation was the same as that in Chapter 2 for bacterial adhesion experiments. *Pseudomonas aeruginosa* strain PAK was kindly provided by Dr. Stephen Lory (Harvard Medical School).[102] Frozen stocks were recovered onto Tryptic Soy Agar plates grown at 37 °C for 14 h. Single colonies were inoculated into 12 mL of modified Mian's minimal medium (Mian's) [4,70] and grown while shaken at 250 rpm at 37 °C until the optical density reached 0.15. Modified Mian's minimal medium consists of sodium phosphate monobasic monohydrate (7.5 mM), potassium phosphate anhydrous (16.8 mM), magnesium sulfate heptahydrate (10 mM), sodium nitrate (23.5 mM), and sodium acetate (10 mM) in ultrapure water and filter sterilized [4,70]. The pH of the Mian's medium is 7.4. Bacteria were then diluted into fresh modified Mian's medium to a concentration at $\sim 5 \times 10^6$ colony forming units per mL (cfu/mL). In some experiments, bacteria were centrifuged at 6000 rcf (6000 x g) for 10 min, and washed and resuspended in desired solutions of $\sim 5 \times 10^6$ cfu/mL. No detectable viability change was observed in the resuspended solutions. Viable cell counts onto MacConkey agar were performed to validate bacteria concentration. Each bacterial-adhesion study was performed with a separate and freshly prepared culture.

Zeta potential of the *Pseudomonas aeruginosa* bacteria was measured with a Brookhaven Zeta Pals (Holtsville, NY). After growth to a concentration of $\sim 5 \times 10^6$ cfu/mL, as described above, 10 sets of measurements were done on two separate occasions and averaged. *P. aeruginosa* strain PAK bacteria suspended in Mian's minimal medium at pH = 7.4 showed slightly negative zeta potentials of -12 ±3.3 mV. Thus, *Pseudomonas aeruginosa* carries a slight negative charge due to the lipopolysaccarides and organic acids on its surface.[54,103]

3.3.3 Hydrogel synthesis

Hydrogel membranes of p-HEMA were synthesized by UV-initiated free-radical polymerization [104]. 2 mL of HEMA and 2.7 mL of distilled/deionized water were mixed thoroughly with 15 μL of EGDMA. Nitrogen gas was bubbled through the solution to remove oxygen, which may hinder polymerization. 6 mg of the initiator, Daracure TPO, was added, and the solution was mixed while shielded from light. Monomer solution was polymerized immediately between two microscope slides (Fisher Scientific, Waltham, MA) separated by 80-μm-thick plastic shim stock (McMaster Car, Elmhurst, IL) and secured by clamps. Membranes consisting of 30-100% MAA or 30-100% AA by volume were made by substituting the HEMA component with the desired fraction of MAA or AA. Since membranes of MAA or AA are fragile, EGDMA cross-linking volume was increased to 60 μL. Additionally, the initiator was increased to 24 mg. Because the cross-linking agent is very hydrophobic, the amount of water added to the monomer solution was replaced with a solution of 75% water and 25% acetonitrile by volume. Before each experiment, hydrogel membranes were presoaked overnight in the solution of interest and then cut into 10-mm diameter sections.

In some experiments, hydrogel beads ~4 μL in volume were synthesized in a similar fashion by pipetting 2-μL droplets of the monomer solution into a Sigmacote™ treated, glass vial containing 25 mL of Silicone DC 200 fluid (laboratory grade, Accurate Chemical and Scientific Corp, Westbury, NY) and UV polymerized. Similar to the membranes, hydrogel beads were presoaked overnight in the solution under study.

3.3.4 Membrane wettability

Surface wettability is argued as a modulator of biofouling.[105,106] To assess wettability of the synthesized hydrogel membranes, aqueous contact angles with captive air bubbles were measured. Except for securing the substrates, the procedure was identical to that of Lin and Svitova.[107] Synthesized membranes were placed on a polystyrene plate and needed no further securing. Cover glasses were secured to a polytetrafluoroethylene (PTFE) block with (PTFE) tape.

Figure 3.1 reports advancing contact angles of p-HEMA, p-MAA, clean glass, and silanated-glass surfaces measured in PBS (pH = 7.4). Clean and silanated glass surfaces served as controls for hydrophilic and hydrophobic materials respectively. p-HEMA membranes were pretreated with PBS (pH 7.4), whereas p-MAA membranes were pretreated with PBS (pH 7.4) with 100-mM $MgCl_2$. Clean glass and p-MAA membranes are hydrophilic with advancing contact angles ~ 20 °, the resolution of our optics at low angles. Conversely, p-HEMA and silanated glass are relatively hydrophobic with advancing contact angles of 59 ± 7.6 ° and 102 ± 4.7 °, respectively. Receding angles for all surfaces were 20 °, except for silanated glass with a receding angle of 90.6 ± 6 °. Thus, as gauged by contact angles, the ionic-homopolymer hydrogel, p-MAA, is considerably more hydrophilic than is p-HEMA. Co-polymerization of methacrylic acid with p-HEMA hydrogels increases the water content of the gel surfaces and in addition to their wettability [98]

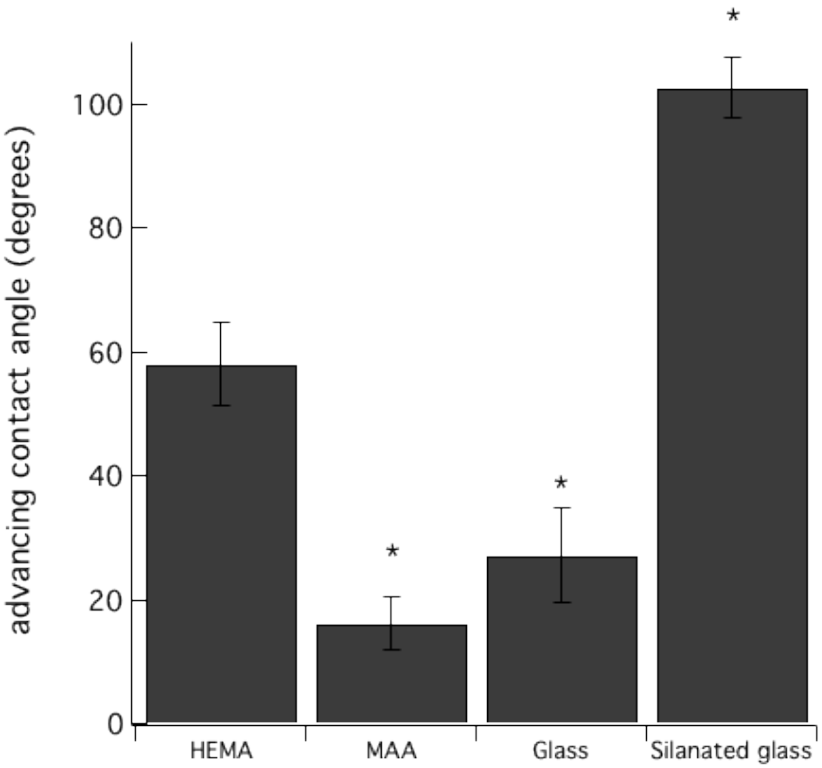


Figure 3.1 Advancing contact angles for surfaces: p-HEMA pretreated with PBS (pH=7.4), p-MAA pretreated with PBS (pH=7.4) with 100-mM $MgCl_2$, clean glass, and silanated glass each immersed in aqueous PBS (pH=7.4) (* denotes statistically significantly different data with comparison to p-HEMA with a p-value <0.05)

3.3.5 Hydrogel swelling/shrinking

Polyelectrolyte hydrogels respond to pH and salt concentration[108-111] typically manifested by swelling/shrinking due to extension/collapse of polymer chains.[110,111] Thus, to gain information on the hydrogel matrix charge, swelling experiments were performed. Swelling/shrinking of selected hydrogels was measured by placing a single hydrogel sphere of initial volume ~4 μL (~ 1-mm diameter) into a glass cuvette containing the aqueous solution of interest. The camera of a Krüss Drop Shape Analysis System 10 (Krüss, Hamburg, Germany) was focused onto the hydrogel sessile bead resting on the bottom of the cuvette. Images were transferred to a PC computer where drop-shape-analysis software (Drop Shape Analysis Version 1.90.0.11, Krüss, Hamburg, Germany) calculated the gel volume every 5 min. Swelling/shrinking results are presented as the average of two or more experiments.

Figure 3.2 shows the swelling/shrinkage response of cross-linked p-MAA in terms of the ratio of the transient bead volume, V, to its final volume, V_f, in Figure 3.2a, or to its starting volume, V_o, in Figure 3.2b. The beads in Figure 3.2a were initially saturated for several days in distilled/deionized water (pH = 6.2) and then exposed to PBS at pH = 7.4. A

four-fold increase in volume ensued. Conversely, Figure 3.2b illustrates that when p-MAA beads initially saturated with PBS (pH=7.4) were exposed to 100-mM NaCl in PBS (pH = 7.4), they shrank by about 10 %. These two results strongly suggest that appended carboxylic side groups in the p-MAA polymeric network are ionized at pH =7.4 in agreement with the expected pKa of less than 7.[66,112,113] Experiments performed on p-MAA and p-AA membranes showed similar results (data not shown). It is concluded that p-HEMA membranes copolymerized with p-MAA or p-AA are anionic at pH=7.4 corresponding to that of Mian's medium.

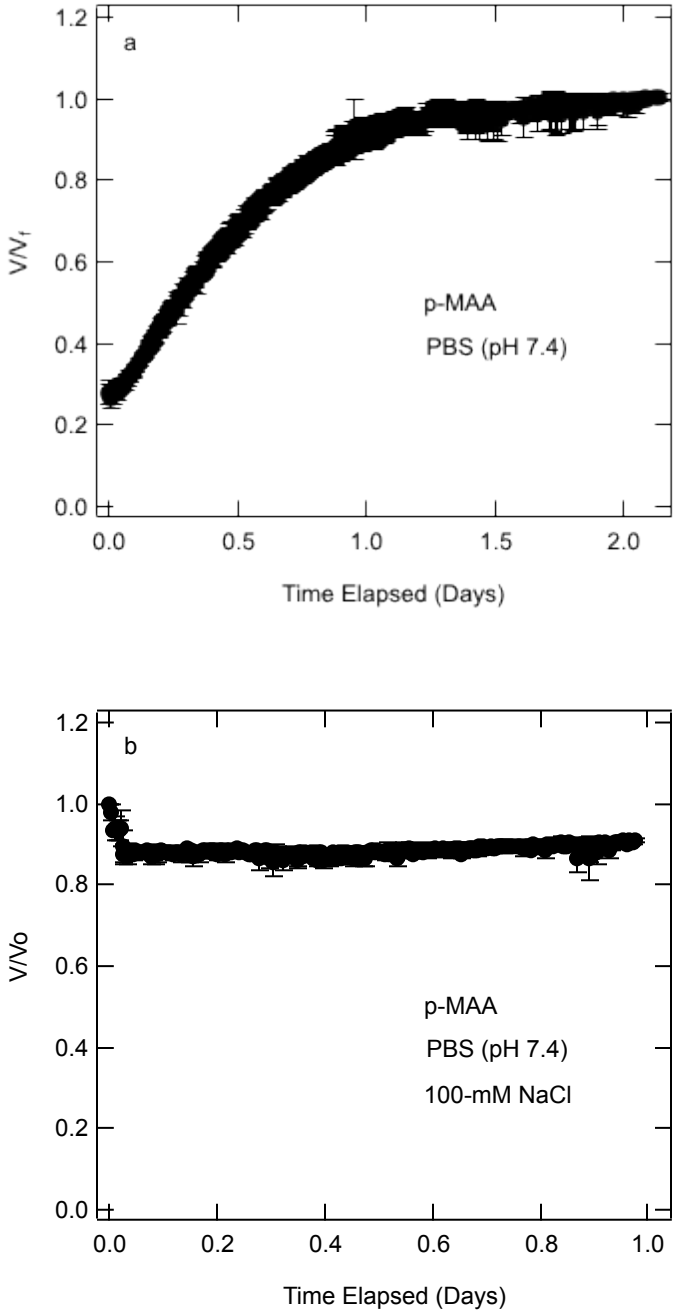


Figure 3.2 Volume swelling/shrinking kinetics of 4-μL p-MAA beads: a.) initially soaked in distilled/deionized water (pH=6.2) and immersed in PBS (pH 7.4) b.) initially soaked in PBS (pH=7.4) and immersed in PBS (pH 7.4) with 10 mM NaCl

3.3.6 Bacteria association assays

Pseudomonas aeruginosa association with transparent surfaces was visualized under phase-contrast, time-lapse microscopy in a parallel-plate flow chamber at a surface shear rate of 0.2 s^{-1} as described in Chapter 2.[89] Cover glasses (Fisher Scientific, 18 cir) for the assays were cleaned by saturated EtOH with KOH and then washed with distilled/deionized water. To make a cover-glass surface hydrophobic, cleaned cover slips were silanated with a chlorinated organopolysiloxane by dipping into SigmaCote™ (Sigma Aldrich) [114] for 5 s. Treated cover glasses were then baked overnight at 80 °C followed by repeated rinsing first with distilled/deionized water and then by ethanol.

Image processing was accomplished the with IMAGE J software (NIH). All bacteria visible were enumerated within the ~ 4-μm focal depth from the membrane surface. In this region, bacteria were bound and stationary or unbound and moving. Bound bacteria were defined not to move within a 20-s time period. This 20-s interval was chosen for convenience. Experiments with captured frames 0.3 s apart showed no difference in results. The number of bound bacteria was determined via image processing with Image J by subtracting bacteria that moved in between captured frames taken 20 s apart. Unbound bacteria include those that approach the surface but do not bind, bacteria that move on or along the surface, and bacteria that detach between each frame.[89]

Bacteria uptake is reported as mean +/- the standard deviation of three or more experiments. Student T-test determined the statistical significance when comparing two groups. p-values of less than 0.05 were considered significant. All adhesion measurements were performed at ambient temperature.

3.4 Results and Discussion

3.4.1 Bacterial uptake

The surface number density of wild-type PAK bacteria in Mian's medium at pH 7.4 accumulating on the surface versus time is shown in Figure 3.3 for a p-HEMA membrane initially soaked in PBS (pH 7.4). Open circles in Figure 3.3 correspond to bacteria within the 4 -μm depth of focus from the surface and thus represent all bacteria directly adjacent to or on the membrane surface. After a few minutes of suspended bacteria injection into the optical flow cell, PAK bacteria steadily accumulated at an average rate of 230 bacteria/mm^2/min, as dictated by convective diffusion.[89] At the surface density of 10^4 bacteria/mm^2, surface coverage is less than 3 %. Hence, surface accumulation is a isolated-entity event.[89]

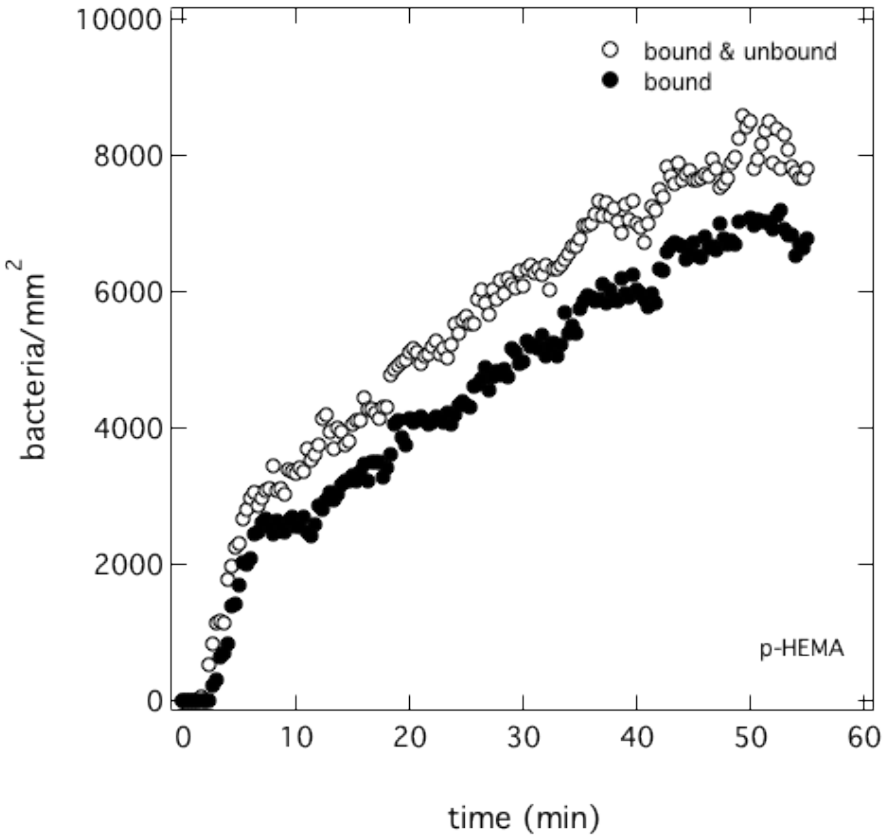


Figure 3.3 Surface uptake kinetics of PAK suspended at $5x10^6$ cfu/mL in Mian's medium accumulating on a p-HEMA surface pretreated in PBS (pH=7.4). Open circles correspond to total bacterial accumulation. Filled circles reflect bound bacteria.

The number density of surface-associated bacteria between each frame is represented by filled circles in Figure 3.3. Bound bacteria (bacteria stationary for 20 s or more) also accumulated steadily over time similarly to that found in Chapter 2 with an O_2Optix lens. They accounted for 85% of the total number of bacteria at the p-HEMA surface.

Figure 3.4 shows the corresponding surface-association kinetics of PAK bacteria in Mian's medium at pH 7.4 but now exposed to a 70% p-HEMA 30% p-MAA membrane pretreated with PBS (pH= 7.4). Drastically different binding histories are seen compared to PAK exposed to 100% p-HEMA in Figure 3.3. In Figure 3.4, the number density of bacteria at the anionic-membrane surface peaks at approximately 20 min. Afterwards, the number of bacteria at the surface diminishes even though bacteria at $5x10^6$ cfu/mL continued to be injected.

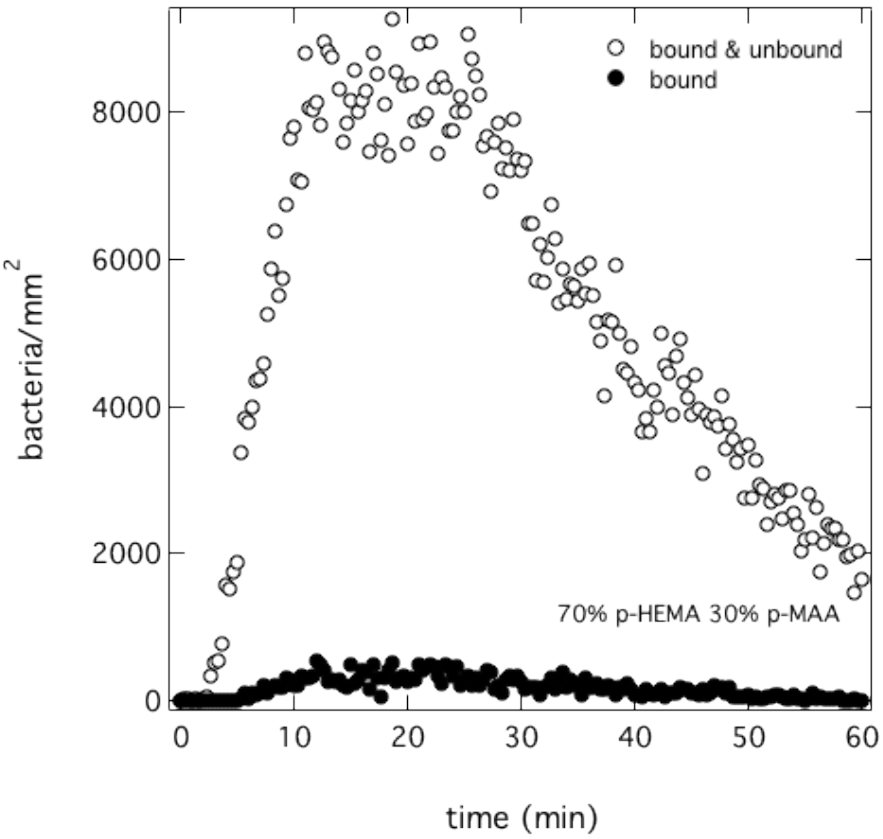


Figure 3.4 Surface uptake kinetics of PAK at $5x10^6$ cfu/mL suspended in Mian's medium accumulating on a 70% p-HEMA /30% p-MAA surface pretreated in PBS (pH=7.4). Open circles correspond to total bacterial accumulation. Filled circles reflect bound bacteria.

Filled circles taken over the same time interval reveal that less than 10% of the bacteria at the surface were bound to the membrane. This result is in stark contrast to the adhesion kinetics of PAK on a p-HEMA surface. Ultimately in Figure 3.4, the total number of bound and unbound bacteria remaining at the surface is less than about 1000 bacteria/mm^2 at the end of the 1-h experiment.

Similar uptake experiments for PAK in Mian's medium were performed with homopolymers of p-MAA and p-AA each pretreated with PBS (pH=7.4). Figure 3.5 graphs the total (bound and unbound) bacterial-accumulation histories for these two hydrogels. Essentially identical results are seen compared to the p-MAA/p-HEMA-copolymer membrane in Figure 3.4: rapid accumulation of bacteria, followed by rapid depletion to very low adhesion densities. The fractions of bound bacteria in Figure 3.5 are very low, similar to that in Figure 3.4.

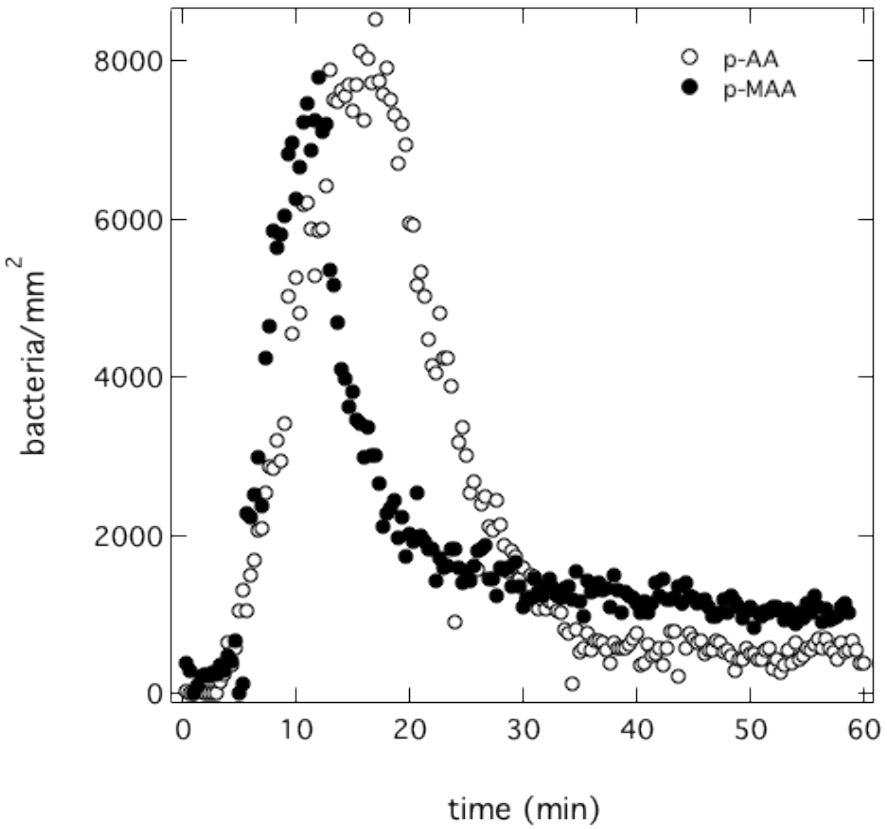


Figure 3.5 Total surface uptake kinetics of PAK at $5x10^6$ cfu/mL suspended in Mian's medium accumulating on anionic-polycarboxylate homopolymers p-MAA (open circles) and p-AA (filled circles) each pretreated in PBS (pH=7.4)

The rapid accumulation and depletion of the PAK bacteria at the membrane surface is described as a "burst". Three distinct time regimes occur in a burst: 1) fast accumulation of unbound bacteria at the membrane (i.e., faster than for p-HEMA), 2) rapid depletion, and 3.) few bacteria eventually binding.

A PAK burst is observed only when p-MAA or p-AA is present in the hydrogel. Apparently, the addition of charged repeat units to the hydrogel matrix plays an important role in the burst phenomenon. To investigate whether membrane charge is necessary for a burst, p-MAA homopolymer membranes were pretreated with deionized/distilled water (pH 6.2) instead of PBS (pH 7.4). Open triangles in Figure 3.6 reveal the lack of a bacterial burst when the membrane initially is at pH = 6.2. This result confirms the pre-requisite of membrane charge in initiating a burst.

The importance of membrane charge in PAK bursts suggests that classical double-layer electrostatic forces play a role[115]. At high enough indifferent electrolyte concentration, these forces diminish. Accordingly, p-MAA membranes were pretreated with 100-mM NaCl in PBS (pH=7.4) and were exposed to PAK bacteria in Mian's medium. At these electrolyte concentrations, the Debye length is less than 1 nm. Far from disappearing, the filled circles in Figure 3.6 clearly demonstrate that bursting is unaffected

by excess indifferent electrolyte. This result is also consistent with the minor shrinkage observed in Figure 3.2b for immersion of p-MAA gel into 100-mM aqueous NaCl at pH = 7.4 Bacterial uptake kinetics at even higher NaCl pretreatment concentrations was difficult to assess due to rapid changes in membrane conformation during the flow-cell experiments. Nevertheless, it is concluded that traditional electrostatic double-layer interaction between the bacterium and the hydrogel surface does not initiate bursting.

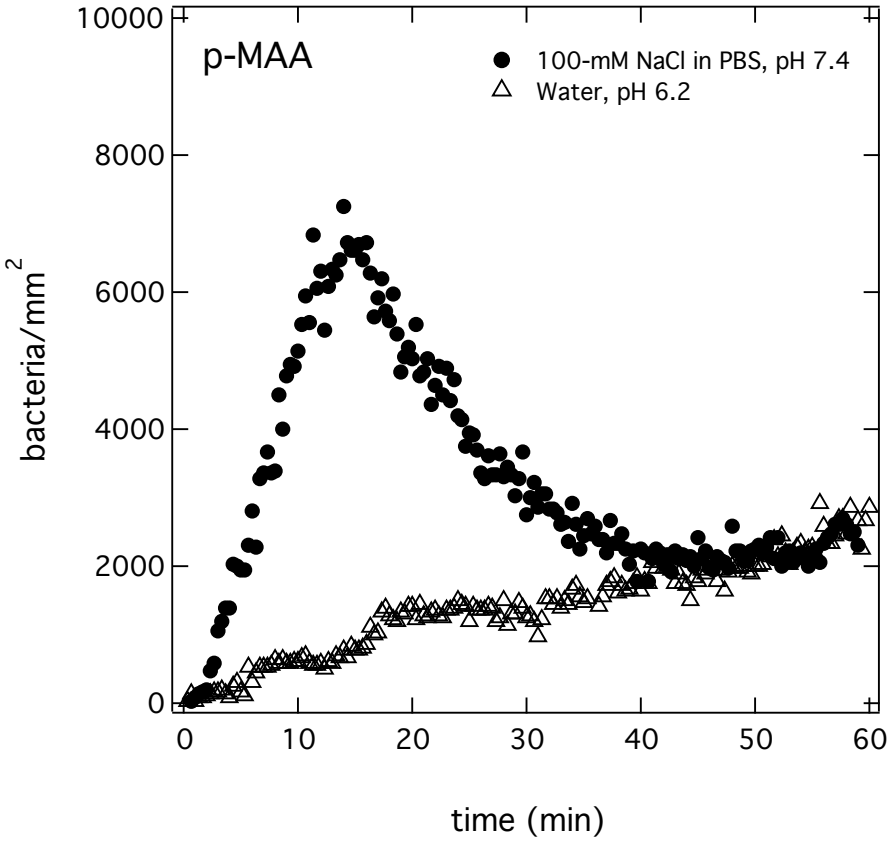


Figure 3.6 Total surface uptake kinetics for PAK at $5x10^6$ cfu/mL suspended in Mian's medium accumulating on p-MAA membranes with differing pretreatments: aqueous 100-mM NaCl in PBS solution (pH=7.4) (filled circles) or distilled/deionized water (pH=6.2) (open triangles).

Mian's medium contains divalent cations, namely magnesium, that interact specifically with anionic carboxylates.[116] To establish whether magnesium cation interacts specifically with the polycarboxylate gels, swelling/shrinkage experiments were performed on p-MAA gel beads in the presence of magnesium. Results are shown in Figure 3.7. When $MgCl_2$ at 10 mM is added to the aqueous PBS solution (pH=7.4), the beads initially swollen in PBS (pH=7.4) shrink by 37%. Specific counterion binding of magnesium cations is the most likely explanation for this significant collapse of the anionic p-MAA hydrogel.

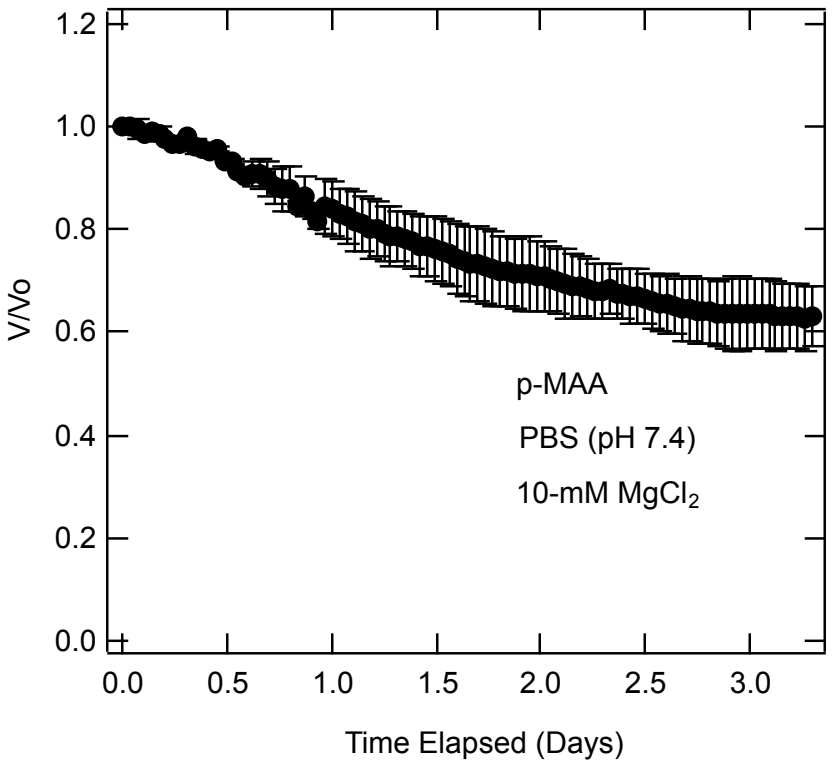


Figure 3.7 Volume shrinking kinetics of 4-μL p-MAA beads initially soaked in PBS (pH=7.4) followed by immersion in PBS (pH 7.4) with 10-mM $MgCl_2$.

Figure 3.8 reports the role of divalent cations in controlling PAK bursting on anionic p-MAA membranes. Uptake kinetics of PAK in Mian's medium (pH=7.4) is shown when the membrane is pretreated with various magnesium-salt-containing solutions: Mian's medium (pH=7.4), 10-mM $MgCl_2$ in aqueous PBS (pH=7.4), and 100-mM $MgCl_2$ in aqueous PBS (pH=7.4). When the presoaking solution contains magnesium cations, PAK bursting is clearly curtailed. The higher is the aqueous magnesium concentration, the more effective is the burst remission. The final number density of bacteria at the membrane surface is less than 2000 bacteria/mm^2 even after 1 h of exposure to bacteria.

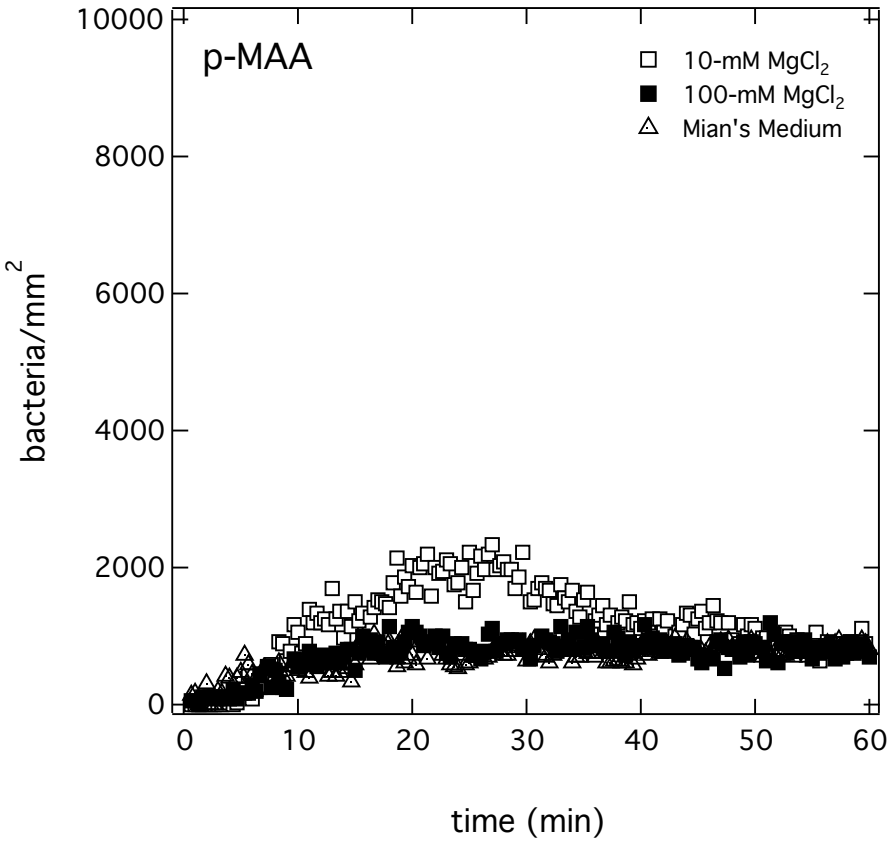


Figure 3.8 Total surface uptake kinetics of PAK at $5x10^6$ cfu/mL accumulating on p-MAA membranes pretreated in Mian's medium (open triangles), in 10-mM $MgCl_2$ aqueous PBS solution (pH=7.4) (open squares), and in 100-mM $MgCl_2$ aqueous PBS solution (pH=7.4) (closed squares). Open triangles are partially hidden.

Figures 3.4-8 suggest that anionic PAK bursts at the surface of anionic hydrogels when magnesium is present in the flowing suspension but not initially in the hydrogel. Therefore, removal of magnesium cations from the suspending medium should eliminate depletion. Bacteria-attachment assays were perfomed with p-AA hydrogels presoaked in PBS (pH=7.4) but with the suspending Mian's medium (pH=7.4) devoid of magnesium salt. To accomplish this, PAK bacteria, initially grown in Mian's medium, were centrifuged, washed, and resuspended in Mian's medium but without $MgSO_4$. Removal of magnesium from the suspending medium had no detectable effect on bacteria viability (data not shown). As demonstrated in Figure 3.9a, no burst was observed at a p-AA membrane even after 1 h of bacterial exposure. However, once the injected bacteria solution was brought to 10-mM $MgCl_2$, a burst immediately occurred. The results confirm that magnesium in the aqueous suspension is required for PAK burst. The fact that bursts occur either with aqueous $MgCl_2$ or with $MgSO_4$ rules out any influence of salt anions.

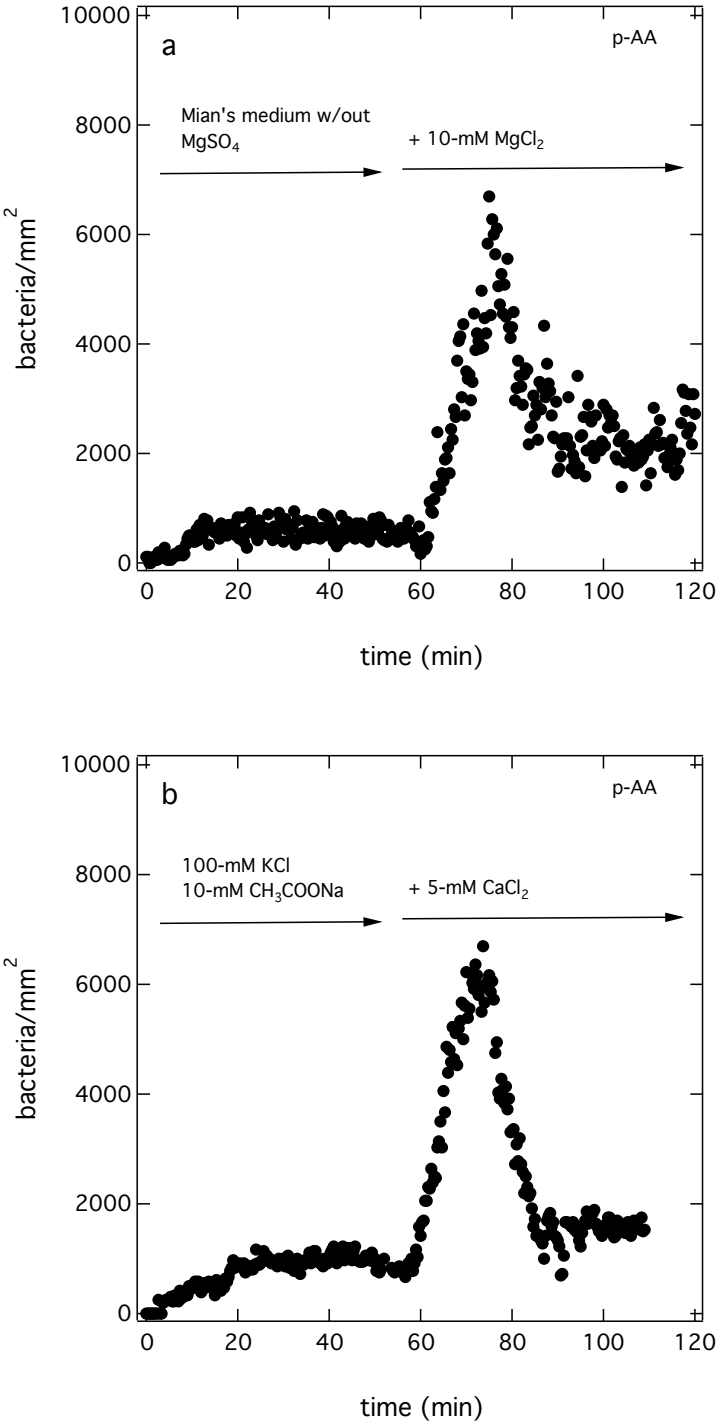


Figure 3.9 Burst initiation with divalent cations. Total surface uptake kinetics of PAK at $5x10^6$ cfu/mL on a p-AA membrane pretreated in PBS (pH=7.4). a.) Initially the injected suspension medium is Mian's without $MgSO_4$ (pH=7.4). After 1 h, 10-mM $MgCl_2$ was added to the flowing bacterial suspension. b.) Initially, the injected suspension medium is 100-mM KCl and 10-mM CH_3COONa at pH=7.4. After 1 h, 5-mM $CaCl_2$ was added to the flowing bacterial suspension.

Identical experiments were conducted with $CaCl_2$ replacing $MgCl_2$. To prevent calcium phosphate from precipitating in PBS and in Mian's medium, a KCl solution (100-mM KCl with 10-mM CH_3COONa) was used both to pretreat the membrane (instead of PBS) and to suspend the bacteria (instead of Mian's). Sodium acetate served as a carbon source (same as in Mian's) for the bacteria, and, thus, maintained bacteria viability. The solution pH was adjusted to 7.4 with small amounts of NaOH. Figure 3.9b displays the results. Without calcium ions in the suspending medium, again no burst is observed. Once $CaCl_2$ is added to the suspension medium, a burst appears. It is conclude that calcium cations also specifically ion bind with the anionic polycarboxylate gels.

Another means for removing magnesium cation from the Mian's suspending medium is via chelation. Figure 3.10 demonstrates that ethylene diamine tetraacetic acid (EDTA) successfully inactivates magnesium cations from both the solution and the anionic gels. p-MAA beads previously shrunken with $MgCl_2$ in Figure 3.7 recover their initial swelling when exposed to EDTA in PBS (pH 7.4). Thus, EDTA was used to restore membranes that had previously absorbed divalent cations. A burst should then occur once the divalent cations are removed from the membrane, and the membrane is exposed to more bacteria in the presence of aqueous divalent cations. In Figure 3.11, PAK bacteria were suspended in Mian's medium (pH = 7.4) and flowed over a p-AA membrane pretreated in PBS (pH = 7.4). After 1 h, EDTA at an equal concentration to magnesium sulfate (10 mM) was incorporated in the suspending medium for about 50 min. During this period, EDTA chelated the magnesium cations from the bulk solution and from the membrane. After the 50-min chelating period, 10-mM of $MgCl_2$ was then added to the EDTA/Mian's bacterial suspension and flowed past the membrane. Figure 3.11 clearly shows that upon addition of more magnesium cations into the bacterial suspension, another burst occurred. Identical results were found for calcium ions with EDTA on a p-AA membrane (data not shown).

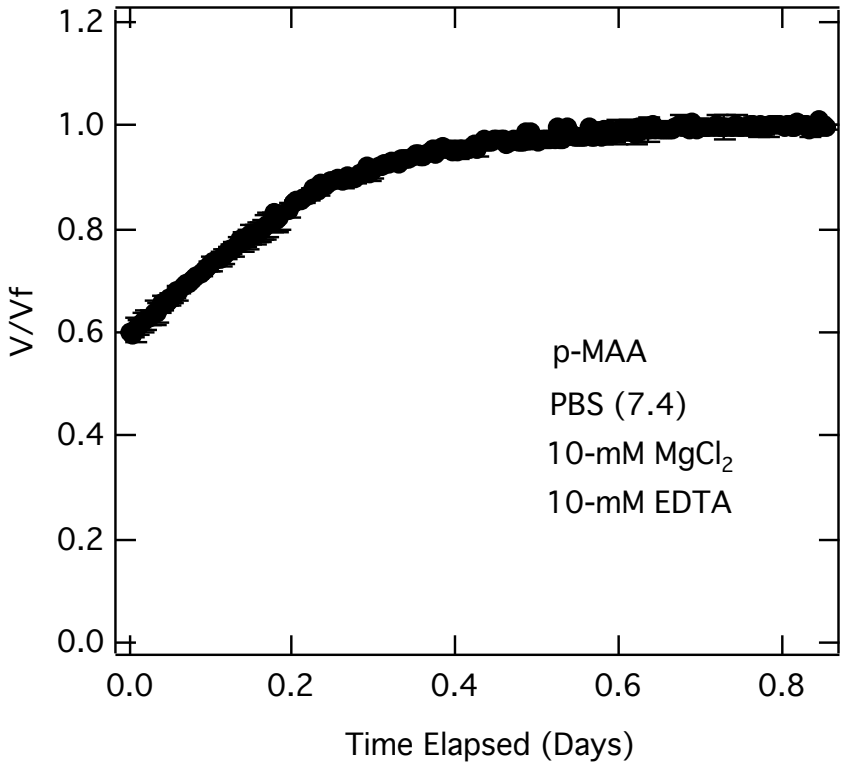


Figure 3.10 Volume swelling kinetics of 4-μL p-MAA beads upon exposure to EDTA. p-MAA was initially soaked in PBS (pH=7.4) followed by immersion in PBS (pH 7.4) with 10-mM $MgCl_2$ (see Figure 3.7). At the end of shrinkage in Figure 3.7, 10-mM EDTA was added to the $MgCl_2$/PBS solution.

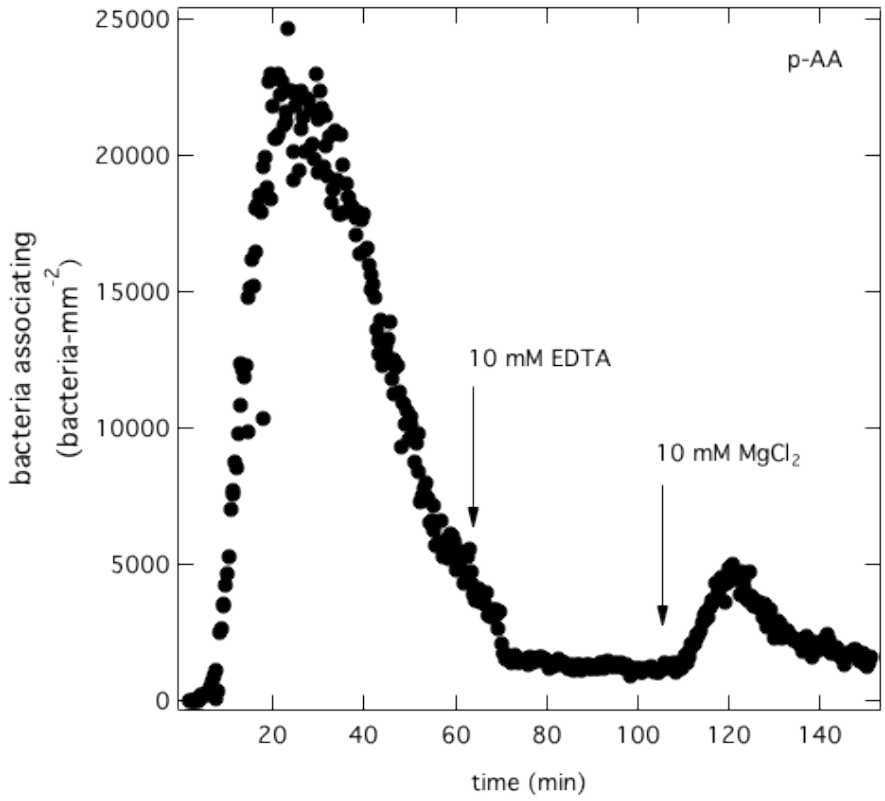


Figure 3.11 Magnesium burst recovery with EDTA. Total surface uptake kinetics of PAK at $5x10^6$ cfu/mL in Mian's medium (pH=7.4) for p-AA membranes pretreated in PBS (pH=7.4). After 1 h, 10-mM EDTA is added to the suspending solution. After about 2 h, 10-mM $MgCl_2$ is added to the suspending solution.

Calcium divalent cation bridging was also stopped with addition of EDTA as shown in Figure 3.12. In this case, PAK at $5x10^6$ cfu/mL in aqueous 100-mM KCl, 10-mM CH_3COONa, 5-mM $CaCl_2$ (pH=7.4) was exposed to p-AA membranes pretreated in 100-mM KCl, 10 mM CH_3COONa (pH=7.4). A burst occurs but there is not enough Ca^{+2} to fully collapse anionic polymer chains. An equilibrium of bacteria strongly associating with the membrane persists. 5-mM EDTA is added to the suspending solution and all the bacteria leave the hydrogel surface. After an additional 30 min, 5-mM $CaCl_2$ is added to the suspending solution and a small burst is recovered.

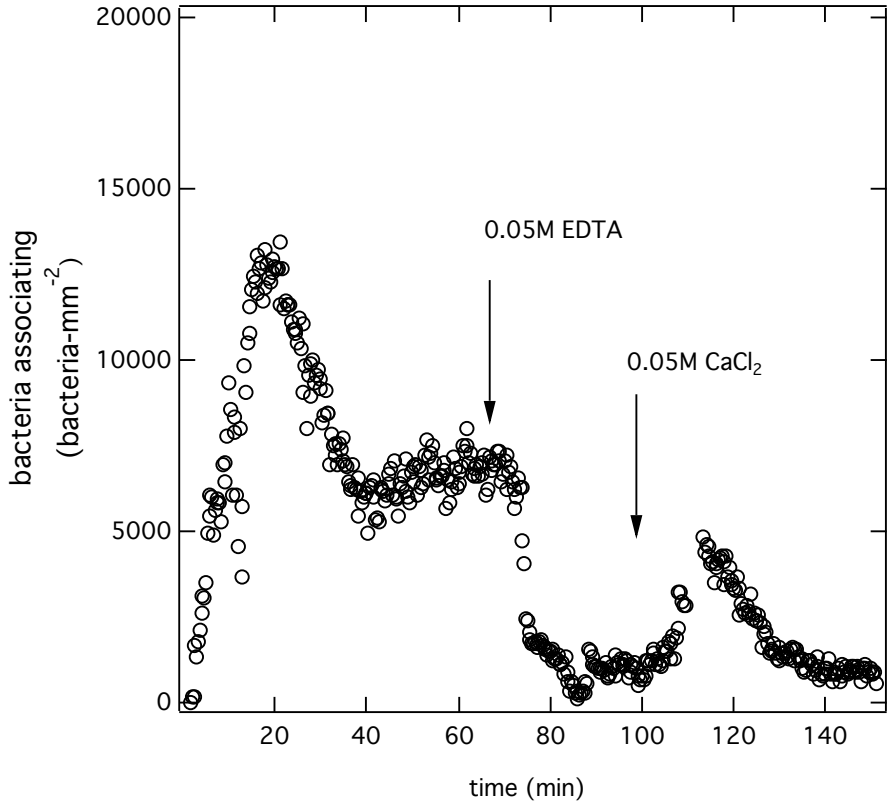


Figure 3.12 Calcium burst recovery with EDTA. Total surface uptake kinetics of PAK at $5x10^6$ cfu/mL in aqueous 100-mM KCl, 10-mM CH_3COONa, and 5-mM $CaCl_2$ (pH=7.4) for p-AA membranes pretreated in 100-mM KCl and 10-mM CH_3COONa (pH=7.4).

3.4.2 Burst etiology

PAK bursts commence when the hydrogel surface is anionic and when the suspending medium contains divalent ions, but the membrane initially does not. Thus, in addition to membrane charge, a gradient in divalent-ion concentration between the suspending solution and the membrane appears requisite. Bacteria migration in concentration gradients towards an attractant or away from a repellent (i.e., chemotaxis) is well documented.[117,118] Specifically, *P. aeruginosa* migrates in the direction of increasing concentration of organic acids used as a carbon source.[118] The presence of magnesium is apparently also required [12,119]. However, no free acids are present in the experiments. Although bacteria adhered to a surface do respond to chemical stimulae [120], there is no documentation of *P. aeruginosa* attraction to MAA or AA. Further, such attraction, if present, does not explain the bacterial-depletion sequence of a burst. Chemotaxis driven by divalent-cation concentration gradients also cannot explain the burst phenomenon because such gradients are present in other PAK uptake experiments that do not exhibit bursts, including those for p-HEMA, O2Optix™ [89], and p-MAA membranes pretreated with distilled/deionized water (see also Figure 3.4) Accordingly, chemotaxis is rejected as the origin of PAK bursting on anionic hydrogel surfaces.

During the burst, the number of bacteria affixed at the membrane surface is very low. In fact, accumulated bacteria appear to diffuse along the membrane surface without strong binding. This observation suggests an attractive force maintaining the bacteria within about a body diameter of the surface. Classical Hamaker forces are sensibly independent of aqueous electrolyte concentration[121,122] and, hence, are inappropriate to bursting. As pointed out earlier, Figures 3.4-10 argue for a specific electrostatic attraction. The importance of divalent cations to bursting in Figures 3.9, 3.11 and 3.12 suggests cationic bridging between negatively charged sites on the anionic bacterium and on the anionic hydrogel surface. Indeed, there is documentation that divalent cations act as a bridge for binding between anionic bacteria surface and substrate surfaces.[62,123] Figure 3.13 illustrates schematically the proposed picture. It suggests that the bridging attraction is local and weak. Nonpermanently bound bacteria may swim away from the surface overcoming the bridging attractive force. They adsorb and desorb reversibly from the membrane on a time scale shorter than the frame speed. Reversible cation bridging explains the initial large accumulation of nonbound PAK on anionic-hydrogel surfaces in Figures 3.3 and 3.4 relative to that on nonionic p-HEMA in Figure 3. Subsequent bacterial depletion, however, is not accounted for.

On the left of Figure 3.13, the membrane surface is immersed in indifferent electrolyte at pH 7.4. Carboxylic-acid side groups are deprotonated causing polymer chains to repel [110,111] and the gel to expand. Figure 3.2a confirms this charge-induced swelling. When exposed to divalent-cation salts, the gel surface ion binds the cations at the anionic charged surface. Some of the surface divalent-ion-bound sites permit cation bridging with PAK and give rise to the enhanced adhesion seen initially in a burst.

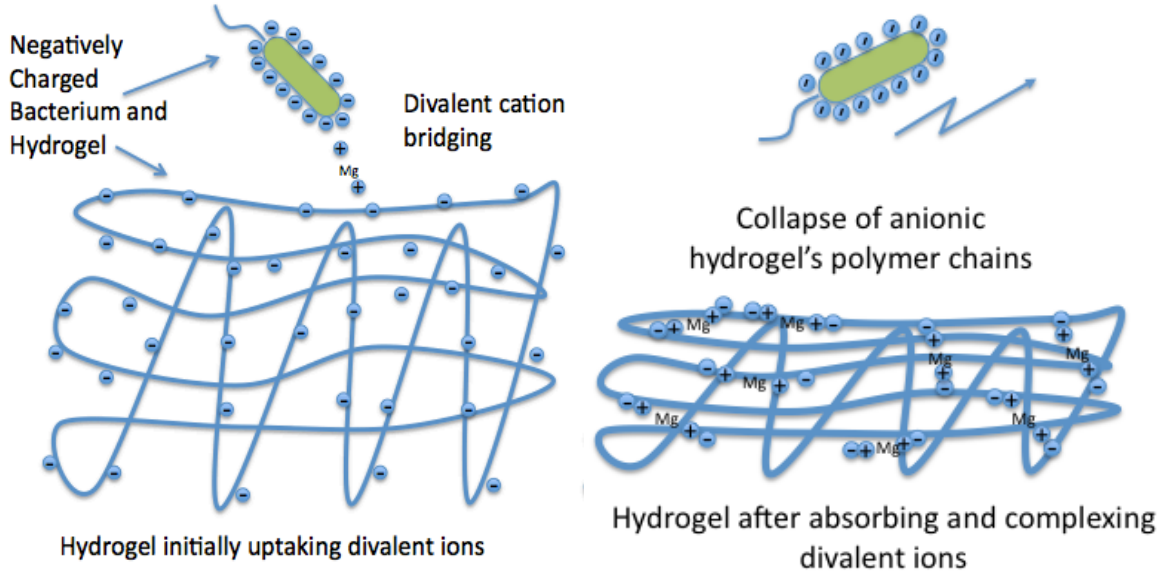


Figure 3.13 Schematic of proposed bridging/collapse mechanism for PAK bursting. Initially, the hydrogel is expanded allowing divalent-cation bridging between bacteria and surface. Later, the hydrogel collapses destroying surface bridging sites and releasing accumulated bacteria.

Upon longer contact of the membrane with aqueous divalent cations, more absorb into the polymer matrix, ion bind, and bridge internally with nearby carboxylated side groups. Nonspecific-bound sodium counterions release in an ion-exchange process.[110] The resulting matrix bridging-charge neutralization contracts the hydrogel, as pictured on the right of Figure 3.12 and confirmed in Figure 3.7. Gel collapse buries some surface bridging sites making them no longer available to nonpenetrating bacteria. Previously associated bacteria then escape from the surface. Divalent cation binding within the anionic gel is reversible to chelation with EDTA. Once the aqueous divalent cations are inactivated, the gel again swells, as established in Figure 3.10. Gel-surface ion-binding sites re-establish. Hence, as documented in Figure 3.11, re-introduction of aqueous divalent-cation salt permits another PAK burst.

Membranes pretreated with distilled/deionized water at pH 6.2 do not exhibit bacterial bursting burst because they are not negatively charged enough. In concert with the proposed bridging/collapse model, divalent cations have a much more pronounced effect relative to monovalent cations on both bursting and gel shrinkage.

The third criterion for a burst is that densities of bound bacteria on the surface are low. Figure 3.13 emphasizes this point (see also Figure 3.8). Adhesion rates of bound PAK in supernatant Mian's medium are almost zero for p-MAA pretreated with 100-mM $MgCl_2$ in PBS. In contrast, the comparable bound adhesion rate of PAK in Mian's medium for p-HEMA is much larger. Figure 3.14 also reveals that similar bound adhesion rates for clean glass are small, whereas those for silanated glass are large. This later result suggests that

wild-type PAK bacteria do not bind well to hydrophilic materials. Some studies suggest that hydrophilic materials resist fouling.[25,105,106] Upon comparing the bound adhesion rates in Figure 3.14 with the corresponding advancing contact angles in Figure 3.1, a definite correlation that low-contact-angle surfaces (more hydrophilic) resist PAK adherence is found, whereas high-contact-angle surfaces (more hydrophobic) do not. Hence, the reason for the small strong binding of PAK on anionic hydrogels is enhanced water wettability when the gel is charged and of higher water content.

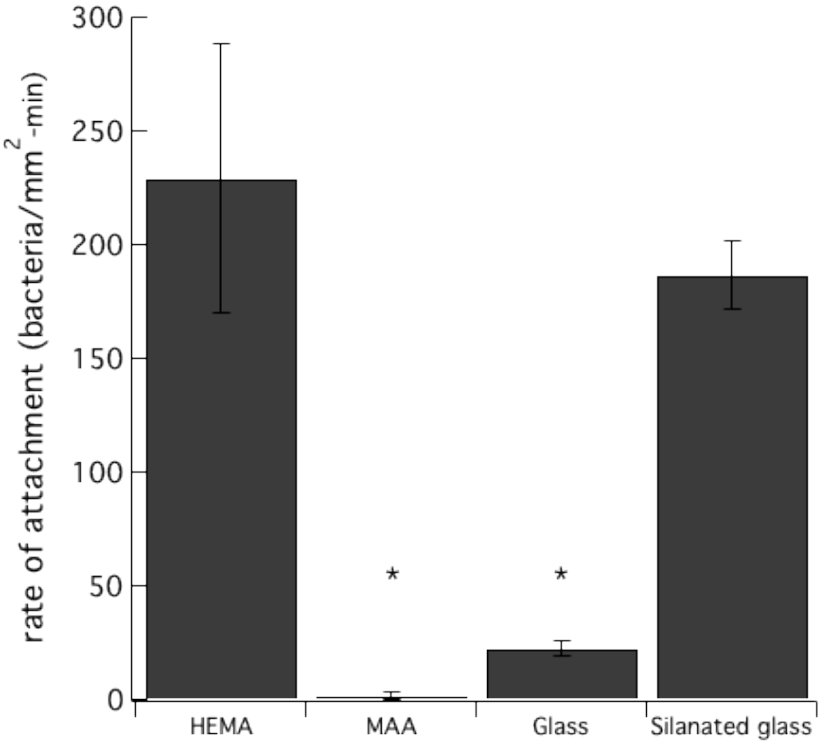


Figure 3.14 PAK total uptake rates at $5x10^6$ cfu/mL on p-HEMA pretreated with PBS (pH=7.4), p-MAA pretreated with PBS (pH=7.4) with 100 mM $MgCl_2$, glass, and silanated glass. (* denotes statistically significantly different data with comparison to p-HEMA with a p-value <0.05).

However, correlation of bacterial binding with surface wettability is not universal.[23,26] PAK bacteria binds equally well to p-HEMA and silanated glass despite an enormous difference in advancing contact angle. Clearly surface hydrophilicity is not the complete deciding factor for bacterial binding. Perhaps there is a threshold hydrophilicity that must be achieved to prevent strong adhesion.

3.5 Conclusions

Wild-type PAK strain of *Pseudomonas aeruginosa* exhibits a burst- attachment phenomenon on anionic hydrogel membranes when the suspending medium contains divalent cations and the membrane initially does not. Early-time accumulation rates are larger than on counterpart nonionic hydrogels. The initial high accumulation rate is followed by spontaneous bacterial detachment to a low number of strongly bound bacteria. The bursting phenomenon arises from reversible divalent-cation bridging between the anionic bacterium and anionic charged sites on the hydrogel surface. As divalent cations penetrate the hydrogel lattice, the gel collapses destroying surface binding sites and releasing most of the initial surface accumulation of bacteria. Few strongly bound PAK bacteria remain on the gel surface most likely due to increased hydrophilicity compared to the nonionic hydrogels. This study emphasizes the delicate balance of physical and chemical forces that play important roles in the interaction of bacteria with solid surfaces. In the experiments presented here, the hydrogel ionic content was at least 30% by monomer volume. In comparison, soft-contact lenses that incorporate charged copolymers may do so at only a few percent [124]. At these low charged copolymer fractions, bursting may not be as evident.

Chapter 4: Effects of Polymeric Surfactants On Silicone Hydrogel Soft Contact Lens Wettability and Bacterial Adhesion of *Pseudomonas aeruginosa*

4.1 Abstract

Prevention of *Pseudomonas aeruginosa* binding to soft-contact lenses (SCLs) may curtail sight-threatening microbial keratitis. Substrate surface wettability is known to modulate adhesion of *P. aeruginosa*. This study investigates the use of aqueous food-grade polymeric surfactants for enhanced wettability and antibacterial adhesion of SCLs under leaching conditions. Specifically, Pluronic® F127 (PF) and three ethylene oxide-butylene oxide (EOBO) surfactants were studied with four commercially available silicone-hydrogel contact lenses: Pure Vision™, Acuvue Advance™, Acuvue Oasys™ and O_2Optix™. Dilute aqueous PF and EOBO surfactants impregnated all four soft-contact lenses as demonstrated by surface-tension decline for leached surfactant. For PF surfactant, significant surface-wettability improvement upon rinsing occurred only after overnight leaching. EOBO surfactant showed a similar pattern with O_2Optix™ lenses. EOBO-pretreated Pure Vision™ lenses, however, showed fast leaching and a significant change in surface energy towards better wettability. Adhesion assays of *P. aeruginosa* showed a small decrease in the binding rate of PAK bacteria for EOBO-pretreated Pure Vision™ lenses, but not for EOBO-pretreated O_2Optix™ lenses. *P. aeruginosa* strain-PAO1 bacteria adhesion to all lenses was independent of surface wettability. Despite the ability of polymeric surfactants to lower advancing contact angles under leaching conditions, increased lens wettability is not a universal panacea for antifouling of soft-contact lenses.

4.2 Introduction

Microbial keratitis is the most serious complication associated with soft-contact-lens wear.[125] Bacterial adhesion to soft-contact lenses is a major risk factor for microbial keratitis;[2] recent studies have shown that bacteria-laden soft-contact lenses can cause infection in a murine model.[4] Thus, an attractive method for preventing sight-threatening microbial keratitis is to preclude bacterial adhesion to soft-contact-lens surfaces.

Pseudomonas aeruginosa is one of the most-often implicated bacterium in contact-lens-related microbial keratitis.[53] *P. aeruginosa* is an opportunistic pathogen that normally infects immune-compromised individuals.[126] However, it infects otherwise healthy soft-contact-lens wearers.[3,127] In addition, the bacterium causes difficult-to-treat and devastating infections.[126] Because of the bacterium's ability to resist antibiotics and to evolve further antibiotic resistances,[128] an antifoulant rather than an antimicrobial agent is worth exploring.

Hydrophilic surfaces have been demonstrated to resist *P. aeruginosa* fouling.[129] Methods for adhesion prevention include hydrophilic poly(ethylene oxide) brush layers [130] and aqueous surfactants.[131] For a surfactant to work in on-eye application, however, it must modify the lens external surface under leaching conditions.[132] Food-grade polymeric surfactants are currently employed in soft-contact-lens solutions to impart better wettability and wearability and are, thus, a promising avenue for exploration. [132,133]

This study investigates the ability of block co-polymer surfactants Pluronic® F127 (PF) and ethylene oxide/butylene oxides: $EO_{45}BO_{12.3}$, $EO_{45}BO_{13.8}$ and $EO_{45}BO_{16.2}$ to modify the external surface of selected commercial soft-contact lenses. Lenses initially loaded with surfactant were assayed for resistance to bacterial adhesion by two *P. aeruginosa* strains, PAK and PAO1. Adhered bacteria were enumerated under surfactant-free-suspension flow through a parallel-plate optical cell by phase-contrast video microscopy. [89]

4.3 Materials and Methods

4.3.1 Materials

Contact lenses were obtained from ABB ConCise Contact Lens (Alameda, CA). PF was purchased from BASF (Ludwigshafen, Germany). EOBO surfactants were kindly provided by Alcon Labs (Fortworth, TX). Phosphate-buffered saline pH 7.4 (PBS, molecular biology grade), sodium phosphate monobasic monohydrate, potassium phosphate anhydrous, magnesium sulfate heptahydrate, and sodium nitrate (reagent grade) were purchased from Sigma-Aldrich (St. Louis, MO). Ethanol, potassium hydroxide, and sodium acetate (reagent grade) were purchased from Fisher Scientific. All chemicals were used as received. Distilled/deionized water was obtained via a Milli Q system (Millipore, Billerica, MA). Tryptic soy agar and MacConkey agar were purchased from Becton, Dickinson and Company (Franklin Lakes, NJ).

4.3.2 Contact-Lens Preparation

Four commericial silicone-hydrogel lenses: Pure Vision™ (PV), Acuvue® Advance™ (AVA), Acuvue® Oasys™ (AVO) and O_2Optix™ (O2O) were used in this study. Table 1 documents pertinent properties of theses lenses.[60,134] Lenses were transferred aseptically from blister packs (commercial containers containing individual lenses stored in proprietary aqueous solution) and placed into 20-mL PBS solutions or PBS with surfactant solutions for two days.

Table 4.1
Contact Lens Properties[60,134]

Commericlal Name	Manufacturer	Material	FDA Group	Water Content	Surface Treatment
Pure Vision™	Bausch and Lomb, Inc.	Balafilcon A	III	36%	Plasma Oxidation
Acuvue® Advance™	Johnson and Johnson Vision Care	Galyfilcon	I	47%	*PVP in reaction mixture
Acuvue ® Oasys™	Johnson and Johnson	Senofilcon A	I	38%	*PVP in reaction mixture
O_2Optix™	CIBA Vision	Lotrafilcon B	I	33%	25 nm plasma coating

*PVP = poly(vinyl pyrrolidone)

4.3.3 Surfactants

Pluronic® F127 (PF) and a set of ethylene oxide/butylene oxide surfactants: $EO_{45}BO_{12.3}$, $EO_{45}BO_{13.8}$ and $EO_{45}BO_{16.2}$ were studied. PF is a triblock copolymer of poly(ethylene oxide)$_x$/ poly(propylene oxide)$_y$/poly(ethylene oxide)$_x$ with a molecular weight of 12.6 kDa [135]. The subscripts x and y indicate the average number of monomer units where x is 101 and y is 56. The EO_nBO_m surfactants are diblocks of poly(ethylene oxide)$_n$/poly(butylene oxide)$_m$ with a molecular weight of about 3 kDa. They are distinguished by their subscripts: n is the average number of EO monomers, and m is the average number of BO monomer units. Each surfactant solution was prepared at 0.05 wt/vol% in PBS which is well above their critical aggregation concentrations. Ambient-temperature equilibrium surface tensions of the PF and EOBO solutions at this concentration were 38 mN/mm and 35 mN/mm, respectively. The surface tension of nascent PBS was 72 mN/m.

4.3.4 Contact-Angle and Surface-Tension Measurements

Contact-angle and surface-tension measurements were performed as previously described by Lin and Svitova.[107] All reported angles are the average advancing contact angle from 3 or more experiments with standard deviations. Lenses suspended in the solution of interest (surfactant in PBS or in nascent PBS) were captured with tweezers and dipped 10 times in clean PBS to rinse surface residual material which may contaminate the contact-angle and surface-tension measurements. Soft-contact lenses were secured to a specially designed polytetrafluoroethylene (PTFE) holder, exposing the anterior contact-lens surface.[107] The contact-lens holder was placed into an optical glass cuvette containing 40 mL of fresh PBS solution to initiate leaching. A sessile bubble of approximately 100 μL was formed in the PBS solution via a syringe pump (Model 1250, J-KEM® Scientific, St Louis, MO). Upon engagement with the contact-lens surface, the captive bubble was imaged via a camera (Krüss, Hamburg Germany) interfaced with a PC and monitored with an in-house Labview™ program. The angle at which the three-phase contact line of the bubble started to move was recorded as the advancing/receding angle.[107] Retraction of air from the bubble created a liquid advancing angle between the air bubble and contact-lens surface. Injection of air gave the corresponding liquid receding angle. Due to the curvature of the contact lenses, the lower limit in the assay is 15 degrees. Receding contact angles for all lenses in aqueous PBS were less than 15 degrees, the precision of detection and are not

shown. Contact angles were measured quickly after immersion of the lens into the surfactant-free PBS solution, typically less than 1 min.

In some cases after bubble detachment to about 1 cm above the contact-lens surface, the resulting sessile bubble was used to measure the air/water surface tension via drop-shape analysis (Drop Shape Analysis Version 1.90.0.11, Krüss, Hamburg, Germany). Bubble tension was assessed within about 1 min after retraction from the contact-lens surface. To prevent evaporation during surface-tension measurements, aluminum foil sealed the cuvette and bubble holder. In extended surfactant-leaching experiments, the lens was left overnight for at least 10 h in the contact-lens holder and cuvette filled with nascent PBS solution while the sessile-bubble surface tension was continuously recorded.

4.3.5 Bacteria Preparation

Pseudomonas-aeruginosa strain PAK was kindly provided by Dr. Joanne Engel (University of California, San Francisco) with permission from Dr. John Mattick (University of Queensland Australia).[68] PAO1 was kindly supplied by Dr. Suzanne Fleisizg (UC Berkeley). Frozen stocks were recovered onto Tryptic Soy Agar plates grown at 37 °C for 14 h. Single colonies were inoculated into 12 mL of modified Mian's minimal medium (Mian's) [4] and grown while shaken at 250 rpm at 37 °C until the optical density reached 0.15 at 650 nm measured with a Spectronic 21D spectrophotometer (Milton Roy). Bacteria were then diluted by fresh modified Mian's medium to a concentration of ~$5x10^6$ colony forming units per mL (cfu/mL) as determined by viable cell counting.[136]

Bacteria used for hydrocarbon-adhesion assays were prepared in a similar fashion. A single colony was inoculated into 100 mL of Mian's minimal medium and allowed to grow while shaking to an optical density at 650 nm of 0.15 as measured by theSpectronic 21D spectrophotometer. Cells were harvested and centrifuged at 6000x (6000xg) for 10 min and the supernatant discarded. The bacteria pellet was then washed by resuspension in fresh, sterile Mian's minimal medium. The wash step was repeated, and the bacteria were resuspended to an optical density at 600 nm of 0.2, as measured with a spectrophotometer (Biophotometer Plus, Eppendorf, Hamburg Germany).

4.3.6 Bacterial-Adhesion Assays

Pseudomonas-aeruginosa association with transparent surfaces was visualized under phase-contrast, time-lapse microscopy in a parallel-plate flow chamber at a surface shear rate of 0.2 s^{-1}.[136] Cover glasses (Fisher Scientific, 18 cir) for the assays were cleaned by ethanol saturated with KOH and then washed with distilled/deionized water. To hydrophobize glass, cleaned cover slips were silanated with a chlorinated organopolysiloxane by dipping into SigmaCote™ (Sigma Aldrich)[114] for 5 s. Treated cover glasses were then baked overnight at 80 °C followed by repeated rinsing, first with distilled/deionized water, and then by ethanol. Contact lenses suspended in solutions of interest were rinsed with sterile PBS by dipping 10 times. 10-mm diameter sections were then cored and mounted into the flow cell.

Image processing was accomplished with IMAGE J software (NIH). All bacteria visible were enumerated within the ~ 4-μm focal depth from the membrane surface. In this region, bacteria were either bound and stationary or unbound and moving.[136]

Bacteria uptake is reported as mean +/- the standard deviation of three or more experiments. Student T-test determined the statistical significance when comparing two

groups. p-values of less than 0.05 were considered significant. All adhesion measurements were performed at ambient temperature.

4.3.7 Bacteria-Hydrocarbon-Adhesion Assay

Bacteria-hydrocarbon-adhesion assays were performed as described previously by Rosenberg et al. [137] with some modification. 4mL glass tubes with a 1-cm diameter used for the experiments were cleaned by ethanol saturated KOH and rinsed repeatedly with distilled water, followed by distilled/deionized water and allowed to air dry. 1 mL of the prepared bacteria suspension was transferred to a 4-mL glass tube. Next, 1 mL of n-hexadecane was slowly pipetted above the aqueous bacteria suspension. The glass tubes were sealed, vortexed for 2 min, and allowed to quiesce for 30 min to allow phase separation. At this point, an emulsion of bacteria and hexdecane at this point was visible near the hexadecane/water interface. Bacteria culture resting near the bottom of the tube was then carefully extracted with a pipette while not disturbing the emulsion layer. The optical density of the extracted culture at 600 nm was then measured with the Biophotometer Plus spectrophotometer and recorded. All experiments were conducted three times in triplicate with triplicate controls using no hexadecane. The fraction bacteria partitioning to the hydrocarbon/aqueous phase interface is reported as unity minus the optical density of the experimental sample divided by the optical density of the control.

4.4 Results

4.4.1 Wettability

Figure 4.1 shows advancing contact angles for PV, AVA, AVO, and O2O lenses initially exposed to PBS for 2 days (dark bars). All angles were taken within a minute after immersing the rinsed lenses into aqueous PBS. The four lenses in aqueous PBS exhibit intermediate wettability, except for PV which is somewhat hydrophobic. Upon pretreatment with PF surfactant at 0.05 wt/vol% for 2 days and rinsing ten times in PBS, no dramatic increase in wettability was found for any of the lenses, as demonstrated by the small changes in advancing contact angles. In the same fashion, with initial loading with all of the EOBO surfactants 0.05 wt/vol% (shaded and open bars), all lenses showed complete wetting except the O2O lens.

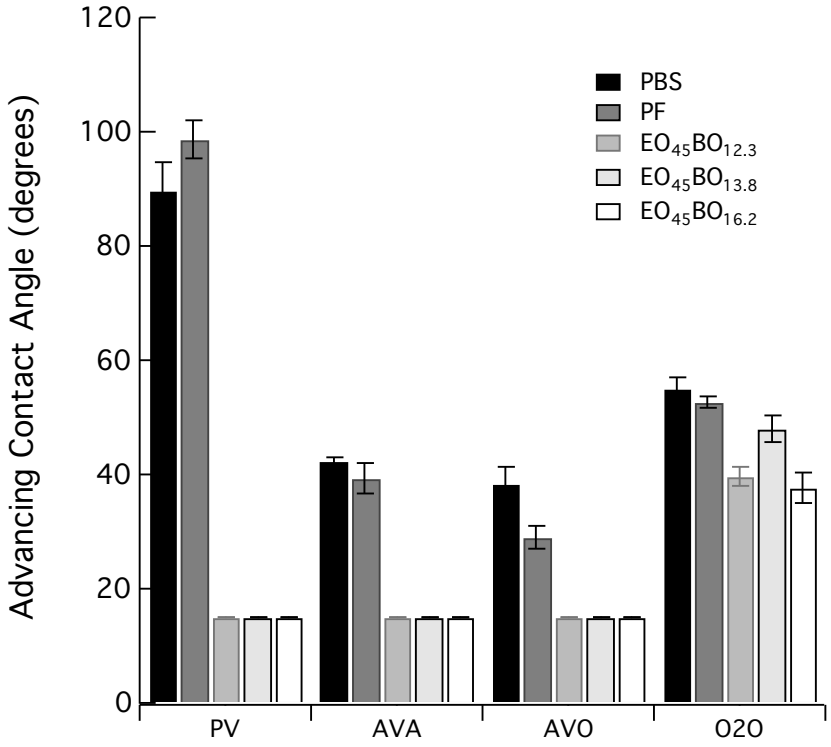


Figure 4.1 Advancing contact angles for lenses initially loaded with PBS, PBS with PF surfactant, or PBS with $EO_{45}BO_{12.3}$, $EO_{45}BO_{13.8}$, or $EO_{45}BO_{16.2}$ surfactant. In each experiment, lenses were rinsed prior to immersion in nascent PBS.

At first glance, Figure 4.1 suggests that any PF surfactant initially adsorbed on all lenses and all EOBO surfactants adsorbed on the O2O lenses were washed away leaving insufficient coverage to improve wettability. Conversely, EOBO surfactants on the PV, AVA, and AVO lenses remained at the lens external surface in spite of rinsing and subsequent leaching. To gain insight into the depletion of surfactant by the rinsing and leaching process, once the advancing angle was measured, the captive bubble was quickly retracted from the lens surface and its dynamic surface tension was measured by drop-shape analysis of the resulting sessile bubble. Only PV and O2O lenses were chosen for this experiment because they exhibited the largest advancing contact angles in PBS. Likewise, only $EO_{45}BO_{16.2}$ surfactant was chosen since there is little difference among advancing contact angles in Figure 4.1 for the three EOBO surfactants. Figures 4.2 and 4.3 show results for $EO_{45}BO_{16.2}$ surfactant initially loaded into PV and O2O lenses. In Figure 4.2 for PV lenses where wettability improved, the surface tension of the sessile bubble just after retraction from the lens surface was 40 mN/m, rising to 43 mN/m after about 1 h. Since surface depletion by washing is expected, $EO_{45}BO_{16.2}$ surfactant most likely leached out of the PV lens matrix to repopulate the lens external surface. Thus, the effectiveness of $EO_{45}BO_{16.2}$ towards wettability improvement of PV lenses can be explained by uptake of the

surfactant into the lens interstices followed by sufficient and rapid supply to the external surface to overcome rinsing. The prolonged minimal rise in bubble surface tension is apparently due to slow desorption of surfactant from the air/water interface into the clean PBS solution.

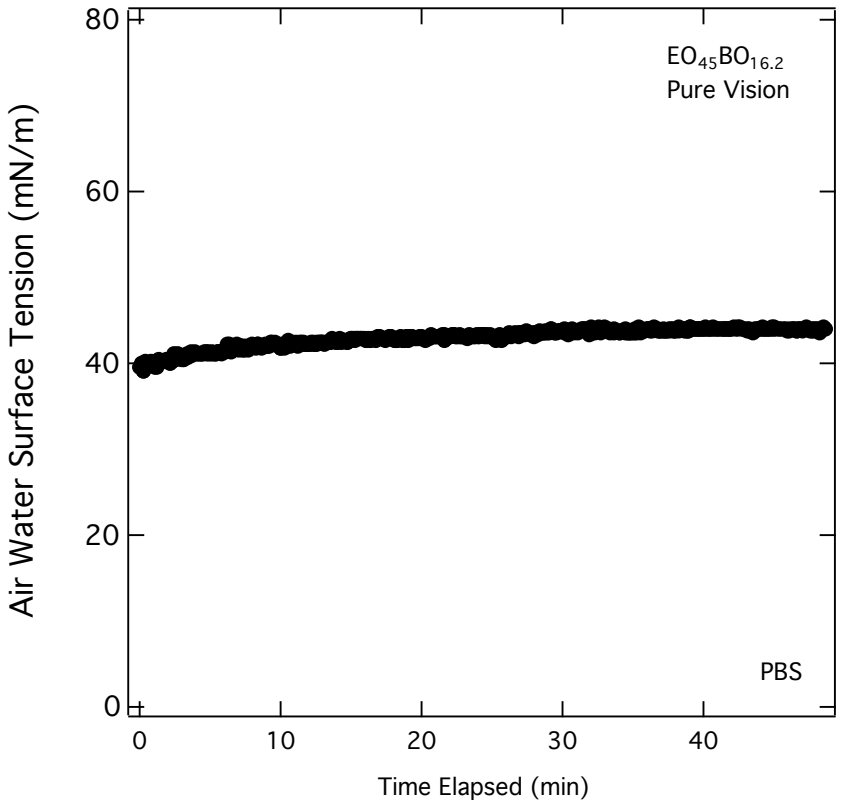


Figure 4.2 Transient surface tension of PBS solution as $EO_{45}BO_{16.2}$ leaches from Pure Vision

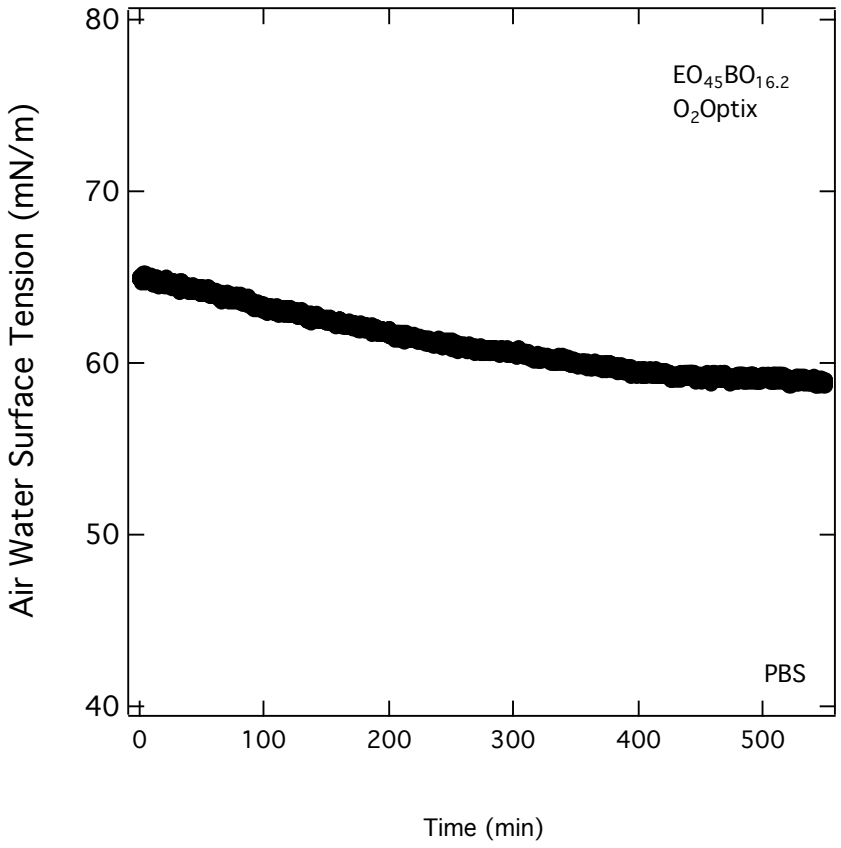


Figure 4.3 Transient surface tension of PBS solution as $EO_{45}BO_{16.2}$ leaches from O_2Optix

Figure 4.3 shows the companion detached-bubble dynamic surface tension for O2O lenses initially pretreated with $EO_{45}BO_{16.2}$ surfactant. For this case, lens water wettability in Figure 4.1 was not improved. Accordingly, there is a comparatively small decline in the initial bubble tension from 72 to about 65 mN/m compared to 40 mN/mm for the PV lens. Afterwards, there is an even smaller decline in tension over a 10-h period. Figure 4.3 is interpreted as insufficient surfactant leaching from the O2O lens matrix to the external surface. Accordingly, the initial surface tension of the detached bubble is not much different from that of the surfactant-free PBS solution. The subsequent small tension decline is due to very slow leaching of $EO_{45}BO_{16.2}$ from the O2O lens matrix and diffusion to the air/water interface of the detached sessile bubble. Thus, for the O2O lens, there is inadequate surfactant partitioning into the hydrogel matrix and/or very slow leaching rates.

To provide more evidence for the polymeric surfactants penetrating the lenses, PV and O2O lenses were preloaded with PF or $EO_{45}BO_{16.2}$ surfactant, rinsed, and left overnight in the cuvette to release surfactant into the PBS solution. Advancing contact-angle results following this procedure are shown in Figure 4.4. After prolonged leaching, both PF-pretreated lenses in Figure 4.4 a and c and $EO_{45}BO_{16.2}$-pretreated O2O lenses in Figure 4.4d showed complete wetting. This result confirms that the lenses uptake and release the surfactant. However, PV lenses loaded with $EO_{45}BO_{16.2}$ in Figure 4.4b did not exhibit

complete wetting after overnight leaching even though complete wetting ensued immediately after rinsing. Instead, this surfactant/lens combination reverted back to high advancing contact angles of 90 degrees. Return to lens hydrophobicity is likely to due extensive leaching and dilution of the $EO_{45}BO_{16.2}$ surfactant.

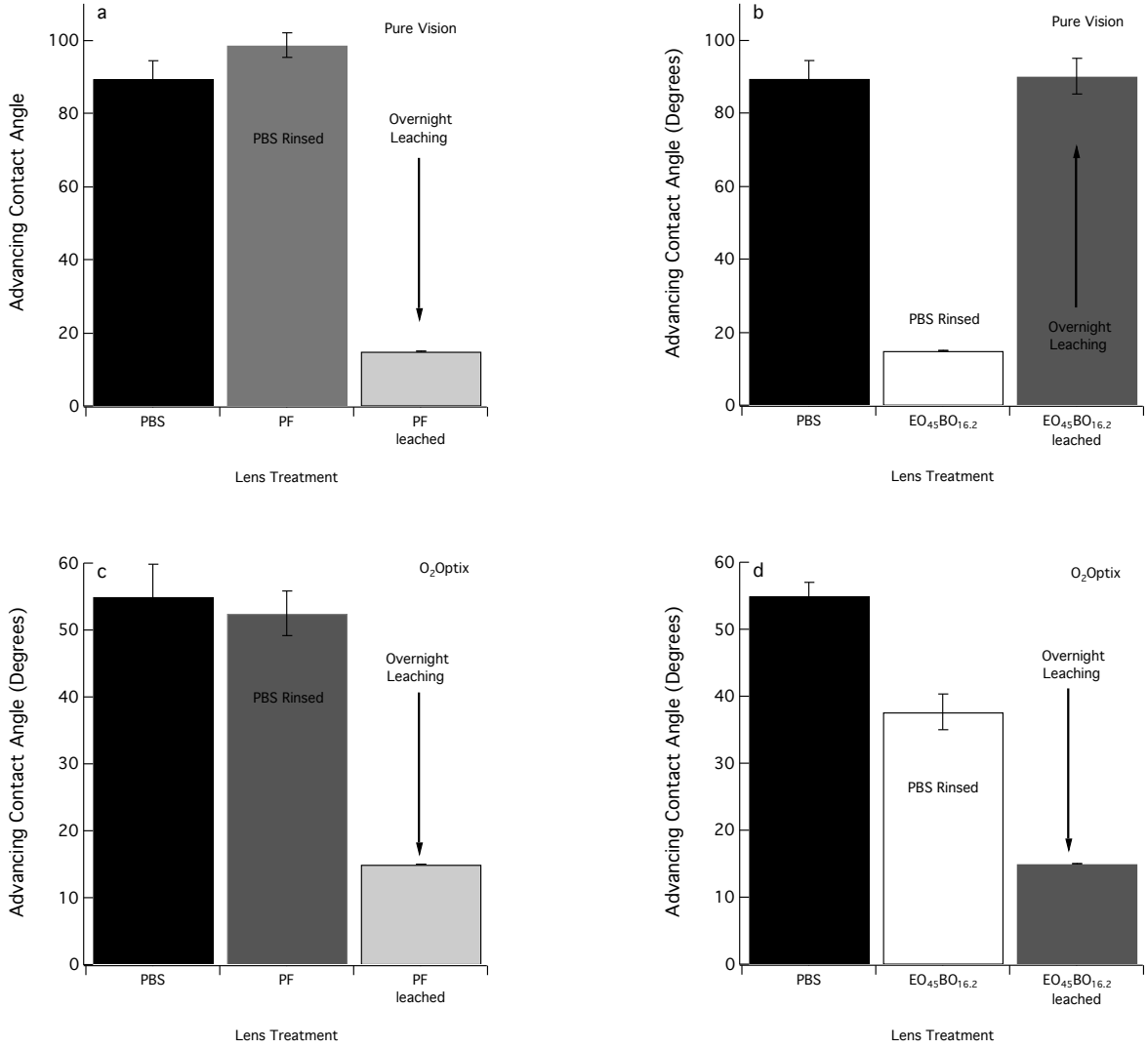


Figure 4.4 Water advancing contact angle of PV and O2O lenses after leaching of PF and $EO_{45}BO_{16.2}$ surfactants overnight. Lenses were initially pretreated with surfactant, rinsed, and then left in PBS overnight. Angles were measured in PBS solution.

4.4.2 Bacterial Adhesion

Chapter 3 demonstrates that PAK bacteria do not adhere well to hydrophilic glass (20 ± 2 bacteria/mm^2-min) but they do adhere well to hydrophobic Sigmacote™-treated glass (180 ± 15 bacteria/mm^2-min) [129]. Advancing contact angles of hydrophilic glass and Sigmacote™-treated glass are 20° and 100°, respectively, [129] consistent with the premise of

hydrophilic surfaces minimizing bacterial adhesion.[23,24] Likewise, PAK adhered very poorly to anionic pMAA membranes (~ 0 bacteria/mm^2-min) that exhibit a 15 ° advancing contact angle in aqueous PBS, as shown in Chapter 3.

For the contact lenses in Figure 4.1, only EOBO surfactants lowered the advancing contact angle of the lenses immediately after rinsing. Consequently, PAK bacterial-adhesion experiments were conducted for $EO_{45}BO_{16.2}$-pretreated PV and O2O lenses. Results in Figure 4.5 show that impregnation of PV lenses with $EO_{45}BO_{16.2}$, which lowered significantly the advancing contact angle after rinsing, also reduced the rate of adhesion of PAK bacteria compared to the control, but not completely. Bacterial adhesion on $EO_{45}BO_{16.2}$-pretreated O2O lenses remained the same as that for the PBS control, which is consistent with the observed lack of significant surfactant-induced wettability improvement in Figure 4.1.

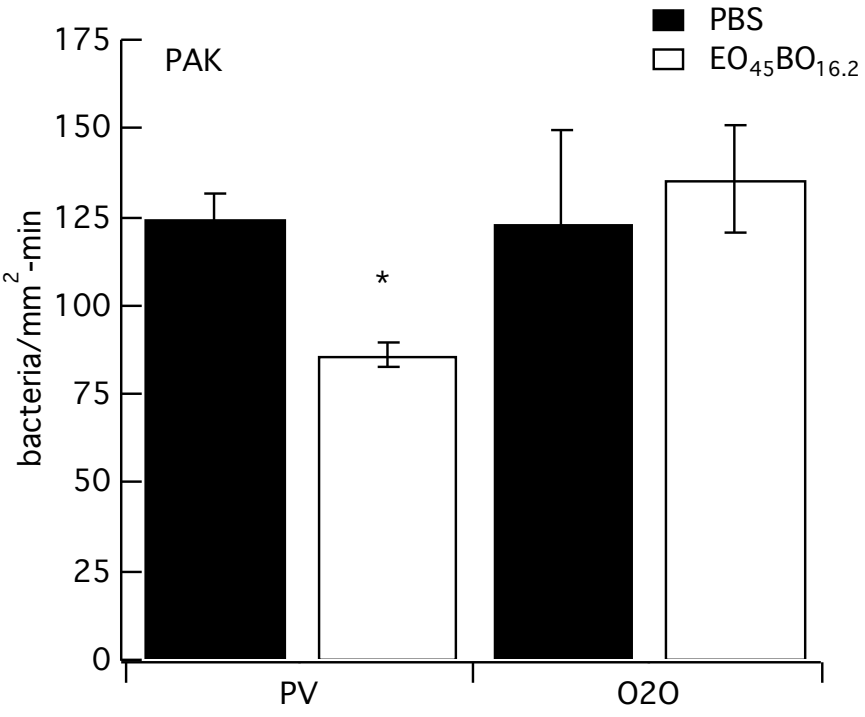


Figure 4.5 Rate of PAK bacteria association to PV and O2O lenses upon pretreatment with PBS or with PBS and $EO_{45}BO_{16.2}$ surfactant. (* designates a p value < 0.05 compared to PBS control)

The exact same experiments as in Figure 4.5 were done with strain PAO1 of *Pseudomonas aeruginosa*. Figure 4.6 demonstrates that strain-PAO1 bacteria did not lower adhesion appreciably for either PV or O2O lenses pretreated with $EO_{45}BO_{16.2}$ surfactant, even though wettability was improved with the PV lens. Companion experiments were then conducted on bacterial adhesion for strain PAO1 on glass versus PAO1 on Sigmacote™-

treated glass. PAO1 bound well both to hydrophilic clean glass and to hydrophobic Sigmacote™-treated glass at rates of 220 ± 6 and 209 ± 10 bacteria/mm^2-min, respectively. Thus, strain PAO1 bound equally well to hydrophilic and hydrophobic glass surfaces. This strain appears immune to the wettability of the substrate surface.

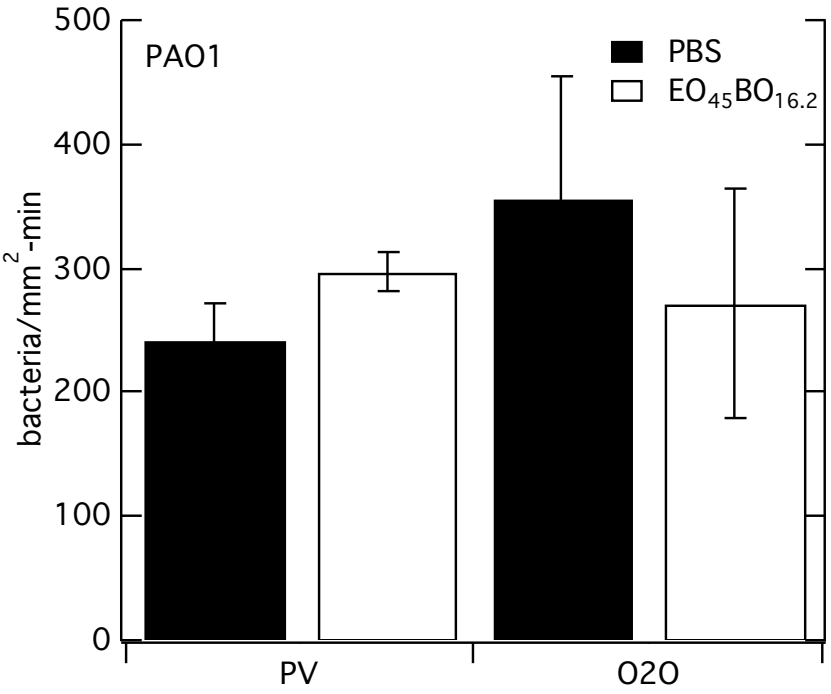


Figure 4.6 Rate of PAO1 bacteria association to PV and O2O lenses upon pretreatment with PBS or with PBS and $EO_{45}BO_{16.2}$.

Finally, hydrocarbon-adhesion assays were performed to determine whether there is a difference in surface hydrophobicity between PAO1 and PAK bacteria strains. Results show that more PAK bacteria adhered to the hydrophobic hexadecane/water interface compared to PAO1 at 72% ± 8 for PAK relative to 40 ± 4% for PAO1. According to this gauge, PAK is more hydrophobic than is PAO1. This result suggests that adhesion of the more highly hydrophobic bacteria is more sensitive to substrate wettability. The more hydrophobic PAK strain dislikes a strongly hydrophilic surface more than does the less hydrophobic PAO1 strain.

4.5 Discussion

4.5.1 Wettability

This study investigates whether food-grade polymeric surfactants can improve the water wetting of commercial silicone-hydrogel soft contact lenses under leaching conditions and

whether resulting improvement in surface hydrophilicity can diminish bacterial adherence. Achieving wetting improvement of silicone-hydrogel commercial SCLs with aqueous polymeric surfactant during leaching conditions is multifaceted. The proposed physical picture of the wetting process with the EOBO class of aqueous polymeric surfactant is highlighted in Figure 4.7. The hydrogel network permits dissolved surfactant to adsorb to the external lens surface and, provided that the surfactant is smaller than the gel mesh size, to enter the water-saturated portion of the gel network. Once inside the gel, surfactant may adsorb to aqueous-exposed polymer strands, depending on architecture and chemical structure. Thus, surfactant absorbs into the gel matrix, and adsorbs both onto the internal gel polymer and onto the external gel surface. Data in Figures 4.1-4.4 and from others[132] indicate that all three processes occur in the systems studied here, although how much surfactant uptake occurs in each state was not assessed. The uptake process is complete when the impregnated surfactant achieves equilibrium with the surrounding aqueous solution.

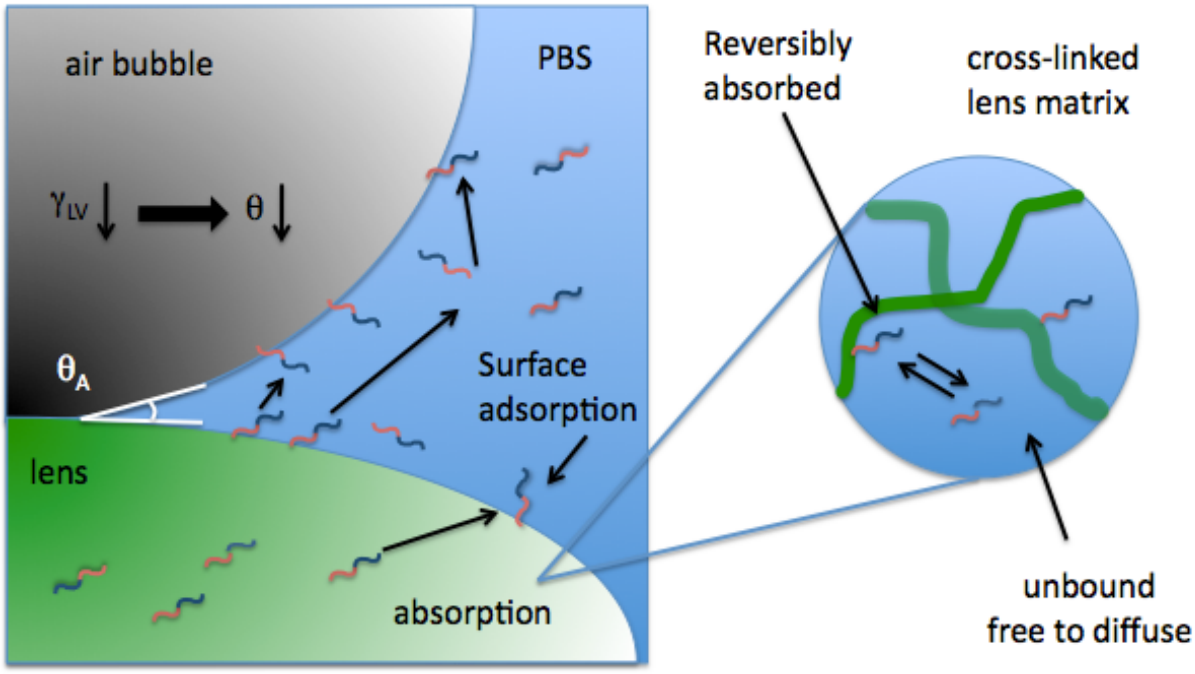


Figure 4.7 Illustration of mechanism of lens wetting by aqueous surfactants. Illustration is for diblock surfactants, such as EOBO. Light shading represents the hydrophobic (tail) moiety and dark shading represents the hydrophilic (head) moiety.

Upon rinsing, immersion in nascent PBS solution, and contact with an air bubble, surfactant in and on the lens surface desorbs, provided the surfactant does not remain irreversibly attached over the time frames studied, here of order hours. The leaching studies in Figures 4.2-4.4 and those of Ketelson et al.[132] strongly suggest partial to total reversibility of EO/PPO and EO/BO- class surfactants on SCL hydrogel materials. Because the bulk aqueous solution initially contains no surfactant in Figure 4.7, surfactant on the bubble surface and on the lens external surface desorbs into solution. Concomitantly,

surfactant diffuses from the gel thereby supplying additional surfactant to both of these interfaces. Eventually, surfactant depletes from the lens matrix and from the bubble surface depending on the ratio of final surfactant mass in the solution to that initially loaded into the gel.

During the gel leaching process in Figure 4.7, lens wettability can be improved when there is enough surfactant present at the lens external surface and at the air/water interface to lower the contact angle. Sustained lowering of the contact angle depends on the amount of surfactant initially in the lens network and on the rate of diffusion supply from the gel matrix.

Figure 4.1 is explained by slow release after rinsing of PF surfactant from all lenses at the 0.05 wt/vol% concentration. There is, thus, no improvement in water wettability. EOBO surfactant in the PV, AVA, and AVO lenses quickly releases after rinsing and lowers the contact angle. For the O2O lenses, release rates are too slow to improve wettability immediately after rinsing, similar to the PF surfactant.

Surface-tension dynamics of the detached air bubble in Figure 4.2 for $EO_{45}BO_{16.2}$ surfactant released from PV lenses show that enough surfactant desorbs from the gel matrix and diffuses back to the lens external surface after rinsing to lower the bubble surface tension to 40 mN/m, close that of the 0.05 wt/vol% aqueous PBS solution (i.e., 35 mN/m). The prolonged minimal rise in bubble surface tension in Figure 4.2 is likely due to desorption of surfactant from the air/water interface into the clean PBS solution. Rapid back supply of $EO_{45}BO_{16.2}$ to the lens external surface explains the effectiveness of this surfactant in lowering the contact angle of the PV lens in Figure 4.1.

Conversely in Figure 4.3, the dynamic surface tension of the detached sessile bubble for $EO_{45}BO_{16.2}$ surfactant initially loaded into O2O lenses indicates that the surfactant does not resaturate the external lens surface after rinsing. Here, the initially detached bubble has a surface tension of 65 mN/m, essentially that of nascent PBS solution (i.e., 72 mN/m). The subsequent very slow decline surface tension arises because surfactant slowly leaches into the surfactant-free PBS solution to populate the air/water interface. In this case, $EO_{45}BO_{16.2}$ does not desorb from the gel polymer and diffuse back to the external surface of the O2O lens quickly enough to improve wettability after rinsing. The dynamic-tension data in Figures 4.2 and 4.3, thus, confirm the results in Figure 4.1 that EOBO surfactant improves the wettability of PV because of fast release, but not that of O2O lenses because of slow depletion kinetics.

Figure 4.4 confirms the importance of surfactant uptake and release kinetics discussed above in wettability alteration of hydrogel surfaces. Here the prolonged leach time allows PF surfactant to repopulate the external surface of both PV and O2O lenses. The advancing contact angle is successfully reduced. Similarly, $EO_{45}BO_{16.2}$ now improves the wettability of the O2O lens, as a longer leach time is given for the surfactant to resaturate the lens external surface. For the $EO_{45}BO_{16.2}$ surfactant with the PV lens, which was quickly leached upon rinsing, we argue that surfactant now leaches completely into the PBS solution. With not enough surfactant eventually remaining in and on the lens, wettability is no longer improved.

Figures 4.1-4.4 highlight the intricate balance of surfactant chemistry and architecture in surfactant-induced wettability alteration of hydrogels. The surfactant must adsorb to the external lens surface and have the ability to alter wettability. In addition, it must have sufficient internal-uptake amounts and release rates from the gel to supply

sufficient surfactant to the external surface under leaching conditions. The PF surfactant molecule is larger than the EOBO surfactant molecule with a molar mass of 12.6 kDa relative to ~3 kDa, respectively. Thus, all else being equal, PF surfactant leaches more slowly than does the EOBO species. PF and EOBO surfactant also differ structurally and chemically. Ketelson et al.[132] found that hydrophobic surfactants have higher affinity with aqueous hydrogels due to stronger interaction with the hydrophobic moieties of the polymer. As noted, PF is a triblock co-polymer of PEO/PPO/PEO, whereas EOBO is a diblock-block co-polymer of PEO/PBO. The hydrophilic/lipophilic balance (HLB) is a measure of the how hydrophilic a surfactant is. Following Griffin, HLB values range from 0-20.[138] The larger is the HLB number, the more hydrophilic is the surfactant. The HLB of PF is 14.6, whereas the HLB for $EO_{45}BO_{12.3}$ = 13.9; $EO_{45}BO_{13.6}$ = 13.3; and $EO_{45}BO_{16.2}$ = 12.6. Thus, EOBO surfactant is more hydrophobic than PF surfactant. Hydrophobic differences of PPO and PBO moieties may also play a role in how the lenses uptake and retain surfactant. It is likely that the more hydrophobic EOBO structure is better retained to hydrophobic external surfaces, such the hydrophobic surface of PV.[139]

Lens chemistry and structure are also important to wettability alteration. Relative hydrophobicity of the gel chains clearly plays a central role in surfactant uptake. Mesh size and tortuosity of the gel influence transport rates.[140] Lens structure is apparently the reason for the relatively slow release kinetics of the EOBO surfactant from the O2O lens and the inability to improve wettability after a rinse. Likewise, lens surface coatings can determine whether or not an adsorbed surfactant improves gel-surface wettability. As shown in Table 4.1, PV and O2O lenses have very different surface treatments.

In this work, lens wettability is assayed by the advancing contact angle against air as dictated by the Young Dupré equation[141]

$$\cos\theta=(\gamma_{sg}-\gamma_{sl})/\gamma_{lg} \qquad (4\text{-}1)$$

where θ is the contact angle, γ_{sg} is the solid/gas interfacial energy, γ_{sl} is the solid/liquid interfacial energy, and γ_{lg} is the liquid/gas surface tension. Let $(\gamma_{sg}-\gamma_{sl})$ denote the adhesion tension.[141] Thus, changes in contact angle are a result not only of changes in the adhesion tension of the solid surface, but also changes in the surface tension of the liquid/gas interface. Surfactant adsorbed to the liquid/gas interface reduces the surface tension and, accordingly, lowers the contact angle. Presumably, bacterial adhesion responds only to the gel external-surface adhesion energy. Consequently, for this application wettability improvement by the surfactant should primarily raise the adhesion tension.

To establish whether the PF and EOBO surfactants alter the adhesion tension, both the contact angle and the liquid/gas surface tension must be measured. The initial tensions in Figures 4.2 and 4.3 give the surface tension directly after lens rinsing and, hence, permit calculation of the adhesion tension. Table 4.2 shows the results. The rise in adhesion tension for PV lenses after exposure to $EO_{45}BO_{16.2}$ surfactant and rinsing is 36 mN/m, whereas for O2O the rise is 12 mN/m. PV lenses show perfect wetting with $EO_{45}BO_{16.2}$ after rinsing and indeed exhibit improvement in adhesion tension. O2O lenses display a smaller rise in adhesion tension and a correspondingly small decline in contact angle.

Therefore, these two surfactants do raise the lens surface adhesion energies and partially influence wettability by adsorption at the lens/aqueous interface.

Table 4.2 Adhesion Tensions

	θ_A(°)	γ_{lg} (mNs/m)	Adhesion Tension (γ_{sg}-γ_{sl}) (mN/m)	Δ Adhesion Tension (mN/m)
PV/PBS	90	72	0	
PV/$EO_{45}BO_{16.2}$	15	37.7	36	36
O2O/PBS	55	72	41	
O2O/$EO_{45}BO_{16.2}$	38	68	54	12

4.5.2 Bacterial Adhesion

It has been previously documented that PAK bacterial adhesion can be less for hydrophilic materials compared to hydrophobic materials.[23,24] For the contact lenses in Figure 4.5, only the PV hydrogels treated with $EO_{45}BO_{16.2}$ surfactant exhibited low contact angles after rinsing and could be expected to diminish bacterial uptake. However, Figure 4.5 shows only a slight reduction of PAK uptake. Thus, although strain-PAK uptake is reduced for glass, pMAA, and pAA water-wet surfaces, surfactant-induced water wetting of the PV hydrogel does not provide complete reduction in PAK adhesion. Even though the contact angle was reduced after rinsing, surfactant adsorbed to the external gel surface did not completely interfere with PAK uptake. Perhaps, allowing more time for leaching might provide more surfactant resistance to bacterial adhesion.

Strain PAO1 adhesion in Figure 4.6 was immune to surfactant-induced wettability improvement consistent with the observed equality of bacterial uptake rates on hydrophilic glass and various hydrophobic surfaces. This observation suggests a difference in surface wettablity between the two bacterial strains. Since the PAK strain appears more hydrophobic than does the PA01 strain, it is more sensitive to wettability alteration of a solid substrate.

PAK and PAO1 are both motile, invasive strains of *P. aeruginosa* with active pili.[44,142,143] Binding differences for differing strains of *P. aeruginosa* have been documented.[58] There are a number of varying bacterial-surface components that differ between the two strains including: lipopolysaccharides, protein secretion, and effectors.[144,145] More in depth studies are needed to ascertain which factors contribute to PAK and PAO1 binding to solid substrate surfaces.

4.6 Conclusions

Food-grade polymeric surfactants, PF and EOBO, are capable of increasing the water wettability of soft-contact lenses under leaching conditions. In order to increase wetttability of the contact-lens surface, the surfactant absorbs into the lens matrix and adsorbs onto the polymer chains. Upon exposure to surfactant-free aqueous solutions, the surfactants leach out of the gel matrix and adsorb at the lens external surface. The studied surfactants increase lens wettability by decreasing the air/water surface tension and by increasing the adhesion tension of the lens external surface. Achieving water wetting of porous soft-contact-lens surfaces has only minimal effect on PAK uptake. Reduction of PAO1 bacteria adhesion by improved wetting was not possible. This result emphasizes the subtle differences in bacterial strains and, thus, the difficulty of preventing adhesion.

References

[1] Mah-Sadorra JH, Yavuz GA, Najjar DM, Laibson PR, Rapuano CJ, Cohen EJ. Trends in contact lens-related corneal ulcers. Cornea 2005;24:51-58.

[2] Bourcier T, Thomas F, Borderie V, Chaumeil C, Laroche L. Bacterial keratitis: predisposing factors, clinical and microbiological review of 300 cases. British Journal of Ophthalmology 2003;87:834-838.

[3] Keay L, Edwards K, Naduvilath T, et al. Microbial keratitis - Predisposing factors and morbidity. Ophthalmology 2006;113:109-116.

[4] Tam C, Mun JJ, Evans DJ, Fleiszig SMJ. The Impact of Inoculation Parameters on the Pathogenesis of Contact Lens-Related Infectious Keratitis. Investigative Ophthalmology & Visual Science 2010;51:3100-3106.

[5] McDonnell PJ. Eximer-Laser Corneal Surgery - New Strategies and Old Enemies. Investigative Ophthalmology & Visual Science 1995;36:4-8.

[6] Fleiszig S, Evans D. The pathogenesis of bacterial keratitis: studies with Pseudomonas aeruginosa. Clinical Experimental Optometry 2002;85:271-278.

[7] Alexandrakis G, Alfonso EC, Miller D. Shifting trends in bacterial keratitis in South Florida and emerging resistance to fluoroquinolones. Ophthalmology 2000;107:1497-1502.

[8] Fick R. *Pseudomonas aeruginosa, the opportunistic pathogen*. Boca Raton: CRC Press; 1992.

[9] de Kerchove AJ, Elimelech M. Impact of alginate conditioning film on deposition kinetics of motile and nonmotile *Pseudomonas aeruginosa* strains. Appl Environ Microbiol 2007;73:5227-5234.

[10] Jyot J, Ramphal R. Flagella and Pili of Pseudomonas aeruginosa. In: Rehm B (ed), *Pseudomonas: model organism, pathogen, cell factory*:85-.

[11] Berg HC. *Random walks in biology*. Expanded ed. Princeton, N.J.: Princeton University Press; 1993:152 p.

[12] Moench TT, Konetzka WA. Chemotaxis in Pseudomonas aeruginosa. Journal of Bacteriology 1978;133:427-429.

[13] Harmsen M, Yang LA, Pamp SJ, Tolker-Nielsen T. An update on Pseudomonas aeruginosa biofilm formation, tolerance, and dispersal. FEMS Immunol Med Microbiol 2010;59:253-268.

[14] Chhabra M, Prausnitz JM, Radke CJ. A single-lens polarographic measurement of oxygen permeability (Dk) for hypertransmissible soft contact lenses. Biomaterials 2007;28:4331-4342.

[15] Guillon M, Maissa C. Tear exchange - does it matter? In: Sweeney DF (ed), *Silicone Hydrogels: the rebirth of continuous wear contact lenses.* Woburn, MA: Butterworth Heinemann; 2000:76-89.

[16] Tighe B. Silicone hydrogel materials-how do they work? In: Sweeney DF (ed), *Silicone Hydrogels: the rebirth of continuous wear contact lenses.* Woburn, MA: Butterworth Heinemann; 2000:1-21.

[17] Holden BA, Sankaridurg PR, Jalbert I. Adverse events and infections: which ones and how many. In: Sweeney DF (ed), *Silicone Hydrogels: the rebirth of continuous wear contact lenses.* Woburn, MA: Butterworth Heinemann; 2000:151-213.

[18] Fleiszig SMJ, Lee EJ, Wu C, et al. Cytotoxic strains of Pseudomonas aeruginosa can damage the intact corneal surface in vitro. CLAO Journal 1998;24:41-47.

[19] An YH, Dickinson RB, Doyle RJ. Mechanisms of Bacterial Adhesion and Pathogenesis of Implant and Tissue Infections. In: An YH, Friedman RJ (eds), *Handbook of bacterial adhesion: principles, methods, and applications*: Humana Press; 2000:1-28.

[20] Busscher HJ, Weerkamp AH. Specific and Nonspecific Interactions in Bacterial Adhesion to Solid Substrata. Fems Microbiology Reviews 1987;46:165-173.

[21] Carnoy C, Scharfman A, Vanbrussel E, Lamblin G, Ramphal R, Roussel P. Pseudomonas-aeruginosa Outer-Membrane Adhesins For Human Respiratory Mucus Glycoproteins. Infection and Immunity 1994;62:1896-1900.

[22] Fletcher EL, Fleiszig SMJ, Brennan NA. Lipopolysaccaride in adherence of *Pseudomonas-aeruginosa* to corena and contact-lenses. Invest Opthalmol Vis Sci 1993;34:1930-1936.

[23] Salerno MB, Logan BE, Velegol D. Importance of molecular details in predicting bacterial adhesion to hydrophobic surfaces. Langmuir 2004;20:10625-10629.

[24] Garcia-Saenz MC, Arias-Puente A, Fresnadillo-Martinez MJ, Paredes-Garcia B. Adherence of two strains of Staphylococcus epidermidis to contact lenses. Cornea 2002;21:511-515.

[25] Henriques M, Sousa C, Lira M, Elisabete M, Oliveira R, Azeredo J. Adhesion of *Pseudomonas aeruginosa* and *Staphylococcus epidermidis* to silicone-hydrogel contact lenses. Optom Vis Sci 2005;82:446-450.

[26] Bruinsma GM, van der Mei HC, Busscher HJ. Bacterial adhesion to surface hydrophilic and hydrophobic contact lenses. Biomaterials 2001;22:3217-3224.

[27] Kodjikian L, Casoli-Bergeron E, Malet F, et al. Bacterial adhesion to conventional hydrogel and new silicone-hydrogel contact lens materials. Graefes Arch Clin Exp Ophthalmol 2008;246:267-273.

[28] Miller MJ, Ahearn DG. Adherence of *Pseudomonas-aeruginosa* to hydrophillic contact-lenses and other substrata. J Clin Microbiol 1987;25:1392-1397.

[29] Taylor RL, Willcox MDP, Williams TJ, Verran J. Modulation of bacterial adhesion to hydrogel contact lenses by albumin. Optom Vis Sci 1998;75:23-29.

[30] Thuruthyil SJ, Zhu H, Willcox MDP. Serotype and adhesion of *Pseudomonas aeruginosa* isolated from contact lens wearers. Clin Experiment Ophthalmol 2001;29:147-149.

[31] Vermeltfoort PBJ, Rustema-Abbing M, de Vries J, et al. Influence of day and night wear on surface properties of silicone hydrogel contact lenses and bacterial adhesion. Cornea 2006;25:516-523.

[32] O'Toole GA, Kolter R. Flagellar and twitching motility are necessary for *Pseudomonas aeruginosa* biofilm development. Mol Microbiol 1998;30:295-304.

[33] Ramphal R, Koo L, Ishimoto KS, Totten PA, Lara JC, Lory S. Adhesion of *Pseudomonas-aeruginosa* pilin-deficient mutants to mucin. Infect Immun 1991;59:1307-1311.

[34] Fletcher EL, Weissman BA, Efron N, Fleiszig SM, Curcio AJ, Brennan NA. The role of pili in the attachment of *Pseudomonas aeruginosa* to unworn hydrogel contact lenses. Curr Eye Res 1993;12:1067-1071.

[35] Skerker JM, Berg HC. Direct observation of extension and retraction of type IV pili. Proc Natl Acad Sci U S A 2001;98:6901-6904.

[36] Zolfaghar I, Evans DJ, Fleiszig SMJ. Twitching motility contributes to the role of pili in corneal infection caused by *Pseudomonas aeruginosa*. Infect Immun 2003;71:5389-5393.

[37] Comolli JC, Hauser AR, Waite L, Whitchurch CB, Mattick JS, Engel JN. *Pseudomonas aeruginosa* gene products PilT and PilU are required for cytotoxicity in vitro and virulence in a mouse model of acute pneumonia. Infect Immun 1999;67:3625-3630.

[38] Gupta SK, Berk RS, Masinick S, Hazlett LD. Pili and lipopolysacharide of *Pseudomonas-aeruginosa* bind to glycolipid asialo gm1. Infect Immun 1994;62:4572-4579.

[39] Hahn HP. The type-4 pilus is the major virulence-associated adhesin of *Pseudomonas aeruginosa* - A review. Gene 1997;192:99-108.

[40] Klausen M, Heydorn A, Ragas P, et al. Biofilm formation by *Pseudomonas aeruginosa* wild type, flagella and type IV pili mutants. Mol Microbiol 2003;48:1511-1524.

[41] Lillehoj EP, Kim BT, Kim KC. Identification of *Pseudomonas aeruginosa* flagellin as an adhesin for Muc1 mucin. Am J Physiol-Lung Cell Mol Physiol 2002;282:L751-L756.

[42] Hazlett LD, Rudner XL. Investigations on the role of flagella in adhesion of *Pseudomonas-aeruginosa* to mouse and human corneal epithelial. Ophthalmic Res 1994;26:375-379.

[43] Silverma.M, Simon M. Flagellar rotation and mechanisms of bacterial motility. Nature 1974;249:73-74.

[44] Arora SK, Ritchings BW, Almira EC, Lory S, Ramphal R. The *Pseudomonas aeruginosa* flagellar cap protein, FliD, is responsible for mucin adhesion. Infect Immun 1998;66:1000-1007.

[45] Chambers D, Scott F, Bangur R, et al. Factors associated with infection by *Pseudomonas aeruginosa* in adult cystic fibrosis. Eur J Respir Dis 2005;26:651-656.

[46] Laroche L, Thomas F, Chaumeil C, Borderie V, Bourcier T. Bacterial keratitis: Predisposing factors, clinical and microbiological review of 300 cases. Invest Ophthalmol Vis Sci 2003;44:4764.

[47] Lyczak JB, Cannon CL, Pier GB. Establishment of *Pseudomonas aeruginosa* infection: lessons from a versatile opportunist. Microbes Infect 2000;2:1051-1060.

[48] Mun JJ, Tam C, Kowbel D, et al. Clearance of *Pseudomonas aeruginosa* from a Healthy Ocular Surface Involves Surfactant Protein D and Is Compromised by Bacterial Elastase in a Murine Null-Infection Model. Infect Immun 2009;77:2392-2398.

[49] Ramphal R, McNiece MT, Polack FM. Adherence of *Pseudomonas aeruginosa* to the injured corena - a step in the pathogenesis of corneal infections. Ann Ophthalmol 1981;13:421-425.

[50] Morgan PB, Efron N, Brennan NA, Hill EA, Raynor MK, Tullo AB. Risk factors for the development of corneal infiltrative events associated with contact lens wear. Invest Ophthalmol Vis Sci 2005;46:3136-3143.

[51] Choy MH, Stapleton F, Willcox MDP, Zhu H. Comparison of virulence factors in Pseudomonas aeruginosa strains isolated from contact lens- and non-contact lens-related keratitis. J Med Microbiol 2008;57:1539-1546.

[52] Willcox MDP, Holden BA. Contact lens related corneal infections. Biosci Rep 2001;21:445-461.

[53] Cheng KH, Leung SL, Hoekman HW, et al. Incidence of contact-lens-associated microbial keratitis and its related morbidity. Lancet 1999;354:181-185.

[54] Bruinsma GM, Rustema-Abbing M, van der Mei HC, Busscher HJ. Effects of cell surface damage on surface properties and adhesion of Pseudomonas aeruginosa. Journal of Microbiological Methods 2001;45:95-101.

[55] Mattick JS. Type IV pili and twitching motility. Annu Rev Microbiol 2002;56:289-314.

[56] Merz AJ, So M, Sheetz MP. Pilus retraction powers bacterial twitching motility. Nature 2000;407:98-102.

[57] Silverma M, Simon M. Flagellar rotation and mechanisms of bacterial motility. Nature 1974;249:73-74.

[58] Borazjani R, Levy B, Ahearn D. Relative primary adhesion of Pseudomonas aeruginosa, Serratia marcescens and Staphylococcus aureus to HEMA-type contact lenses and an extended wear silicone hydrogel contact
lens of high oxygen permeability. Contact Lens & Anterior Eye 2004;27:3-8.

[59] Choo JD, Holden BA, Papas EB, Willcox MDP. Adhesion of Pseudomonas aeruginosa to Orthokeratology and Alignment Lenses. Optom Vis Sci 2009;86:93-97.

[60] Santos L, Rodrigues D, Lira M, et al. The influence of surface treatment on hydrophobicity, protein adsorption and microbial colonisation of silicone hydrogel contact lenses. Contact Lens & Anterior Eye 2007;30:183-188.

[61] Busscher HJ, van der Mei HC. Microbial adhesion in flow displacement systems. Clin Microbiol Rev 2006;19:127-141.

[62] De Kerchove AJ, Elimelech M. Calcium and magnesium cations enhance the adhesion of motile and nonmotile Pseudomonas aeruginosa on alginate films. Langmuir 2008;24:3392-3399.

[63] Marshall KC, Stout R, Mitchell R. Mechanism of initial event in sorption of marine bacteria to surfaces. J Gen Microbiol 1971;68:3-337.

[64] McClaine JW, Ford RM. Reversal of flagellar rotation is important in initial attachment of Escherichia coli to glass in a dynamic system with high- and low-ionic-strength buffers. Appl Environ Microbiol 2002;68:1280-1289.

[65] Sjoblad RD, Doetsch RN. Adsorption of polarly flagellated bacteria to bacteria surfaces. Curr Microbiol 1982;7:191-194.

[66] Toutain CM, Caizza NC, Zegans ME, O'Toole GA. Roles for flagellar stators in biofilm formation by Pseudomonas aeruginosa. Res Microbiol 2007;158:471-477.

[67] Dasgupta N, Wolfgang MC, Goodman AL, et al. A four-tiered transcriptional regulatory circuit controls flagellar biogenesis in *Pseudomonas aeruginosa*. Mol Microbiol 2003;50:809-824.

[68] Watson AA, Mattick JS, Alm RA. Functional expression of heterologous type 4 fimbriae in Pseudomonas aeruginosa. Gene 1996;175:143-150.

[69] Whitchurch CB, Mattick JS. Characterization of a gene, pilU, required for twitching motility but not phage sensitivity in *Pseudomonas-aeruginosa*. Mol Microbiol 1994;13:1079-1091.

[70] Lakkis C, Fleiszig SMJ. Resistance of *Pseudomonas aeruginosa* isolates to hydrogel contact lens disinfection correlates with cytotoxic activity. J Clin Microbiol 2001;39:1477-1486.

[71] Turner L, Ryu WS, Berg HC. Real-time imaging of fluorescent flagellar filaments. J Bacteriol 2000;182:2793-2801.

[72] Lira M, Santos L, Azeredo J, Yebra-Pimentel E, Oliveira M. Comparative study of silicone-hydrogel contact lenses surfaces before and after wear using atomic force microscopy. J Biomed Mater Res Part B Appl Biomater 2008;85B:361-367.

[73] Lopez-Alemany A, Compan V, Refojo MF. Porous structure of Purevision (TM) versus Focus (R) night & day (TM) and conventional hydrogel contact lenses. J Biomed Mater Res 2002;63:319-325.

[74] Singh PK, Parsek MR, Greenberg EP, Welsh MJ. A component of innate immunity prevents bacterial biofilm development. Nature 2002;417:552-555.

[75] Lévêque MA. Les lois de la transmission de chaleur par convection. Annales des Mines, Memoires Ser 1928;13:201-299.

[76] Lok BK, Cheng YL, Robertson CR. Protein adsorption on crosslinked polydimethlsiloxane using total internal-reflection fluorescence. J Colloid Interface Sci 1983;91:104-116.

[77] Newman J, Thomas-Alyew K. Electrochemical Systems. Hoboken, NJ: Wiley Interscience; 2004:377-415.

[78] Barton JW, Ford RM. Determination of effective transport-coefficients for bacterial migration in sand columns. Appl Environ Microbiol 1995;61:3329-3335.

[79] Chiang P, Burrows LL. Biofilm formation by hyperpiliated mutants of Pseudomonas aeruginosa. J Bacteriology 2003;185:2374-2378.

[80] Jenkins ATA, Ffrench-Constant R, Buckling A, Clarke DJ, Jarvis K. Study of the attachment of Pseudomonas aeruginosa on gold and modified gold surfaces using surface plasmon resonance. Biotechnol Prog 2004;20:1233-1236.

[81] Kirisits MJ, Prost L, Starkey M, Parsek MR. Characterization of colony morphology variants isolated from Pseudomonas aeruginosa biofilms. Appl Environ Microbiol 2005;71:4809-4821.

[82] Stoodley P, Sauer K, Davies DG, Costerton JW. Biofilms as complex differentiated communities. Invest Ophthalmol Vis Sci 2002;56:187-209.

[83] Blasco MD, Esteve C, Alcaide E. Multiresistant waterborne pathogens isolated from water reservoirs and cooling systems. Journal of Applied Microbiology 2008;105:469-475.

[84] Das K, Bose S, Bandyopadhyay A, Karandikar B, Gibbins BL. Surface Coatings for Improvement of Bone Cell Materials and Antimicrobial Activities of Ti Implants. Journal of Biomedical Materials Research Part B-Applied Biomaterials 2008;87B:455-460.

[85] Garg P, Sharma S, Rao GN. Ciprofloxacin resistant Pseudomonas keratitis. Ophthalmology 1999;106:1319-1323.

[86] Liu C, Zhao Q, Liu Y, Wang S, Abel EW. Reduction of bacterial adhesion on modified DLC coatings. Colloids and Surfaces B-Biointerfaces 2008;61:182-187.

[87] Stubblefield BA, Howery KE, Islam BN, Santiago AJ, Cardenas WE, Gilbert ES. Constructing multispecies biofilms with defined compositions by sequential deposition of bacteria. Applied Microbiology and Biotechnology 2010;86:1941-1946.

[88] Selinger DS, Selinger RC, Reed WP. Resistance to Infection of External Eye - Role of Tears. Survey of Ophthalmology 1979;24:33-38.

[89] Tran V, Fleiszig S, Evans D, Radke C. Dynamics of Flagellar and Pilus-mediated Pseudomonas aeruginosa Surface Association with Contact Lenses. Applied and Environmental Microbiology 2011;77:3644-3652.

[90] Drake D, Montie TC. Flagella, motility and invasie virulence of *Pseudomonas-aeruginosa*. Journal of General Microbiology 1988;134:43-52.

[91] Giltner CL, van Schaik EJ, Audette GF, et al. The Pseudomonas aeruginosa type IV pilin receptor binding domain functions as an adhesin for both biotic and abiotic surfaces. Molecular Microbiology 2006;59:1083-1096.

[92] Saiman L, Prince A. Pseudomonas-aeruginosa Pili Bind to ASIALOGM1 Which is Increased On The Surface of Cystic-Fibrosis Epithelial-Cells. Journal of Clinical Investigation 1993;92:1875-1880.

[93] Atabek A, Camesano TA. Atomic force microscopy study of the effect of lipopolysaccharides and extracellular polymers on adhesion of Pseudomonas aeruginosa. J Bacteriol 2007;189:8503-8509.

[94] Blanchard B, Nurisso A, Hollville E, et al. Structural Basis of the Preferential Binding for Globo-Series Glycosphingolipids Displayed by Pseudomonas aeruginosa Lectin I. J Mol Biol 2008;383:837-853.

[95] Myszka K, Czaczyk K. Characterization of Adhesive Exopolysaccharide (EPS) Produced by Pseudomonas aeruginosa Under Starvation Conditions. Current Microbiology 2009;58:541-546.

[96] Epstein A. Soft Contact Lens Fitting. In: Agarwal S, Agarwal A, Apple DJ, et al. (eds), *Textbook of Opthalmology.* New Delhi, India: Jaypee Brothers Medical Publishers; 2002:205-218.

[97] Moradi O, Modarress H, Noroozi M. Experimental study of albumin and lysozyme adsorption onto acrylic acid (AA) and 2-hydroxyethyl methacrylate (HEMA) surfaces. Journal of Colloid and Interface Science 2004;271:16-19.

[98] Nicolson PC, Vogt J. Soft contact lens polymers: an evolution. Biomaterials 2001;22:3273-3283.

[99] Tonge S, Jones L, Goodall S, Tighe B. The ex vivo wettability of soft contact lenses. Current Eye Research 2001;23:51-59.

[100] Amende MT, Hariharan D, Peppas NA. Factors Influencing Drug and Protein-Transport and Release From Ionic Hydrogels. Reactive Polymers 1995;25:127-137.

[101] Johnson BD, Beebe DJ, Crone W. Effects of swelling on the mechanical properties of a pH-sensitive hydrogel for use in microfluidic devices. Materials Science & Engineering C-Biomimetic and Supramolecular Systems 2004;24:575-581.

[102] Strom MS, Lory S. Cloning and Expression of the Pilin Gene of Pseudomonas-aeruginosa PAK in Escherichia-coli. Journal of Bacteriology 1986;165:367-372.

[103] Makin SA, Beveridge TJ. The influence of A-band and B-band lipopolysaccharide on the surface characteristics and adhesion of Pseudomonas aeruginosa to surfaces. Microbiology-Uk 1996;142:299-307.

[104] Kapoor Y, Chauhan A. Drug and surfactant transport in Cyclosporine A and Brij 98 laden p-HEMA hydrogels. Journal of Colloid and Interface Science 2008;322:624-633.

[105] Aye Aye M, Lee W, Mun S, Ahn C, Lee S, Yoon J. Influence of membrane surface properties on the behavior of initial bacterial adhesion and biofilm development onto nanofiltration membranes. Biofouling 2010;26:313-321.

[106] Bennett SM, Finlay JA, Gunari N, et al. The role of surface energy and water wettability in aminoalkyl/fluorocarbon/hydrocarbon-modified xerogel surfaces in the control of marine biofouling. Biofouling 2010;26:235-246.

[107] Lin MC, Svitova TF. Contact Lenses Wettability In Vitro: Effect of Surface-Active Ingredients. Optometry and Vision Science 2010;87:440-447.

[108] Chu Y, Varanasi PP, McGlade MJ, Varanasi S. pH-Induced Swelling Kinetics of Polyelectrolyte Hydrogels. Journal of Applied Polymer Science 1995;58:2161-2176.

[109] De-Wei Y, Olvera de la Cruz M, de Pablo JJ. Swelling and collapse of polyelectrolyte gels in equilibrium with monovalent and divalent electrolyte solutions. Journal of Chemical Physics 2009;131:194907 (194906 pp.).

[110] Toomey R, Tirrell M. Functional polymer brushes in aqueous media from self-assembled and surface-initiated polymers. Annual Review of Physical Chemistry 2008;59:493-517.

[111] Zhang J, Peppas NA. Synthesis and characterization of pH- and temperature-sensitive poly(methacrylic acid)/poly(N-isopropylacrylamide) interpenetrating polymeric networks. Macromolecules 2000;33:102-107.

[112] Chao GT, Deng HX, Huang Q, et al. Preparation and characterization of pH sensitive semi-interpenetrating network hydrogel based on methacrylic acid, bovine serum albumin (BSA), and PEG. Journal of Polymer Research 2006;13:349-355.

[113] Izumrudov V, Sukhishvili SA. Ionization-controlled stability of polyelectrolyte multilayers in salt solutions. Langmuir 2003;19:5188-5191.

[114] van der Heiden AP, Willems GM, Lindhout T, Pijpers AP, Koole LH. Adsorption of proteins onto poly(ether urethane) with a phosphorylcholine moiety and influence of preadsorbed phospholipid. Journal of Biomedical Materials Research 1998;40:195-203.

[115] Hermansson M. The DLVO theory in microbial adhesion. Colloids and Surfaces B-Biointerfaces 1999;14:105-119.

[116] Cannan RK, Kibrick A. Complex formation between carboxylic acids and divalent metal cations. J Am Chem Soc 1938;60:2314-2320.

[117] Berg HC. Chemotaxis in Bacteria. Annual Review of Biophysics and Bioengineering 1975;4:119-136.

[118] Kato J, Kim HE, Takiguchi N, Kuroda A, Ohtake H. Pseudomonas aeruginosa as a model microorganism for investigation of chemotactic behaviors in ecosystem. Journal of Bioscience and Bioengineering 2008;106:1-7.

[119] Ferrandez A, Hawkins AC, Summerfield DT, Harwood CS. Cluster II che genes from Pseudomonas aeruginosa are required for an optimal chemotactic response. Journal of Bacteriology 2002;184:4374-4383.

[120] Deziel E, Lepine F, Milot S, Villemur R. rhlA is required for the production of a novel biosurfactant promoting swarming motility in Pseudomonas aeruginosa: 3-(3-hydroxyalkanoyloxy)alkanoic acids (HAAs), the precursors of rhamnolipids. Microbiology-Sgm 2003;149:2005-2013.

[121] Hamaker HC. The London - Van Der Waals attraction between spherical particles. Physica 1937;4:1058-1072.

[122] Overbeek JTG. Chapter IV and VI. In: Kruyt HR (ed), *Colloid Science I: Irreversible Systems, Chapter IV and VI.* Amsterdam: Elsevier; 1952.

[123] Simoni SF, Bosma TNP, Harms H, Zehnder AJB. Bivalent cations increase both the subpopulation of adhering bacteria and their adhesion efficiency in sand columns. Environmental Science & Technology 2000;34:1011-1017.

[124] Soltys-Robitaille CE, Ammon DM, Valint PL, Grobe GL. The relationship between contact lens surface charge and in-vitro protein deposition levels. Biomaterials 2001;22:3257-3260.

[125] Fleiszig SMJ, Evans DJ. Pathogenesis of Contact Lens-Associated Microbial Keratitis. Optometry and Vision Science 2010;87:225-232.

[126] Bodey GP, Bolivar R, Fainstein V, Jadeja L. Infections Caused By Pseudomonas-aeruginosa. Reviews of Infectious Diseases 1983;5:279-313.

[127] Morgan PB, Efron N, Brennan NA, Hill EA, Raynor MK, Tullo AB. Risk factors for the development of corneal infiltrative events associated with contact lens wear. Investigative Ophthalmology and Visual Science 2005;46:3136-3143.

[128] Livermore DM. Multiple mechanisms of antimicrobial resistance in Pseudomonas aeruginosa: Our worst nightmare? Clinical Infectious Diseases 2002;34:634-640.

[129] Tran V, Sung YS, Radke CJ. Dynamics of Pseudomonas aeruginosa association with anionic hydrogel surfaces in the presence of aqueous divalent-cation salts. Journal of Colloid and Interface Science 2011;To appear.

[130] Roosjen A, Busscher HJ, Nordel W, van der Mei HC. Bacterial factors influencing adhesion of Pseudomonas aeruginosa strains to a poly(ethylene oxide) brush. Microbiology-Sgm 2006;152:2673-2682.

[131] Cloete TE, Jacobs L. Surfactants and the attachment of Pseudomonas aeruginosa to 3CR12 stainless steel and glass. Water Sa 2001;27:21-26.

[132] Ketelson HA, Meadows DL, Stone RP. Dynamic wettability properties of a soft contact lens hydrogel. Colloids and Surfaces B-Biointerfaces 2005;40:1-9.

[133] Subbaraman LN, Bayer S, Gepr S, et al. Rewetting drops containing surface active agents improve the clinical performance of silicone hydrogel contact lenses. Optometry and Vision Science 2006;83:143-151.

[134] Carney FP, Nash WL, Sentell KB. The adsorption of major tear film lipids in vitro to various silicone hydrogels over time. Investigative Ophthalmology & Visual Science 2008;49:120-124.

[135] BASF. Safety data sheet Pluronic* F 127. 2007.

[136] Tran V, Fleiszig S, Evans D, Radke C. Dynamics of Flagellar and Pilus-mediated Pseudomonas aeruginosa Surface Association with Contact Lenses. Applied and Environmental Microbiology 2011.

[137] Rosenberg M, Gutnick D, Rosenberg E. Adherence of Bacteria to Hydrocarbons - A Simple Method For Measuring Cell-Surface Hydrophobicity. Fems Microbiology Letters 1980;9:29-33.

[138] Griffin WC. Calculation of HLB values of non-ionic surfactants. Journal of the Society of Cosmetic Chemists 1954;5:259.

[139] Schillen K, Claesson PM, Malmsten M, Linse P, Booth C. Properties of poly(ethylene oxide)-poly(butylene oxide) diblock copolymers at the interface between hydrophobic surfaces and water. Journal of Physical Chemistry B 1997;101:4238-4252.

[140] Boushehri A, Tang D, Shieh KJ, Prausnitz J, Radke CJ. Water transport through soft contact lenses determined in a fan-evaporation cell. Journal of Membrane Science 2010;362:529-534.

[141] Adamson AW, Gast AP. The Solid-Liquid Interface-Contact Angle. *Physical Chemistry of Surfaces.* New York: John Wiley & Sons, Inc; 1997:347-383.

[142] Vance RE, Rietsch A, Mekalanos JJ. Role of the type III secreted exoenzymes S, T, and Y in systemic spread of pseudomonas aeruginosa PAO1 in vivo. Infection and Immunity 2005;73:1706-1713.

[143] de Kerchove AJ, Weronski P, Elimelech M. Adhesion of nonmotile Pseudomonas aeruginosa on "soft" polyelectrolyte layer in a radial stagnation point flow system: Measurements and model predictions. Langmuir 2007;23:12301-12308.

[144] Knirel YA, Bystrova OV, Kocharova NA, Zahringer U, Pier GB. Conserved and variable structural features in the lipopolysaccharide of Pseudomonas aeruginosa. Journal of Endotoxin Research 2006;12:324-336.

[145] Angus AA, Lee AA, Augustin DK, Lee EJ, Evans DJ, Fleiszig SMJ. Pseudomonas aeruginosa induces membrane blebs in epithelial cells, which are utilized as a niche for intracellular replication and motility. Infection and Immunity 2008;76:1992-2001.

[146] Cheng L, Muller SJ, Radke CJ. Wettability of silicone-hydrogel contact lenses in the presence of tear-film components. Current Eye Research 2004;28:93-108.

[147] Harned HS, French DM. A Conductance Method For The Determination of The Diffusion Coefficients of Electrolytes. Annals of the New York Academy of Sciences 1945;46:267-284.

[148] Stewart SG, Newman J. The use of UV/vis absorption to measure diffusion coefficients in LiPF6 electrolytic solutions. Journal of the Electrochemical Society 2008;155:F13-F16.

[149] Berg HC. *Random walks in biology*. Expanded ed. Princeton, N.J.: Princeton University Press; 1993.

[150] Ford RM, Phillips BR, Quinn JA, Lauffenburger DA. Measurement of bacterial random motility and chemotaxis coefficients: I. Stopped-flow diffusion chamber assay. Biotechnology and Bioengineering 1991;37:647-660.

[151] Axelrod D, Koppel DE, Schlessinger J, Elson E, Webb WW. Mobility measurement by analysis of fluorescence photobleaching recovery kinetics. Biophysical journal 1976;16:1055-1069.

[152] Emanuel A, Olander DR. Diffusion Coefficients of Copper Sulfate in Water and Water in n-Butyl Alcohol. Journal of Chemical & Engineering Data 1963;8:31-32.

[153] Kato J, Kim H-E, Takiguchi N, Kuroda A, Ohtake H. Pseudomonas aeruginosa as a model microorganism for investigation of chemotactic behaviors in ecosystem. Journal of Bioscience and Bioengineering 2008;106:1-7.

[154] Baracchini O, Sherris JC. The chemotactic effect of oxygen on bacteria. The Journal of Pathology and Bacteriology 1959;77:565-574.

Appendix A: Bacterial Adhesion Studies With a Flow-Chamber designed for Viable-Cell Counting

A.1 Abstract

In the main text, all bacteria adhesion experiments were done with an optical flow chamber that allowed for bacteria adhesion to be viewed in-situ via microscopy. However microscopy is not always available. Therefore a larger parallel-plate flow chamber was used in conjunction with viable cell counting to evaluate bacterial adhesion. This flow chamber is simpler to use than the one used in Chapters 2-4 because the soft-contact lenses do not need to be cored and then mounted since optics are not important. This flow chamber was made and used prior to the use of the optical flow chamber. In this study, *Pseudomonas aeruginosa* strain PAO1 adhesion to commercial soft-contact lenses was evaluated with the vialble-cell-count flow chamber. The method was used to determine the efficacy of surfactants Tetronic 1304 and AL-52700 for reduction in bacterial adhesion to Acuvue 2, a traditional hydrogel soft contact lens, and two silicone hydrogels – Acuvue Advance and Pure Vision. Results show bacteria uptake is linear with concentration and exposure time. A simple first-order reversible/irreversible adhesion kinetic model demonstrates bacterial uptake to be linear with concentration and time. The ratio of experimental bacteria uptakes divided by maximum adherence as determined by Lèvêque solution gives the adhesion efficiency. Efficiencies are about 27-47% without significant difference among the three lenses. Polymeric surfactants Tetronic 1304 and AL-52700 were evaluated for surface modification and bacterial adhesion reduction. Tetronic 1304 was only effective in increasing wettability in Acuvue 2 lenses. However, it reduced bacterial adhesion significantly for all three lenses. AL-52700 increased wettability and reduced bacterial adhesion significantly for all three lenses. These results are in contradiction to what was found for PAO1 in Chapter 4 where wettability did not play a role.

A.2 Background

Numerous techniques to measure bacterial adhesion have been employed as described in Chapter 2. As mentioned, use of a well-defined flow system such as a parallel plate flow chamber allows for control over mass transport limitations, especially if the suspension is shaken to prevent bacteria from settling. Flow systems are beneficial because mass transport can be predicted. The shear rate, bacteria concentrations etc. can be controlled thereby allowing quantitative analysis of the results such as kinetics of adhesion. In the studies presented in Chapter 2-4, a small parallel-plate flow chamber under phase microscopy was used. Use of microscopy allows for better insight into how the bacteria are binding. However, prior to creation of the small flow chamber, microscopy was not available. Therefore, previously a flow chamber utilizing viable cell counting to enumerate adhered bacteria was created. This viable-cell-count flow chamber was not intended for use with microscopy and thus there are structural differences between the first flow chamber and the one mentioned in Chapters 2-5. More detail on the first flow chamber is in the Materials and Methods section.

A.3 Materials and Methods

A.3.1 Contact Lenses

For this study, three commercially available soft contact lenses were used: Acuvue 2, Acuvue Advance, and Pure Vision. A popular lens, Acuvue 2 (Vistacon) is an ionic, etifilcon A, traditional HEMA based hydrogel with a water content of 58%. Acuvue Advance (Vistakon) is a non-ionic, galyfilcon, silicone hydrogel lens with a water content of 47%. Pure vision (Bausch & Lomb) is an ionic silcone hydrogel made of balifilcon A with a water content of 36%. Acuvue 2 and Acuvue Advance are marketed for daily wear; Pure Vision lenses are approved for extended wear. Acuvue 2 and Acuvue Advance have no surface treatments; however Acuvue Advance does release a wetting agent, polyvinalpyrrolidone (PVP). Pure Vision's surface is oxygen gas plasma treated thereby leaving behind hydrophilic silicate islands. [146]

A.3.2 Contact angles

Contact angle measurements were performed using the captive-bubble technique. A special contact lens holder secures the lens. A syringe connected to a pump injects air into the system creating the bubble. A finely focused video camera captures images of the contact angles and then sends them to the computer. The contact angles are extrapolated by fitting the lens and bubble curvatures with a polynomial and the angles are recorded in real time. Figure A.1 shows the advancing and receding angles as imaged by the camera. The bottom, dark curved surface is the lens and above this surface is the bubble contacting and forming the advancing and receding angles, respectively.

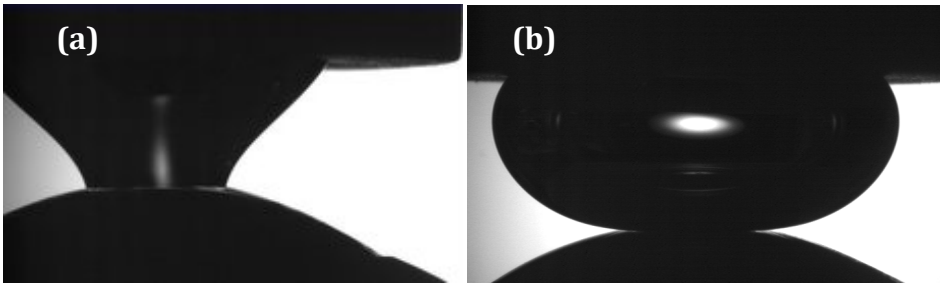


Figure A.1 Advancing(a) and receding angles (b)

All contact angles were measured on the posterior side of the contact lens in 0.1 M phosphate buffered saline (PBS) since vulnerability to bacterial infection is the highest for bacterial attached closest to the corneal surface. All lenses were soaked in solutions of interest in order to remove any wetting agents or preservatives that are contained in the blister packs which the lenses are stored in.

A.3.3 Viable-Cell-Count Flow Chamber

For all adhesion assays, a constant-shear laminar flow-cell was used, as shown in Figure A.2. The flow chamber was constructed of plexiglass. A contact lens was mounted to a Dacron holder that exposed only 6-mm diameter of the center section of the lens to the bacteria flow stream. This design differs from the optical-flow chamber in Chapters 2-4 because an intact-contact lens can be used. The smaller flow chamber demanded a flattened piece of the contact lens be mounted on glass so that light could pass through during microscopy.

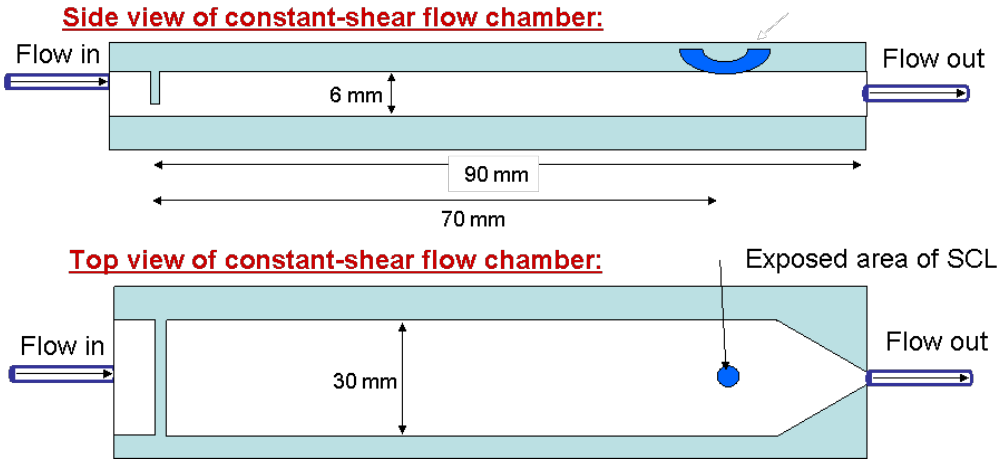


Figure A.2 Schematic of viable-cell count flow cell for bacterial adhesion assays

The viable-cell-count flow-cell was designed to create laminar flow in the flow cell as illustrated in Figure A.2. A relatively low shear rate of $0.35 s^{-1}$ was chosen. In addition, fully developed flow is ensured early in the flow cell. This was tested with flowing dye experiments. In addition, simulations in COMSOL validated the Reynolds number, shear rate and velocity flow field. Figure A.3 shows the COMSOL simulation of the velocity flow field is fully developed early in the flow cell.



Figure A.3 COMSOL results from velocity field in viable-cell counting flow-cell

A.3.4 Bacterial Adhesion Assays

For all adhesion assays a *Pseudomonas aeruginosa* strain, PA01, was used. PA01 is an invasive, laboratory strain that has been completely sequenced. PA01 bacteria grown overnight on Tryptic soy agar plates was re-suspended in nutrient-free PBS to 10^7 cfu/mL and then pumped through the cell in the laminar regime. The flow path allowed the suspended bacteria to contact a small area of the posterior side of the contact lens under study. After a fixed amount of flow time up to 2 h, the flow-cell was flushed for 90 min (10 flow-cell volumes) with nutrient-free, sterile PBS to wash away reversibly bound bacteria.

To quantify the number of irreversibly bound bacteria after exposure to the flow suspension the lenses were homogenized in 0.25 wt. % Triton X aqueous surfactant solution. 15-μL drops of the homogenized solution were then plated, and the bacteria were allowed to grow into individual colonies. The number of colony forming units (*cfu*) was then enumerated. Each colony formed corresponded to a single live progenitor bacterium adhered to the lens. Uptake of viable and irreversibly bound bacteria onto the lenses is reported in *cfu/mm²*.

A.3.5 Addition of Surfactants

Tetronic 1304 and AL-52700 surfactants were supplied by Alcon Labs. Tetronic 1304 is a tetra-functional block co-polymer (PEO-PPO) with a MW of 12,000. AL-52700 is a linear di-block co-polymer (PEO-PBO) with a MW of 4,000. In the bacteria-adhesion studies, all lenses were presoaked in 0.05 wt% surfactant/PBS solutions for 24-40 h and then assayed after rinsing. Lenses were rinsed with PBS by dipping ten times in clean PBS.

A.4 Results and Discussion

A.4.1 Contact Angles

After soaking in PBS for 24-40 h. The advancing contact angle of Pure Vision was about 90°. Acuvue 2 exhibited similar contact angle results to Pure Vision with an advancing contact angle of about 90°. Acuvue Advance, however, had a much lower advancing contact angle of about 40°. All three lenses exhibited small receding angles around 10-20 degrees. A summary of the advancing contact angle results is in Figure A.4.

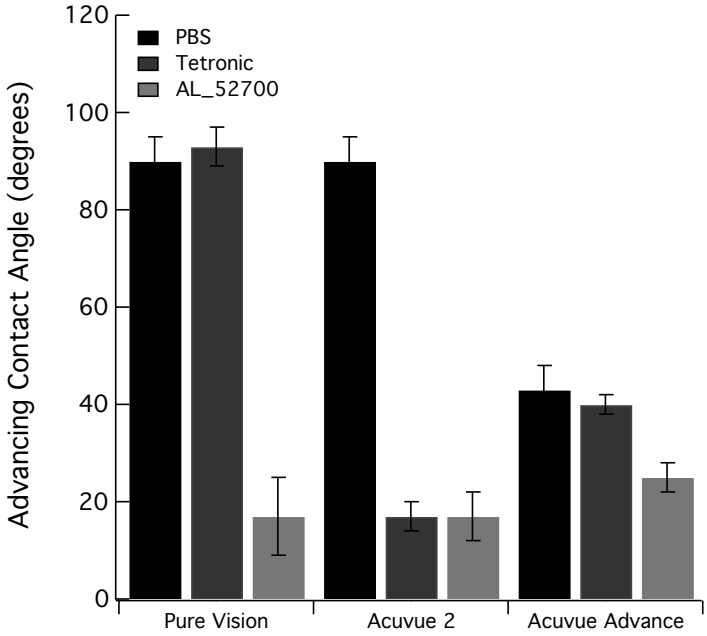


Figure A.4 Advancing contact angles for Pure Vision, Acuvue 2 and Acuvue Advance after soaking in PBS, Tetronic or AL-52700 solutions.

With prior exposure to Tetronic 1304, the advancing and receding angles of Pure Vision and Acuvue Advance did not differ from those after PBS exposure either. However, the addition of Tetronic 1304 significantly changed the advancing angle of Acuvue 2 to about 17°.

Unlike previous results for Tetronic 1304, the advancing contact angle of Pure Vision after soaking in AL-52700 for two days decreased substantially to about 21°. Similar results were obtained for Acuvue Advance and Acuvue 2 in the AL-52700 surfactant. Thus surface hydrophobicity decreased substantially for all three lenses after exposure to AL-52700.

A.4.2 Bacterial Adhesion

With the first constant-shear flow-cell, the bacterial uptake of all three lenses was shown to have a linear relationship with time. Figure A.5 shows the uptake in bacteria versus time for Acuvue 2, Acuvue Advance, and Pure Vision lenses. Within the precision of the experimental technique, there is little difference in uptake between the lenses, although Pure Vision has a slightly higher uptake. Thus, the longer the exposure of the lens to bacteria the higher is the uptake. It should be noted that Borazani et al, also found little difference for *P. aeruginosa* adhesion to balifilcon (Pure Vision) and etifilcon A (Acuvue 2) lenses. [58]

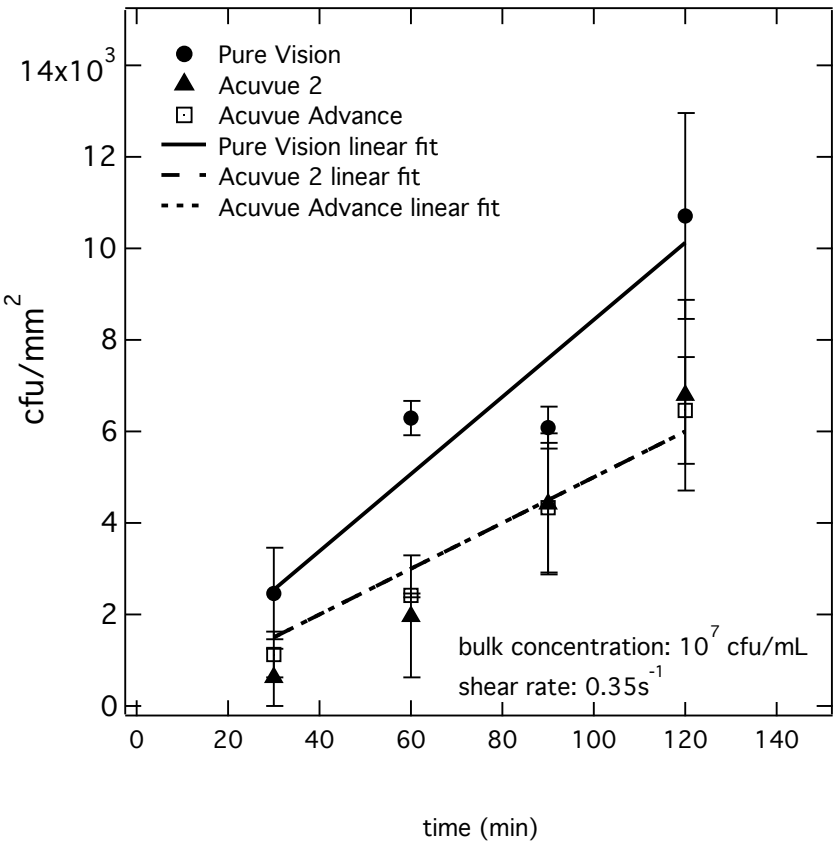


Figure A.5 Bacterial uptake versus time for viable-cell-count flow cell. The error bars are the standard deviations of 2 or more experiments

After two days of presoaking in PBS, bacterial uptake of all three lenses in the viable-cell-count flow cell showed a linear relationship with respect to bulk bacteria concentration. Figure A.6 shows the bacteria uptake vs. bulk bacteria concentration for Pure Vision lenses on a log-log scale. Importantly, even at the highest concentration of bacteria used, the maximum surface coverage is about 1.5%. Additionally, Figure A.6 has a slope of unity. This result indicates that the bacteria adhere as single units rather than in clumps and that there is no interference from previously attached bacteria. This result also suggests that at the concentrations studied, the bacteria do not signal each other to adhere.

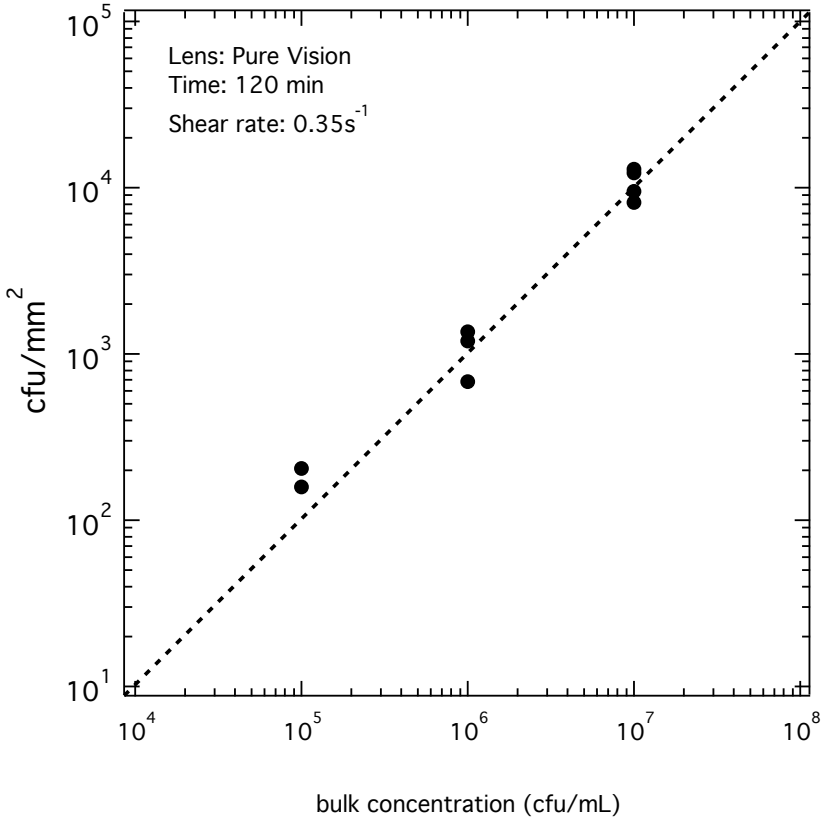


Figure A.6 Bacterial uptake vs. bulk bacteria concentration for Pure Vision lenses

The Lèvêque equation ascertains the maximum rate of bacterial uptake by the expression,

$$R_{\max} = 0.538\left(\frac{\gamma}{x}\right)^{\frac{1}{3}} D^{\frac{2}{3}} C_0 \qquad \text{(A-1)}$$

where R_{max} is the maximum rate as dictated by Lèvêque, γ is the shear rate, x is the distance from the baffle to the contact lens, D is the diffusion coefficient of the bacteria and C_0 is the bulk bacteria concentration in the flow. Once the bacterium diffusion coefficient is known (see Appendix B), the Lèvêque model in Eqn A-1 permits calculation of the maximum bacterium collision frequency with the lens surface. The slope of the lines in Figure A.5 give the rate of viable, irreversible uptake, *R.* Note that the collision frequency of bacteria with the surface of the lens, R_{max}, is much greater than the measured irreversible-bound rates. This result means that only a fraction of bacteria colliding remain irreversibly adhered. This fraction is the adhesion efficiency or R/R_{max}. Results for the adhesion efficiency at a concentration of 10^7 *cfu/mL* are shown in Table A.1. Typical efficiencies for bacterial irreversibly sticking to the lens surface are about 27-46 %. Although Pure Vision lenses seem to adhere more bacteria, the difference is not within our measurement error.

TABLE A.1: ADHESION EFFICIENCY

Lens	Adhesion Efficiency
Acuvue 2	27± 12%
Acuvue Advance	27± 12%
Pure Vision	46±19%

A.4.3 Role of Polymeric Surfactants in Bacterial Adhesion

Figure A.7 reveals that exposure to Tetronic 1304 surfactant significantly decreases the bacterial uptake after 1 hour for all three lenses. This result is not consistent with the hydrophobicity measurements of the lens surface gauged by the contact angle measurements that had shown a decrease in advancing contact angles only for Acuvue 2. Exposure to AL-52700 decreased bacterial uptake for all three lenses consistent with the contact angle measurements.

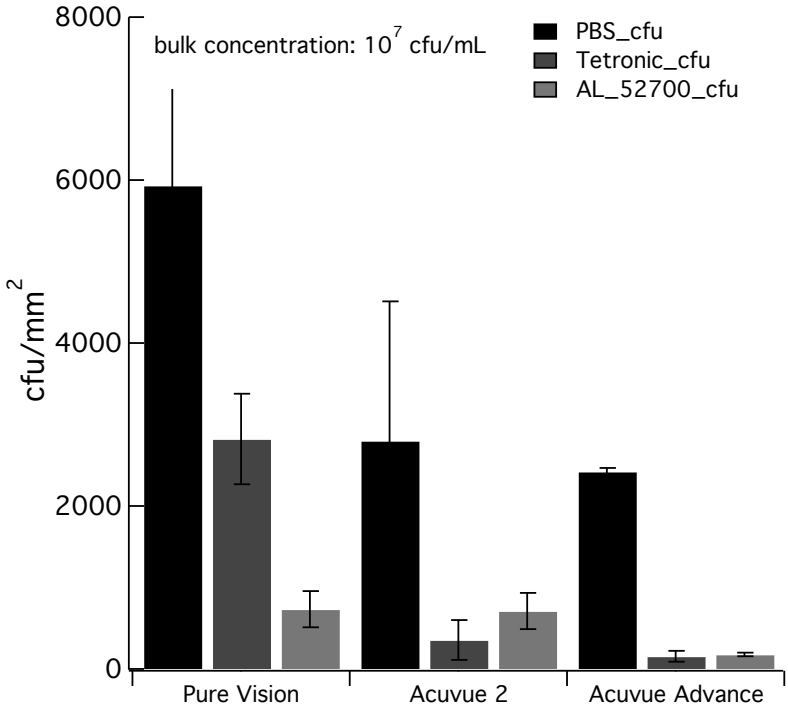


Figure A.7 Effect of surfactant addition in contact lenses on bacterial adhesion

A.4.4 Adhesion kinetic model

To understand the adhesion kinetics, a simple reversible, irreversible adhesion model is proposed. An illustration of this model is shown in Figure A.8. In this model, bacteria transport from the bulk solution to the surface by convective diffusion as dictated by Lèvêque. $k_m = 0.538\left(\frac{\gamma}{x}\right)^{\frac{1}{3}} D^{\frac{2}{3}}$ Initially, bacterial uptake is reversible in the amount per unit area of Γ_R. Reversibly adsorbed bacteria transform into irreversibly attached microbes in the amount per unit of Γ_I. Due to very low bacterial surface coverage, all kinetic steps are assumed as first order.

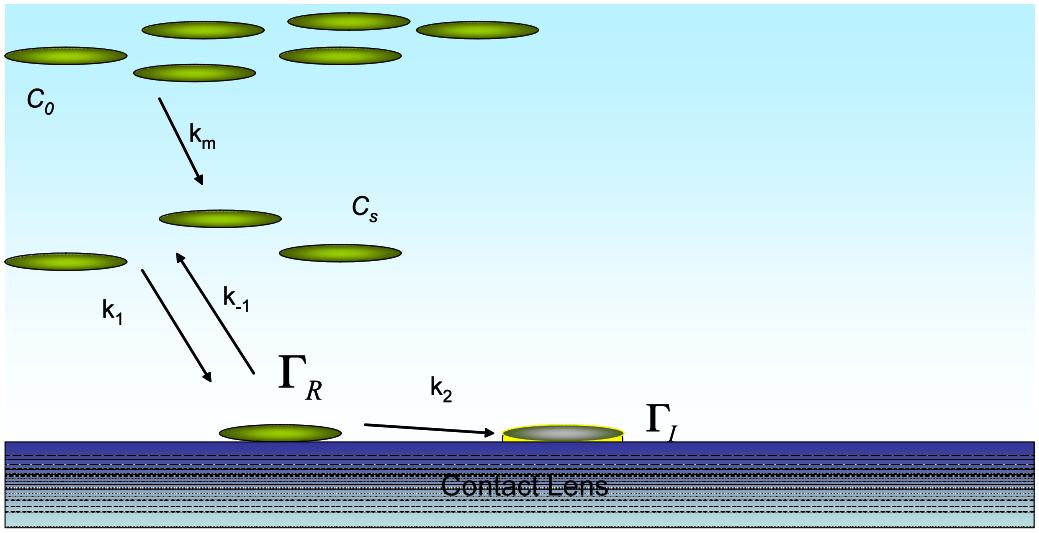


Figure A.8 Kinetic model to describe bacterial adhesion to soft contact lenses.

The kinetic expression for the reversible uptake is then:

$$\frac{d\Gamma_R}{dt} = k_1 C_s - k_{-1}\Gamma_R - k_2\Gamma_R \tag{4}$$

While the irreversible uptake obeys the following expression:

$$\frac{d\Gamma_I}{dt} = k_2\Gamma_R \tag{5}$$

When this model is evaluated for equilibrium of C_s and Γ_R, the bacteria uptake is linear with concentration and time as with the experimental results. The results indicate that the evolution of bacterial uptake at long times is:

$$\frac{d\Gamma_I}{dt} = \frac{k_1 k_2 k_m}{k_{-1}k_m + k_2 k_m + k_1 k_2} C_0 \tag{6}$$

This simple model agrees with observed kinetic behavior. In addition, Bussher et al describes a two step kinetic behavior for *Streptococcus sanguis* adhesion to polymer substrates. Their findings indicate that after an initial period of adhesion where attachment is reversible, the bacteria adhesion increases steadily. [21] Thus the results found in these experiments are similar. These results also indicate that some means for estimating the reversible uptake should be sought.

A.5 Conclusions

A parallel-plate constant-shear laminar flow cell utilizing viable-cell counting was developed to create a reliable bacterial adhesion assay. Results indicate that PA01 adheres to untreated Pure Vision, Acuvue Advance and Acuvue 2 lenses linearly with time and concentration. However, there is no significant difference in adhesion efficiency among the three untreated lenses despite significant differences in material and contact angles. Of the three lenses, the addition of Tetronic 1304 polymeric surfactant only decreased the contact angle of Acuvue 2. However, this surfactant still decreases bacterial adhesion for all the lenses. The addition of AL-52700 polymeric surfactant significantly decreases contact angles and bacterial adhesion for all three lenses. To understand bacterial adhesion efficiency and kinetics, the Lèvêque transport model was employed as a limiting case for maximum bacterial uptake. In order to apply Lèvêque theory, the effective diffusion coefficient of PA01 was set to be $1x10^{6}$ cm^2/s. PA01 adhesion efficiencies on native lenses are about 27-47%.

Furthermore, a simple first order reversible/irreversible adhesion kinetic model demonstrates that bacterial uptake is linear with concentration and time. This model therefore agrees with observed kinetic behavior in the constant-shear flow cells.

Appendix B: Determination of Effective Diffusion Coefficient of motile *Pseudomonas aeruginosa* via Restricted Diffusion

B.1 Abstract

Restricted diffusion (i.e., diffusion in a closed container) is a well-known method for measuring diffusion coefficients of aqueous electrolytes.[147,148] Here, the method has been implemented to determine the effective diffusion coefficients of aqueous swimming-motile *Pseudomonas aeruginosa*. Results illustrate motile bacteria are able to achieve effective diffusion coefficients on the order of 10^{-6} cm^2/s which is three orders of magnitude higher than that predicted by Stokes Einstein for a non-motile particle.

B.2 Introduction

Many strains of *Pseudomonas aeruginosa* are motile due to a single flagellum, which allows the bacterium to swim in straight lines punctuated with random tumbles. This movement gives way to a random walk or random motility coefficient. Random-walk motion can be interpreted as a diffusion coefficient, *D*. Measuring the diffusion coefficient of motile bacteria is a nontrivial task. Methods include using three dimensional tracking [149] and stopped-flow chambers [150]. Bacterial effective diffusion coefficients for motile bacteria are on the order of $10^{-6}cm^2/s$.[149,150]

To evaluate the maximum possible rate of bacterial uptake via the Lèvêque equation as in Chapter 2, the effective diffusion coefficient of the bacterium must be known. There are a number of methods available for measuring diffusion coefficients of colloids. One method of measurement for proteins and large molecules is fluorescence recovery after photobleaching (FRAP).[151] However, bacteria are relatively large and the area that needs to be bleached is therefore large. Attempts to utilize FRAP proved not possible since the time necessary to bleach such a large area of bacteria was long and damaging to the bacteria. In addition, a large concentration of bacteria are required which causes clumping of the bacteria making it impossible to have representative data for individual bacteria moving. 2-D tracking of the bacteria was also attempted but the bacteria moved too quickly out of view. Thus restricted diffusion was explored.

B.3 Methods

B.3.1 Bacteria preparation

PAO1 bacteria were provided by Professor Suzanne Fleiszig at UC Berkeley. Using a polyester-tipped sterile swab (Fisher Scientific), frozen bacteria stocks were aseptically streaked out onto Tryptic Soy agar plates (Becton, Dickinson, and Company, Franklin Lakes, NJ). The plates were incubated at 37 °C overnight at which point bacteria lawns were present on the plates. The bacteria were then resuspended in M9 minimal media to a concentration of $4x10^8$ cfu/mL to provide minimal nutrients during the experiment, which are required for respiration and thus swimming motility.

B.3.2 Restricted Diffusion

The restricted diffusion apparatus utilized was a UV/Vis setup (Ocean Optics, Dunedin, Fl) similar to Stewart et al.[148] An illustration of the setup used is shown in Figure B.1. 0.6 mL of the bacteria suspension was carefully pipetted into a quartz, black-walled cuvette (Starna Cells, Atascadero, CA). The cuvette was 4 mm wide, 1 cm deep and about 3 cm tall. 0.6 mL of sterile water was then carefully pipetted above the bacteria suspension into the cuvette. Sterile water was used because it is less dense then the minimal medium solution. A density difference is required to create a stable interface for restricted diffusion. Additionally, the denser phase must be at the bottom of the cuvette. A dual channel S200-R spectrometer was used. A deep-UV-deuterium bulb was used as a light source, which emitted a focused beam of light into a designated location of the cuvette, and a detector monitored the change in absorbance at 650 nm with time. A specially designed cuvette holder determines where on the cuvette the light source is focused. An extreme solarization-resistant (XSR) cable was spliced after leaving the light source. One half of the

light was sent to a cuvette containing PBS and the other half when to the sample. This allowed for correction of any bulb fluctuations over time.

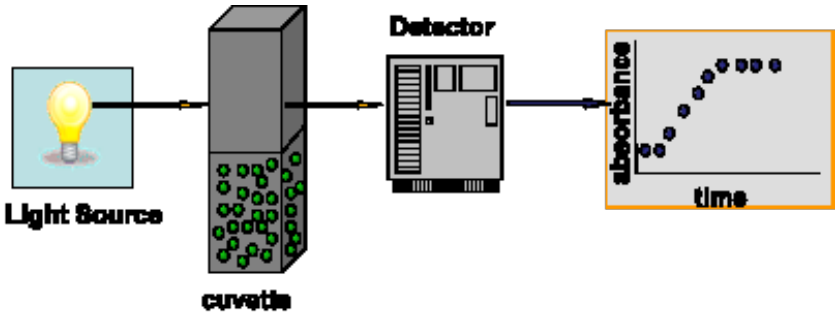


Figure B.1 Schematic of the restricted-diffusion method. Upward diffusion of the bacteria is detected by UV/vis absorbance

B.4 Results and Discussion

Copper sulfate was used as a control to ensure that the method was reliable. Copper sulfate absorbance is linear in the solution concentrations used of 0.5 M and less. Restricted diffusion results are shown in Figure B.2. For simple salts diffusing, the diffusion coefficient can be determined by Eqn B-1 by measuring the change in the absorbance: *A-A** where *A* is the absorbance varying in time and A* is the absorbance at infinite time. *D* is the diffusion coefficient and *L* is the height of the liquid in the cuvette. In these cases, the absorbance can be taken anywhere along the liquid length in the cuvette except at the interface of the two different solutions.

$$\frac{d\left(\ln(A - A^*)\right)}{dt} = -\frac{\pi^2 D}{L^2} \qquad \text{(B-1)}$$

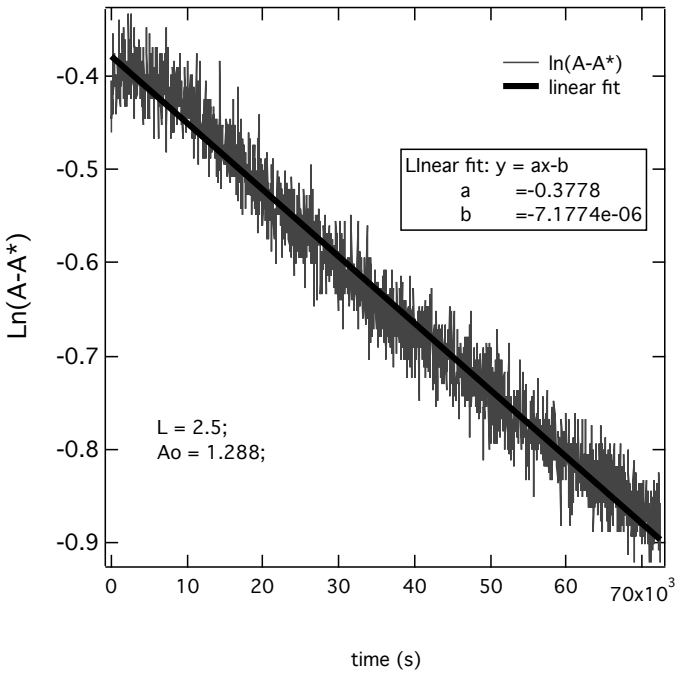


Figure B.2 Restricted diffusion results for 0.5 M copper sulfate at ambient temperature.

With the restricted-diffusion method, the experimental diffusion coefficient was determined to be 4.54 x 10^{-6} cm^2/s which is in excellent agreement with the literature value of 4.47 x 10^{-6} cm^2/s.[152]

For the concentrations of bacteria studied, optical absorbance is also linear with concentration (data not shown). Thus, from the absorbance-versus-time data, a random motility/effective diffusion coefficient is determined. Diffusion fluxes are small so the measurements last hours. During this time frame, the bacteria also settle towards the bottom of the cuvette under the action of gravity. Thus, a continuum diffusion model is necessary to establish the diffusion coefficient from the absorption data must include a term for convective settling flux:

$$\frac{\partial C}{\partial t} + v\frac{\partial C}{\partial x} = D\frac{\partial^2 C}{\partial x^2} \qquad \text{(B-2)}$$

C(t,x) is the local concentration of bacteria with *x* measured from the bottom of the cuvette and *v* is the terminal settling velocity. Based on Stokes law for settling of a randomly oriented rod, the bacteria were estimated as having a settling velocity of 3x10^{-6}cm/s. Solution of Eqn B-1 for zero-flux boundary conditions at the cuvette ends is given in the in Eqn B-3 . Once *C(t,x)* is measured, the solution to Eqn B-1 is bet fit to obtain the bacteria diffusion coefficient.

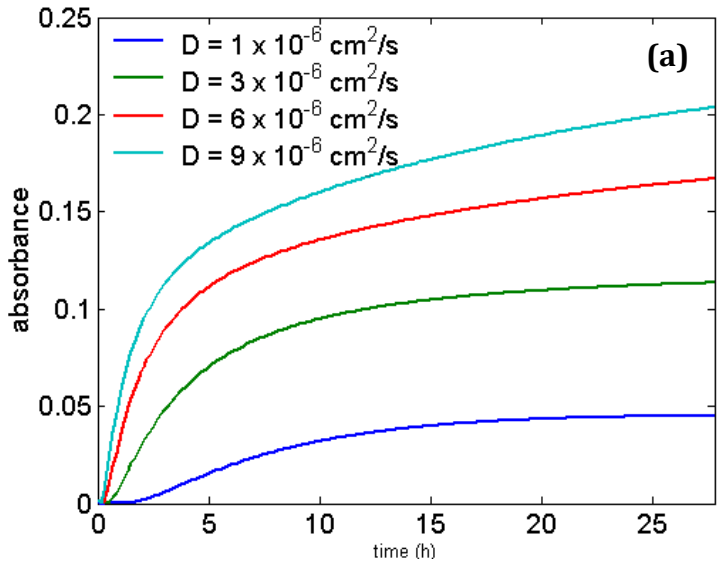
Solution to Eqn B-2:

$$C(x,t) = C_{ss} + \sum_1^\infty A_n e^{-\lambda_n t} e^{ax}\left(\cos(bx) + B\sin(bx)\right) \qquad \text{(B-3)}$$

Where: $\lambda_n = \frac{n^2\pi^2 D}{L^2} + \frac{v^2}{4D}$, $a = v/2D$, $b = \frac{\sqrt{4D\lambda - v^2}}{2D}$, $C_{ss} = \frac{C_0 dv/D}{e^{vL/D} - 1} e^{vx/D}$, $B = \frac{v - aD}{Db}$

$$A_n = \frac{C_0\left[\frac{e^{-ad}(b - aB)\sin(bd) - (a + bB)\cos(bd)}{a^2 + b^2} + \frac{(a + Bb)}{a^2 + b^2}\right] - \frac{C_0 dv}{De^{vL/D} - D}\left[\frac{e^{aL}\left((a - bB)\cos(bL) + (b + aB)\sin(bL)\right)}{a^2 + b^2} - \frac{(a - bB)}{a^2 + b^2}\right]}{\frac{2bL + \sin(2bL)}{4b} + B^2\left(L/2 - \frac{\sin(2bL)}{4b}\right) + \frac{-2B\cos(bL)^2 + 2B}{2b}}$$

To obtain a "best" diffusion coefficient with the restricted diffusion technique, experimental transient absorbance curves were fit according to Eqn B-3. Before doing so, the effects of varying the diffusion coefficient and settling velocity were determined as shown in Figure B.3. Figure B.3a shows the variation in absorbance versus time plots for various values of a diffusion coefficient at a fixed value of 3E-6 cm/s. The diffusion coefficient plays a role in setting the initial slope of the absorbance versus time behavior. Figure B.3b shows the variation in absorbance vs. time plots for various values of a settling velocity. The settling velocity sets the asymptotic behavior as the bacteria concentration profile reaches steady state. Therefore, affects due to the bacteria settling become more relevant at the end of the experiment at long times.



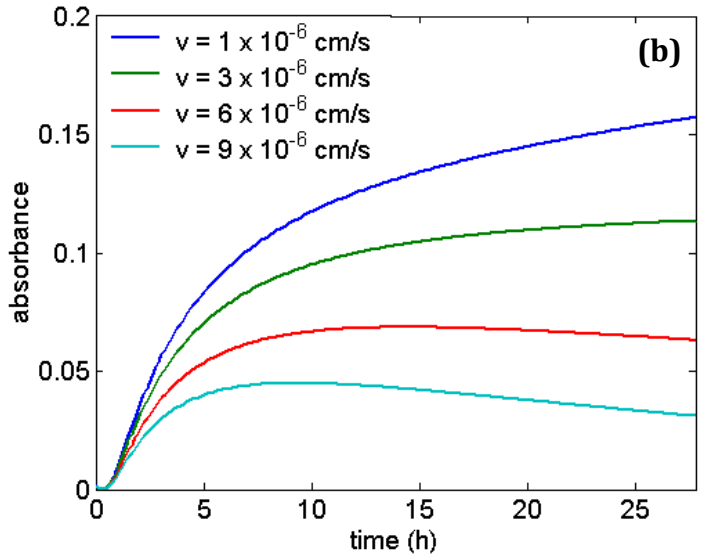


Figure B.3 Variation in absorbance vs. time for various values of (a) diffusion coefficient where v is 3E-6cm/s and settling velocity (b) where D is 3E-6cm^2/s

Figure B.4 shows the results for three separate experiments. The result shows that within the first few hours, the absorbance increases. After a few hours, it rapidly increases and then plateaus. Additionally in Figure B.4 are the "best" diffusion coefficient fits. The fit is done manually by eye. The proposed settling-model does not fit the data well. However, a lower estimate of 2x10^{-6} cm^2/s is obtained as well as upper estimate of 5x10-6 cm^2/s as shown.

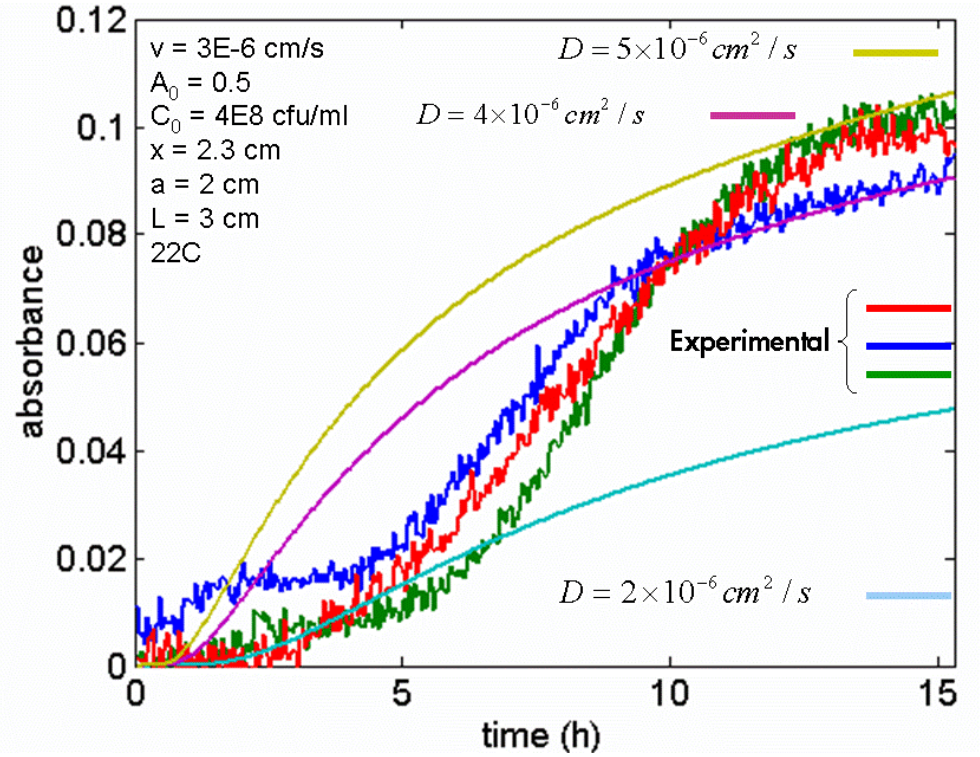


Figure B.4 Restricted diffusion results. Numbers in the upper left of the figure give pertinent dimensions and conditions of the optical cuvette.

It is hypothesized that the dramatic increase after 5 hours is not due to the random swimming behavior of the bacteria. Instead, it is proposed that it is a result of aerotaxis. It is known that *Pseudomonas aeruginosa* swims in directions of an attractant provided there is a chemical gradient. The experiments last for hours and in that time, the bacteria most likely use up the oxygen in the cuvette and can move in directions of oxygen gradients.[153] At the end of the experiments, a layer of bacteria at the top of the cuvette indicative of aerotaxis can be seen.[154]

The hypothesis is that the initial increase in absorbance within the first 5 hours is actually due to random swimming motility. Figure B.5 shows a fit for a diffusion coefficient of 1 x 10^{-6} cm^2/s. This estimation fits well with the predicted delay before absorbance increase and the slope of absorbance increase. Interestingly, Berg demonstrates for *E. coli* and Ford et al. for *Pseudomonas putida* effective diffusion coefficients on the order of 10^{-6} cm^2/s.[149,150] These findings emphasize the strong role that flagellum-driven motility plays in PA01 diffusion flux and how bacteria cannot be treated simply as inanimate colloidal particles.

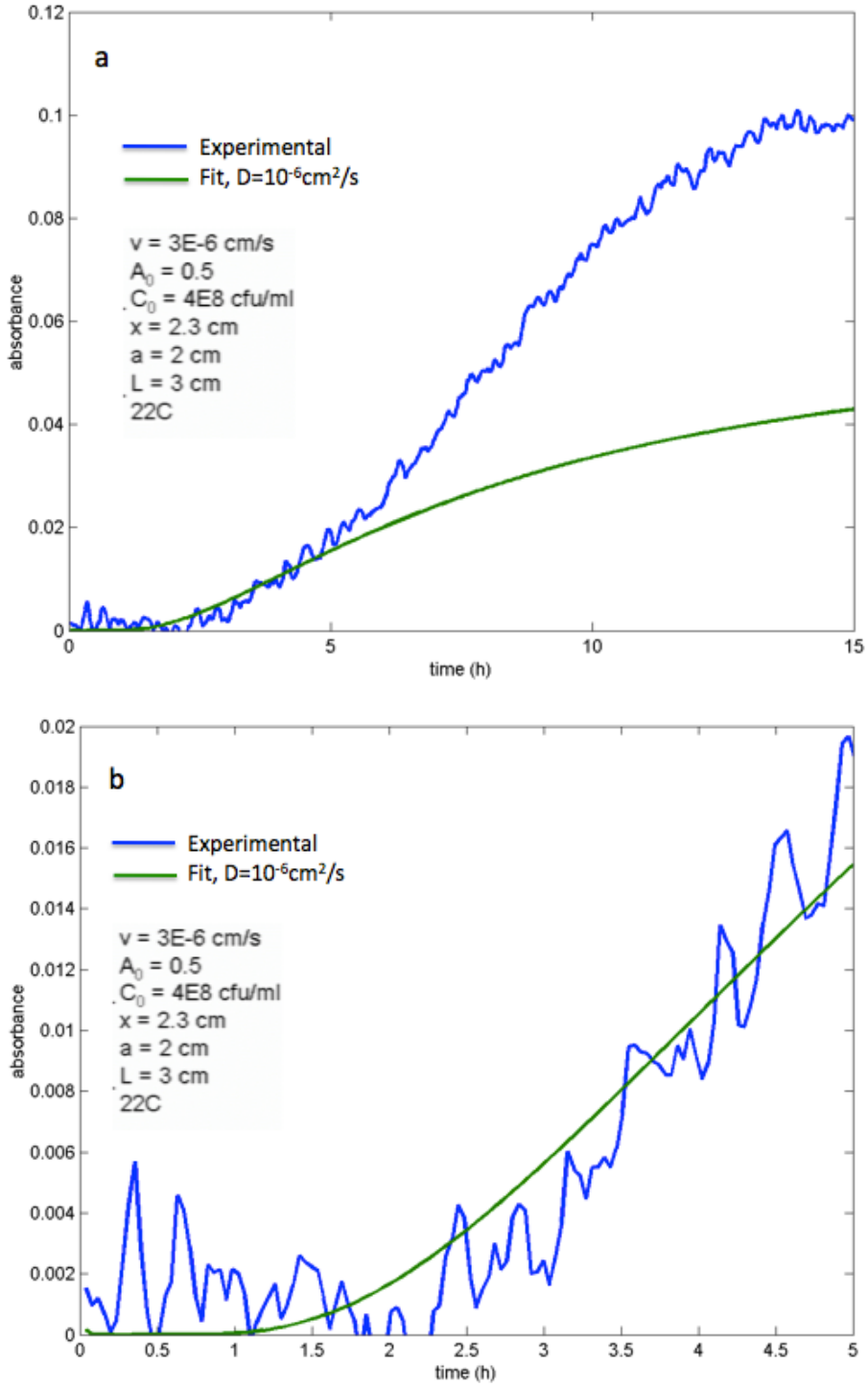


Figure B.5 Restricted diffusion fit for 5 hours.

Appendix C: Optical Flow Chamber Information

C.1 Introduction

For all of the bacterial adhesion uptake experiments as mentioned in Chapters 2-4, an optical flow chamber was utilized. This chamber was designed and constructed so that well-developed laminar flow could be created within the chamber. Therefore, meaningful kinetic measurements could be made. This chapter provides important information regarding the optical flow chamber used for bacterial-adhesion studies. It summarizes, the flow chamber setup in addition to its flow dynamics.

C.2 Flow chamber preparation

A schematic of the optical-flow chamber can be found in Chapter 2. As mentioned, the chamber was made of G-10 epoxy resin. This resin is autoclavable along with the silicone spacers. However, persistent autoclaving is a problem because it causes the silicone spacers to disfigure. This makes it difficult for the spacers to fit the flow chamber and leaking may occur. Thus, another cleaning mechanism was employed as follows.

Prior to each experiment, the flow chamber is washed by soaking in 1% house-hold bleach in distilled water for 14 hours. The flow chamber is then scrubbed with a standard Alconox™ solution and rinsed repeatedly with distilled water. The chamber is then allowed to dry overnight in an oven at 60 °C. Oven drying further sanitizes the chamber. Additionally, it is critical to dry out the silicone spacers prior to an experiment in order for them to fit properly into the flow chamber. After an experiment, the flow chamber is disassembled and soaked in a 1% bleach solution overnight.

C.3 Flow chamber, pump and microscope set-up

For each experiment, an autoclaved 250-mL, glass beaker stores the bacteria in the aqueous solution of interest. The solution is stirred gently with a stir bar. The beaker is covered with aluminum foil to prevent excess contamination from the air. Silicone tubing (size 13, Masterflex, Cole Palmer, Vernon Hill, IL) is placed into the beaker and the tubing connects to the syringe pump entrance port. Exiting the syringe pump, is also silicone tubing about 1.5 feet in length. The end of this silicone tubing is connected to 1.5 ft of polytetrafluoroethylene (PTFE) tubing (0.125 cm diameter, Masterflex), which is then connected to the entrance of the flow chamber. The exiting flow chamber tubing is also about 1.5 ft of PTFE tubing (0.125 cm diameter). The waste stream flows into an autoclaved 250-mL beaker, which is also covered by aluminum foil.

As mentioned in Chapter 2, fluid is pumped into the flow chamber via a syringe pump. Although, a peristaltic pump is possible given the tubing material, it is not recommended. A peristaltic pump creates a pulsing flow, that vibrates the entire flow chamber, and the microscope optics become difficult. Attempts were made to dampen the pulsing but they were not enough to stabilize the optics.

During an experiment, the flow chamber rests on the microscope stage via a specially designed chamber holder made of stainless steel. As mentioned in Chapter 2, 40x and 60x objectives were used for a total of 400x and 600x magnification, respectively. 600x was used for real-time video microscopy because the resolution of the analog camera used was lower than that of the digital camera used to take time-lapse images. A 20x

objective can also be used, but the bacteria are very small and quantification is difficult. 100x cannot be used with a contact lens or synthesized membrane surfaces because the working distance is too small. If the working distance could be increased or the thickness of the membranes thinned, a 100x objective is possible but not necessary for the experiments performed.

C.4 Flow chamber hydrodynamics

COMSOL Multiphyics (COMSOL, Burlington, MA) was used to simulate the flow chamber hydrodynamics. To do so, a 3-dimensional geometry of the flow chamber was simulated to scale in the program. Incompressible Navier Stokes was used. For boundary conditions, the flow chamber inlet was set to the fluid velocity of 0.00736 m/s while the exit was set to a pressure of 0 Pa. All other boundaries were set to no slip. The fluid was set as water with a density of 1000 kg/m^3 and a viscosity of 0.00089 Pa-s. To solve Navier Stokes, the geometry was meshed with 1894 mesh pints and 7876 elements with 2030 boundary elements. The meshing was done automatically with the software. The calculation took 178 s to solve.

The optical flow chamber was designed to create well-defined, fully developed laminar flow across the contact lens surface. In order for this to be achieved, the contact lens must be positioned at an adequate distance away from the entrance port and away from the exit port. A baffle, located at the entrance port helps to distribute the flow. Figure C1 shows that the flow is fully developed well before it reaches where the contact lens is placed.

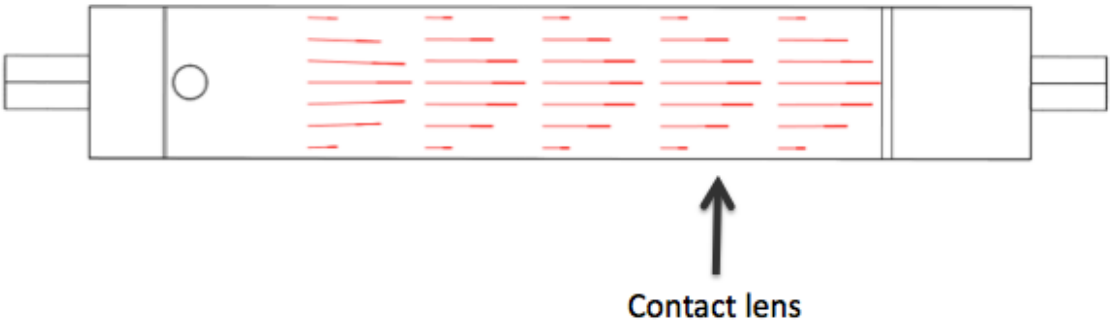


Figure C.1 COMSOL simulated velocity profile of optical-flow chamber.

Laminar flow was also confirmed by calculation of the Reynold's number. COMSOL Multiphysics was also used and as shown in Figure C.2 the Reynold's number is small throughout the flow chamber for the flow conditions used. In all experiments, laminar flow through the flow chamber was achieved. As demonstrated in Figure C.2 the Reynolds number is less than 16, well within the laminar flow regime.

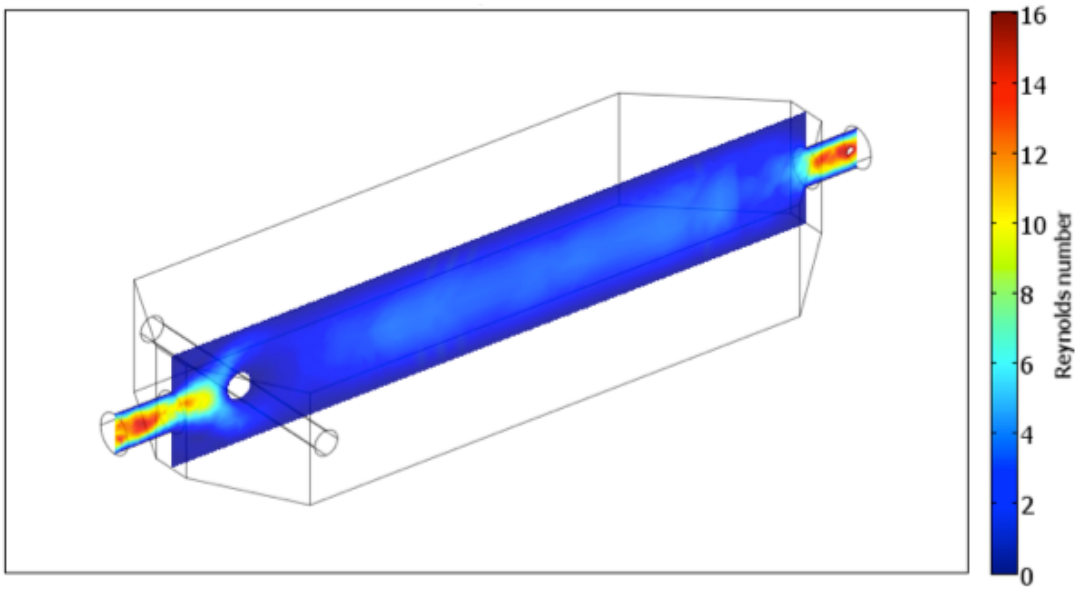


Figure C.2 COMSOL simulated Reynold's number in optical-flow chamber.

As mentioned in Chapter 2, the shear rate at the bottom wall where the contact lens is located is 0.2 s^{-1}. Figure C.3 shows a COMSOL simulation of the shear rate throughout the flow chamber. The shear rate is 0.2s^{-1} throughout the flow chamber.

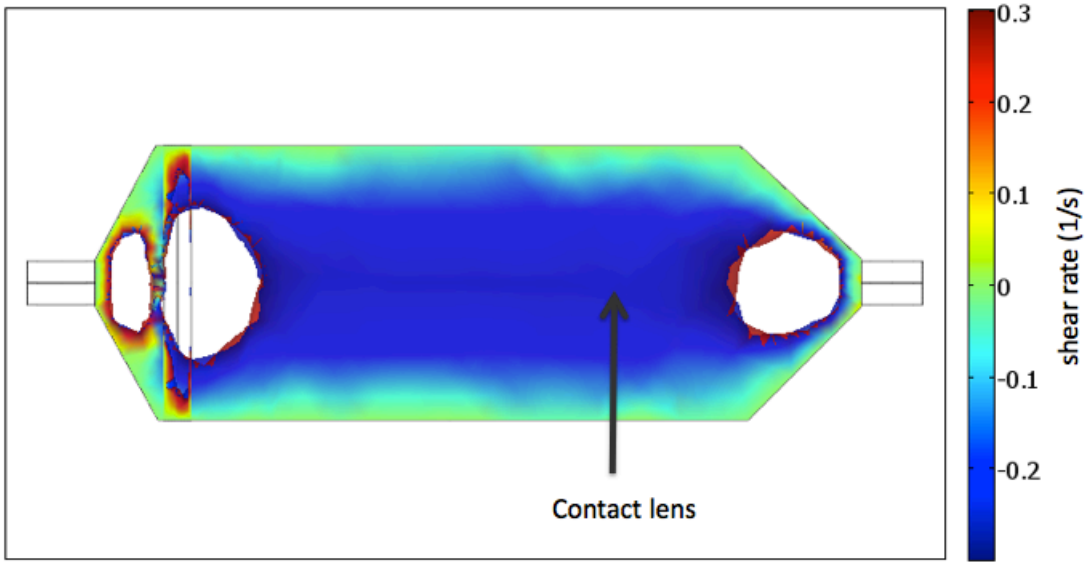


Figure C.3 COMSOL simulated shear rate of optical-flow chamber. The range in the color bar are -0.3 s^{-1} to 0.3 s^{-1}

As mentioned in Chapter 2, nonmotile bacteria reach the contact lens surface much later than that of swimming capable bacteria. Figure C.4 shows the fluid velocity at the bottom surface of the flow chamber. At the viewing depth visible with microscope, the velocity is about 10 μm/s. Given the distance from the baffle, where bacteria are forced to the bottom wall, to the contact lens surface, the time required for the bacteria to reach the surface of the contact lens is about 45 minutes. This corresponds well with the experimental results.

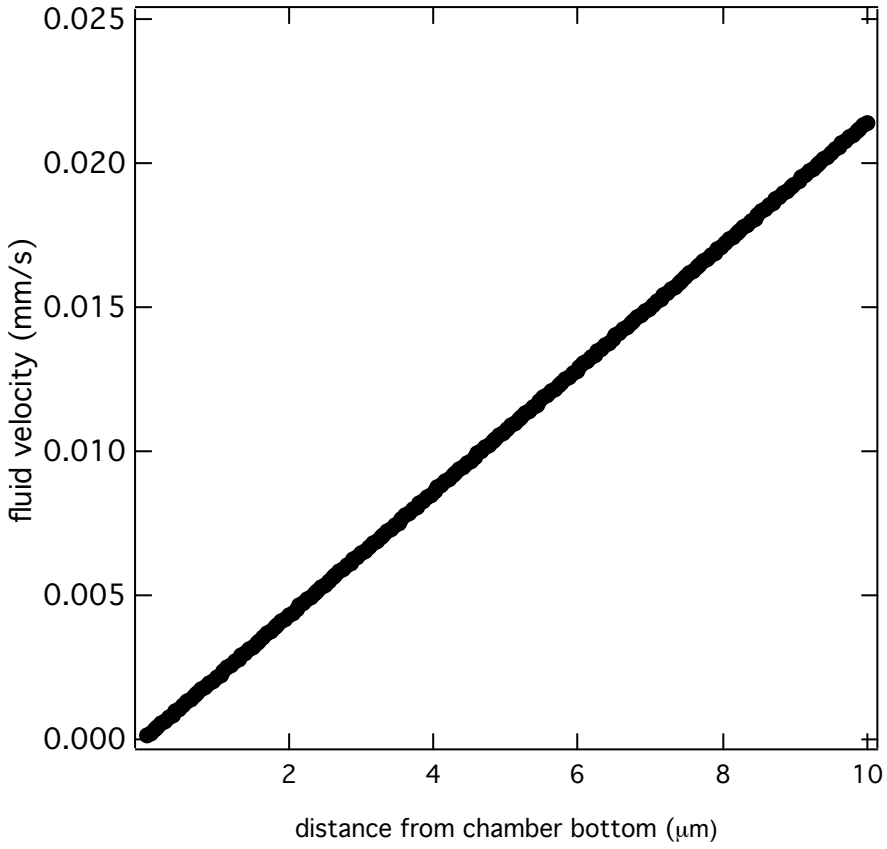


Figure C.4 COMSOL simulated velocity at bottom surface of flow chamber.

Appendix D: Sterile Media Washout After Bacterial Adhesion Experiment

In Chapter 2, it was determined that most wildtype bacteria bind irreversibly to the soft-contact lens surface. To establish further that this statement is valid, a washout experiment was performed as shown in Figure D.1. At the end of a bacterial-adhesion experiment with wildtype PAK to O2O as mentioned in Chapter 2, the flow through the chamber was exchanged to sterile Mian's minimal media. The flow rate stayed the same and essentially the only difference now was that the aqueous medium contained no bacteria. Very few of the bacteria detached confirming irreversible binding.

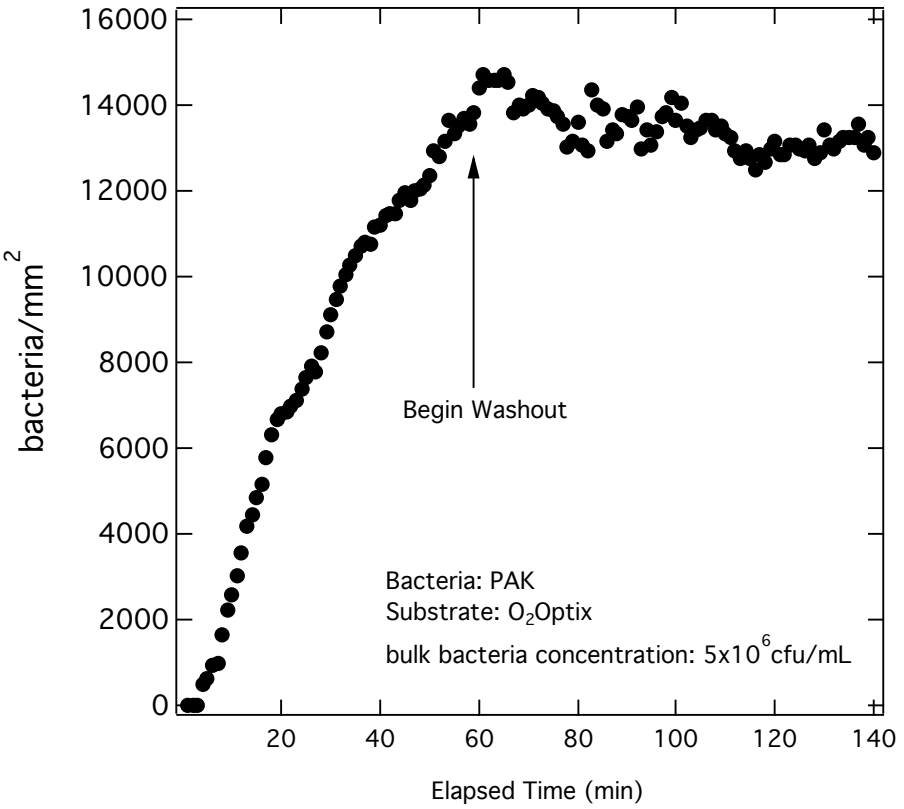
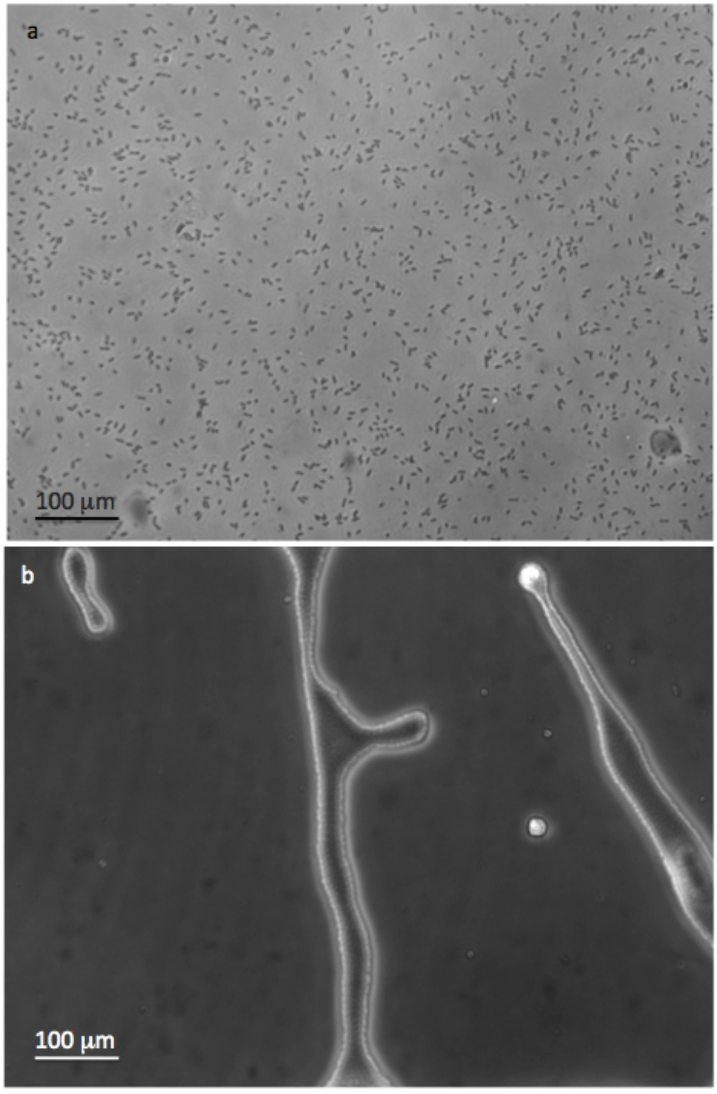


Figure D.1 PAK bacteria associating with O_2Optix lens. Lens was exposed to $5x10^6$ cfu/mL of bacteria suspended in Mian's minimal medium for 1 h and then sterile Mian's minimal medium for 1 h.

Appendix E: Passage of Air Water Interface Across Bound Bacteria

In Appendix A, it was found that different results with viable cell counting versus microscopy occurred for the role of surfactants and adhesion of PAO1. A main difference between microscopy and viable-cell counting is that in viable cell-counting, prior to enumeration of the bacteria, the substrate must pass through the air water interface. Bruinsima et al. showed that passage of the air water interface creates high shear that can remove bacteria.[26] Therefore, after an experiment with PAO1 bacteria binding to an O2Optix lens, the flow chamber was emptied of its liquid contents and the contact lens surface was viewed with the microscope. As shown in Figure E.1, at the end of one hour of PAO1 exposure to an O2Optix lens, the bacteria are evenly distributed on the surface. After the air water interface passes across the bacteria bound surface, it was found all of the bacteria had moved and many of them had moved/aggregated. This shows that the passage of the substrate through an air water interface, is a large artifact in measuring bacterial adhesion.



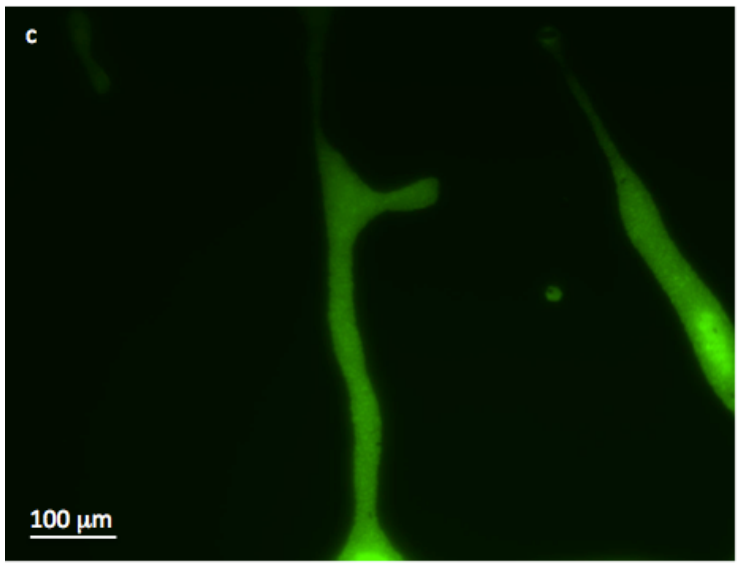


Figure E.1 GFP labeled PAO1 at O_2Optix lens after passage of air water interface. Magnification is at 400x. Lens was exposed to $5x10^6$ cfu/mL of bacteria suspended in Mian's minimal medium for 1 h and then the medium in the flow cell was drained. a.) phase-contrast image before washout b.) phase-contrast image after washout c.) GFP fluorescence image of a.